Future-ready Nordic homes

Responding to the Changing Climate with Free-running Buildings

Marko Ljubas

Master thesis in Energy-efficient and Environmental Buildings
Faculty of Engineering | Lund University

Lund University

Lund University, with eight faculties and a number of research centers and specialized institutes, is the largest establishment for research and higher education in Scandinavia. The main part of the University is situated in the small city of Lund which has about 112 000 inhabitants. However, several departments for research and education are located in Malmö. Lund University was founded in 1666 and has today a total staff of 6 000 employees and 47 000 students attending 280 degree programmes and 2 300 subject courses offered by 63 departments.

Master Programme in Energy-efficient and Environmental Building Design

This international program provides knowledge, skills, and competencies within the area of energy-efficient and environmental building design in cold climates. The goal is to train highly skilled professionals, who will significantly contribute to and influence the design, building, or renovation of energy-efficient buildings, taking into consideration the architecture and environment, the inhabitants' behavior and needs, their health and comfort as well as the overall economy.

The degree project is the final part of the master's program leading to a Master of Science (120 credits) in Energy-efficient and Environmental Buildings.

Examiner: Jouri Kanters (Division of Energy and Building Design)

Supervisor: Pieter de Wilde (Division of Energy and Building Design)

Keywords: Free-running buildings, Climate change adaptation, Thermal inertia, Thermal comfort, Indoor climate, Passive building design

Publication year: 2024

Abstract

The increasing urgency of climate change, coupled with the energy crisis and resource scarcity, demands radical and resilient building solutions. Buildings currently consume a significant portion of energy – in the Nordic context, primarily for indoor space conditioning – highlighting their vulnerability to future climate impacts.

Free-running buildings, operating without any energy for heating, cooling, and mechanical ventilation, relying instead exclusively on passive design strategies, arise as a potential countermeasure to this risk. The thesis aimed to evaluate the viability of free-running residential buildings in the Nordic region under contemporary and future climate scenarios. In the available scientific literature, knowledge of whole-year functional free-running buildings was quite limited.

A detailed case study of the Austrian free-running building „2226“ provided a basis for creating a model suitable for the selected six Nordic locations. Parametric simulations conducted in IDA ICE considered various materials of the building enclosure, internal heat gains, sensor-based control systems, and climate scenarios based on historic and present data, as well as the worst-case future climate projections. Parameters were modified to determine the impact of thermal transmittance, thermal inertia, and natural ventilation on building performance, which was assessed through the adaptive thermal comfort model, indoor relative humidity, and carbon dioxide concentration.

The findings demonstrated that in colder Nordic regions, insufficient internal heat gains during winter limited the viability of free-running buildings. However, in milder Nordic climates, free-running buildings could sustain comfort levels in cases of sun-facing window orientation, higher occupancy, and adequate natural ventilation. Future overheating risks were identified but could be mitigated by thermal inertia, particularly if high-mass materials were exposed on the interior building surfaces. Based on the results, simultaneous fulfillment of year-round requirements for thermal comfort and indoor climate solely through passive design measures in Nordic climates was proven challenging, especially during future extreme cold waves and heat waves.

The significance of this research lies in its contribution to the understanding of sustainable and resilient building practices in cold climates. While free-running buildings offer a promising approach to reducing dependence on energy consumption, their viability depends on the optimization of building design and certain occupancy patterns. Further research on hygrothermal behavior is warranted. The thesis paves the way for future exploration and development in the broader field of climate change adaptation.

Acknowledgments

This thesis is the final project of the last two years of my studies in the Master's program in Energy-efficient and Environmental Building Design at Lund University. It has been an incredible opportunity to learn about topics of sustainability in buildings, and I have had an incredible time while studying here. This work would not be possible without the following people.

I am thankful to my supervisor, Pieter de Wilde, for his guidance, insights, and expertise. His feedback and patience in consultations were crucial to the completion of the thesis.
Gratitude also goes to my examiner, Jouri Kanters, for the thorough review and constructive comments.
An extended thanks to my opponents, Alberto Morales Samper and Aryan Ramezani, for their critical review and helpful suggestions.

I would like to thank all my colleagues for their collaboration in projects, camaraderie, and motivation.
Additional thanks to other teachers in the program, for their interesting lectures and discussions.

To my partner and best friend, Iva, I especially thank you for your love, time, kindness, and encouragement.
I am grateful to my brother, my parents, and the rest of my family for their love and support.
Thank you to my friends in Croatia for the long-distance cheer and long video calls.

I would like to express appreciation to everyone in Larix Engineering, where I gained valuable knowledge of thermal comfort and building simulations during my summer internship.
Lastly, I also wish to acknowledge the team behind 2226 for providing me with information about their design principles, Meteotest for providing their tool Meteonorm, and EQUA for providing the software IDA ICE and their customer support in helping generate custom building controls.

Marko Ljubas

Helsingborg, July 2024

Table of Contents

1 Introduction

This chapter provides an overview of the study, detailing the background, overall aim and objectives, and structure of the thesis, comprising literature review, case study of the "2226" building, method, results and discussion, and conclusion.

1.1 Background

In the face of accelerating climate change (Schwalm et al., 2020) and interrelated challenges, such as resource depletion (Schandl et al., 2018), energy crisis (Moriarty & Honnery, 2016), waste generation (Borrelle et al., 2020), and biome destruction (Bellard et al., 2012) – all escalating in severity – one must realize there is limited time, energy, and resources available to tackle them (Armstrong McKay et al., 2022). This necessitates a closer examination of potentially viable measures, particularly within the built environment and buildings, which significantly contribute to overall energy consumption (Pérez-Lombard et al., 2008), and cause high operational (Huang et al., 2018) and embodied carbon emissions (Röck et al., 2020).

It is universally acknowledged that the ensuing climate change will bring forth turbulent and intense weather events (Fischer & Knutti, 2015), and produce many unprecedented consequences, such as the failure of multiple breadbaskets (Gaupp et al., 2020), colossal wildfires (Jolly et al., 2015), global displacement of millions of people (Mustak, 2022), water insecurity (Hanjra & Qureshi, 2010), and many others. Humanity faces a poly-crisis, where complex systems like climate, biome, and economy are interdependent. Solving a poly-crisis is considered a "wicked problem", which implies no satisfactory solutions due to the scale of complexity (Lönngren & van Poeck, 2020). Recognizing these emerging realities, it may be more prudent to redirect limited attention from mitigation to adaptation to the new circumstances (Albert, 2022).

This topic is of immense relevance for everyone navigating high energy bills, fears of supply chain disruptions, power failure, and various possible economic and social shocks, as evident locally with recent electricity price hikes in Sweden (Statistics Sweden, 2024), (Brauer et al., 2024), (Brännlund et al., 2024). In times of increasing unpredictability, aiming for stability might be facilitated best by greater resilience and decreased reliance on the electric grid, fossil fuels, rare-earth metals, and high-tech materials (Michaux, 2021).

Currently, buildings in developed countries consume up to 40 % of primary energy (Allouhi et al., 2015). Space heating dominates the EU's total building energy end-use (Cao et al., 2016). Heating, ventilation, and air conditioning (HVAC) systems account for around 50 % of energy use in buildings, with a significant increase in space conditioning demand expected shortly (Pérez-Lombard et al., 2008). Therefore, as increasingly called for in academia (Malik et al., 2024), the approach of energy sufficiency – maximum reduction of energy use – is especially suitable for buildings. Since HVAC systems are of such significance to human health and comfort, reducing their energy use might alleviate the burdens of the incoming global challenges.

As a response to the listed issues, this thesis proposed to analyze and understand buildings that use no energy for the climate conditioning of indoor spaces. Such buildings are called free-running (*CIBSE Guide A*, 2015), naturally conditioned (de Dear & Brager, 2002), or thermally autonomous (L.-S. Wang et al., 2014) buildings. Building autonomy can be viewed through the lens of energy, water, or similar independence, which means off-grid electricity generation and off-grid fresh water and wastewater systems (Grazieschi et al., 2020). While the summer potential of free-running buildings is well-explored (Huo et al., 2023), there is a significant knowledge gap of their year-round performance. In this study, the climatic/thermal autonomy of buildings was examined closely. The free-running building from a non-Nordic region, the "2226" in Austria, was selected as a case study, with its design and features adapted for simulation in the Nordic countries.

1.2 Overall Aim

The overall aim was to assess the viability and effectiveness of exclusively passive design strategies in ensuring the resilience of residential buildings in the Nordic region amidst the changing climate conditions. The focus was on creating free-running, future-proof homes that can maintain a specified level of comfort without relying on active heating, cooling, or mechanical ventilation systems.

1.3 Objectives

To meet the overall aim of the study, the objectives of the thesis were to:

1. Identify possible passive design strategies applicable to the Nordic context, and understand the underlying mechanisms behind their performance.
2. Specify the performance requirements for thermal comfort and indoor climate quality.
3. Investigate the current and projected Nordic climate conditions to understand risks and vulnerabilities that could be alleviated with the identified passive measures.
4. Evaluate the performance of proposed solutions by comparing the selected passive design strategies.
5. Provide insights into the influence of climate projections on future building performance.

1.4 Structure of the Report

In chapter 2, scientific literature was reviewed to investigate in detail the state-of-the-art knowledge of three main theoretical topics:

a. Climate change projections, including global and regional effects, and modeling of weather files.
b. Passive building design strategies, including design principles, explanation of thermal inertia, natural ventilation, and properties of building materials.
c. Indoor environment requirements, including thermal comfort, indoor air quality, and occupant behavior.

Chapter 3 offers a comprehensive analysis of the case study – multi-functional building “2226” in Austria – providing insight into passive building design and real-world data, enabling verification of the simulation model. Findings from this case study formed a basis for further research on the possibility of free-running buildings in the Nordic context.
In chapter 4, methods used in this study were elaborated, including the creation of the building model, generation of weather files, and setup of the parametric simulation.
Building performance simulation results were presented in the chapter 5, followed by a discussion of key findings.
Chapter 6 provides conclusions to the undertaken work, with proposals for potential future research into the subject matter.

2 Literature Review

This chapter provides an overview of relevant scientific literature, covering the impacts of climate change on buildings, passive design strategies, thermal comfort, and indoor climate, as well as their applications in building performance simulation.

2.1 Climate Change and Scarcity of Resources

The climate emergency has driven climate data analysis, scientific research, public policy, and international regulations, impacting billions of lives, from waste reduction to large-scale energy developments. Sustainability has become a megatrend, despite socioeconomic inertia, greenwashing, and denial in some regions. In the construction sector, it influences everything from design principles to construction methodologies. Fighting climate change is now paramount. Addressing this requires confronting our current situation and future direction. Yet, the mainstream global warming estimations seem to have been significantly underestimated, posing a much greater threat than previously thought (Witkowski et al., 2024). With accelerating climate change, there is a risk of failing to alter future warming trajectories, potentially crossing planetary thresholds leading to global average temperatures not felt on Earth in more than the last 1.2 million years (Steffen et al., 2018). Simultaneously, the world is facing diminishing returns on fossil fuel energy, while the alternatives, seen in clean technology and renewable resources, bring further uncertainties and risks to the viable energy transition (Michaux, 2021).

2.1.1 Climate Change Unfolding

Climate change is, in essence, a result of physical processes. The main driver of climate change is anthropologically induced global warming, resulting from the Earth's energy imbalance (EEI). EEI is a measure of the excess energy trapped on Earth, predominantly due to man-made changes in the atmosphere's composition of greenhouse gases (GHGs). As long as there is more energy absorbed by the planet from solar radiation than it is emitted back to space by longwave radiation, the EEI will continue to warm up the Earth until a new thermal equilibrium is reached.
What is felt today is a delayed response from earlier energy accumulation. Carbon dioxide and other GHGs are the main positive forcing mechanisms. The negative forcing, or cooling effect, is caused by the Earth's albedo and aerosol clouds dispersed in the atmosphere, reflecting partial radiation before it can heat the planet. The net positive forcing is the driver of EEI (von Schuckmann et al., 2023). In the last 20 years, the EEI has more than doubled, mainly due to reduced albedo (Loeb et al., 2021). An increase in EEI is a sign of accelerated global warming.

Assuming a linear long-term warming trend (observed since the 1980s) of +0.2 °C per decade, a warming of 3 °C of surface air temperature is estimated by 2100. In 2023, the global average annual temperature was 1.54 ± 0.06 °C above the pre-industrial baseline, surpassing the threshold of 1.5 °C for the first time throughout the year. For land temperatures alone, the increase was 2.1 °C. A single anomalous year is not sufficient proof of a change in the global warming rate, but it gives cause for concern (Rohde, 2024).
As explained by Hansen et al. (2023), fast-feedback equilibrium warming of total GHG forcing (4.1 W/m²) emitted from the 18th century up to the present yields a temperature increase of 4.8 ± 1.2 °C. Each additional year of record carbon emissions increases the equilibrium warming (presently the growth rate is 0.5 W/m² per decade, which yields a warming rate of almost +0.3 °C per decade).
Unfortunately, the real equilibrium is a sum of anthropogenic activities and the Earth's feedback loops. As biogeophysical feedback loops activate, the proportional relationship between human-emitted GHGs and global temperature rise will break. With the activation of feedback loops, some of the intermediate warming trajectories (< 2 °C) could be crossed out. The largest negative (stabilizing) feedbacks, land and ocean uptake of carbon, have been diminished by human activities. In turn, the positive (destabilizing) feedbacks, such as permafrost thawing, and diebacks of the boreal and Amazon forests, have been increasingly enhanced by human activities. The long-term feedback spanning centuries, such as the decomposition of ocean methane hydrates, oceanic bacterial respiration, and loss of polar ice sheets, have already been triggered (Steffen et al., 2018). Today's concentrations of GHGs in the atmosphere are estimated to yield equilibrium warming of 10 °C when slow feedbacks are considered (Hansen et al., 2023).

When a tipping point is reached, an abrupt change may be expected. The rate of change will hinder the existing biomes from adapting to new conditions, and widespread die-offs could occur as a result. It is suggested that the continued melting of Greenland and West Antarctica ice sheets could affect ocean circulation and ocean temperature, which would in return accelerate the loss of permafrost and boreal forests. Permafrost contains high amounts of future methane emissions, which have a stronger warming impact than carbon dioxide (Kemp et al., 2022).
Warming of 2 °C above pre-industrial temperature levels is suggested as a threshold for runaway warming, as at those temperatures some of the global tipping points are reached, meaning that the processes become self-perpetuating and almost irreversible. Some tipping points could already be tipped, and others could be triggered by a cascading effect, even when the higher levels of warming have not yet occurred (Steffen et al., 2018). Far-future feedbacks are mostly "unknown unknowns" and their potential impact is largely speculative. Among them, some are low-probability, but high-impact, which drives the range of uncertainty and possible risk (Kemp et al., 2022). Feedback loop instabilities and uncertainties, such as cloud behavior, explain how significantly higher average temperatures millions of years ago were possible without the atmosphere's impossibly high amounts of carbon dioxide (Schneider et al., 2019).

In many impact studies, temperature increases above 3 °C are underexamined and underreported. The Intergovernmental Panel on Climate Change (IPCC) reports have focused on impacts of 1.5 °C and 2 °C, the upper limits set by the Paris Agreement in 2015, with any higher levels of warming recognized as extremely high-risk conditions. From the perspective of risk assessment, the opposite should have been done.
Even at moderate warming rates, food and water instability will increase, accompanied by disease spread, higher mortality, and political/economic instability (Kemp et al., 2022). In a worst-case scenario, immense risk is present in food systems, with implied starvations measured in billions of people, not even sparing high-income countries (Richards et al., 2023).

Well-meaning efforts to curb climate change yield unwanted side effects. For example, aerosols, fine airborne particles that block solar radiation, originate from natural sources like wildfires or volcanos, but a large share comes as an anthropogenic by-product of the combustion of fossil fuels, wood, and biomass. They have a cooling effect but also cause health issues and significant deaths (Vohra et al., 2021).
In Europe, regulations have limited the amount of aerosols that can be emitted by industry, leading to better health outcomes, but also faster warming and brighter skies. Most climate models have underestimated the enormity of the impact, as aerosol-cloud modeling is extremely complex, with large uncertainties (Schumacher et al., 2024). New International Maritime Organization regulations on ship fuels to reduce SO_2 emissions have caused drastic and unprecedented warming in heavy-traffic shipping lanes, especially in the North Atlantic (Hansen et al., 2023), (*Climate Reanalyzer*, 2024).
These results are incredibly concerning because they indicate that efforts to achieve carbon neutrality by mid-century will be met with more and more instead of less warming (P. Wang et al., 2023). Reduced aerosols create additional forcing of 0.5 W/m^2 – 1.0 W/m^2, which translates to approximately 2 °C of masked warming (Hansen et al., 2023).

Apart from being characterized by a relatively narrow temperature range (C. Xu et al., 2020), the human livable niche can be examined as a part of stable planetary boundaries, as laid out by Rockström et al. (2009). There are nine mutually interdependent planetary boundaries within which human society can flourish: climate change, ocean acidification, stratospheric ozone, biogeochemical nitrogen and phosphorus cycles, global freshwater use, land system change, the rate of biological diversity loss, chemical pollution, and atmospheric aerosol loading, with three boundaries already exceeded at the time of the report. In a revised study by Richardson et al. (2023), it was concluded that six out of nine planetary boundaries were crossed, with some entering high-risk zones.
The conclusions of these studies reach eschatological proportions. They signal "catastrophe" and call for urgent adjustment. The lack of it could potentially result in human non-survival entering the next centuries, amidst the sixth mass extinction already underway (Ceballos et al., 2015), (Thomas et al., 2004).

2.1.2 Climate Change in Nordic Countries

Measured data shows that the climate of Nordic countries has already changed in relation to the pre-industrial baseline. In general, temperature has increased in all seasons, and in the last 30 years, there has been ever more precipitation. Diurnal temperature variability has decreased in winter and increased in summer (Kjellström et al., 2022). The Nordic region has been warming significantly more than the global average, as

seen in Figure 1 (Berkely Earth, 2024). However, this does not necessarily mean that the observed pattern will continue in the future.

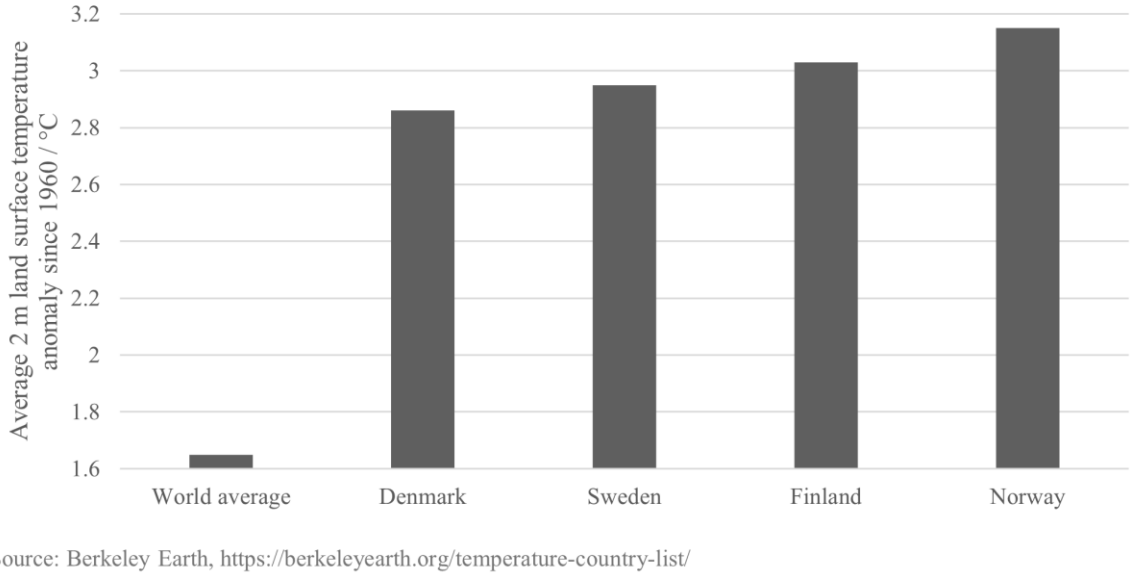

Figure 1. The difference in the rate of warming land surface temperature between the Nordic countries and the global average. Sourced from (Berkely Earth, 2024).

Rain intensity is generally expected to increase, although the predictions between different prediction models vary significantly. This will cause a higher wind-driven rain impact on the building facade, meaning that external building enclosure layers will increase their water content. In many locations across the Nordic region, buildings have historically already displayed problems caused by high moisture and wind-driven rain (Nik et al., 2015). Under the IPCC Representative Concentration Pathway RCP4.5 and RCP8.5 scenarios, the climate is expected to become ”wetter, warmer, and wilder” (The Danish portal for Climate Change Adaptation, 2023). Since the water-holding capacity of air increases by around 6 %/K of warming (Borger et al., 2022), higher humidity levels will lead to amplified global warming, as well as stronger variations in precipitation and severe weather (Patel & Kuttippurath, 2023).

In Denmark, this would mean warmer summer nights, longer and more intense heat waves, and fewer frosty nights. The trend of increased annual precipitation will continue, with prominent winter rainfall (an increase of 25 %). The ”best guess” for temperature increase by the end of the century is 3.4˚C above preindustrial baseline (interval 2.8 °C – 4.3 °C).
In Norway, the same scenarios predict a temperature increase within the range of 3.3 °C and 6.4 °C (Norwegian Centre for Climate Service, 2017). Heavy rainfall will be more intense and more frequent, causing floods. Snowmelt floods, on the other hand, will decrease, as snow cover in lowlands will be almost non-existent. Glaciers are projected to decrease by a third of today’s volume. By 2100, most permafrost will thaw permanently, except for the highest mountains.
In Sweden, the projected temperature increase by the end of the century is between 4.2 °C and 7.0 °C nationally (Swedish Meteorological and Hydrological Institute, 2020). In the southernmost region of Skåne, temperature increase is expected in the interval of 3.5 °C and 6.2 °C, while in the northernmost region of Norrbotten, the interval will be between 4.2 °C and 7.8 °C. The diurnal temperature range will decrease by around 1 °C. Access to water will be reduced in most of southern Sweden, especially in Skåne and around lakes Vänern and Vättern. Precipitation will particularly increase in northern Sweden, especially in winter. Along the coast, the erosion will produce a risk of damage to buildings and infrastructure.
In Finland, the temperature increase will most likely be between 3.4 °C and 8.7 °C, with the highest temperature anomalies expected in winter (UNFCCC, 2017). Future precipitation is more uncertain: there could be up to a 12 % annual decrease or up to a 36 % annual increase. Northern parts of Finland are expected to receive more rainfall. In southern Finland, there may be up to 35 hot days where the daily maximum temperature exceeds 30 °C, and up to seven days where the temperature exceeds 35 °C.

However, there are some boundaries, tipping points, and other phenomena that are either understudied or completely omitted from the IPCC reports and models. One of the overlooked topics is the Atlantic Meridional Overturning Circulation (AMOC), which is a fundamental factor of European climate (Hansen et al., 2016). The AMOC system is one of the most important tipping elements of the Earth's climate. The AMOC has recently weakened, and it may partially or completely shut down sometime during this century. Already today, AMOC is weaker than at any point in the last millennium (Bellomo et al., 2023). Many previous studies independently conclude that a weakened or collapsed AMOC leads to cooling in the northern hemisphere, along with decreased precipitation, especially over the Atlantic and Europe, whereas in the southern hemisphere, further warming is expected. This is caused by reduced heat transport from the tropics to the northern latitudes.

In northwestern Europe, precipitation will increase, due to changes in the behavior of the jet stream. Over land, storms will be more intense, but overall drier. In Nordic countries, the simulated cooling effect will be the most magnified of all regions over the globe, as the average near-surface temperature may cool down by more than 2 °C. A strong decrease in annual average precipitation will be expected, especially amplified along the Norwegian coast (Bellomo et al., 2023). Although the mean number of wet days could decrease, there are going to be positive precipitation anomalies, meaning that significantly wet days are to be expected, with a large amount of daily precipitation. This is also more emphasized in the western parts of Scandinavia. The expected changes in wind directions and wind velocities will lead to a strong contrast between generally dry coasts and generally wet adjacent seas.

Based on paleoclimatic records and future climate simulations, Hansen et al. (2016) show AMOC collapse will yield a rapid, non-linear sea level rise of 2 m – 3 m within several decades, and up to 9 m in the following centuries. Additionally, shifts in temperature gradients will cause severe "superstorms" in Europe, with an increase in intensity and frequency.

Net precipitation in the Nordic countries will decrease by up to –1.8 mm/day, with the sharpest decrease expected in Norway. The storms are expected to be drier, but still more intense. Without the weakened AMOC, we would be expecting significantly wetter anomalies. However, with the weakened AMOC, precipitation can be expected to increase only in the southernmost parts of Norway, the west coast of Sweden, and Denmark (Bellomo et al., 2023).

Findings from simulations of future AMOC behavior indicate an abrupt collapse and a relatively fast cooling effect that takes approximately a century to stabilize. The most intense cooling will be seen across northern Europe, particularly in the area between Iceland, Scandinavia, and the UK. The estimated annual temperature decrease in this area would be up to 15 °C, with the sharpest temperature decline in winter months (up to 35 °C lower February temperatures than today for simulation in Bergen), while in summer months, the temperature drop is between 0 °C and 10 °C (van Westen et al., 2024). These findings are significant and worrisome, as they indicate a potential near-future reality where both cooling and heating loads in buildings are increased.

2.1.3 Impacts of Climate Change on Buildings

Climate change will have varying effects on buildings, some of them being gradual or sudden, moderate or drastic, on a local or a regional level, affecting occupants, energy use and emissions, building subsystems, or building functionality (de Wilde & Coley, 2012). For example, the impact of climate change on building energy demand is well-studied. In most climates, the heating demand is expected to decrease, and the cooling demand is expected to increase (Ciancio et al., 2019). Whether the total energy consumption will decrease or increase is influenced largely by local climate conditions (Bravo Dias et al., 2020). In a high-performance building, the majority of energy consumed is accounted for lighting, equipment, and appliances.

Much of the future electric load will be caused by the increased cooling demand (Robert & Kummert, 2012). Furthermore, it is known that in energy-efficient buildings, many uncertainties such as household size and the occupants' behavior have a relatively greater impact on building performance, which is reflected in frequent deviance between operational and predicted energy use, rendering many such buildings highly sensitive to diverse conditions (Kotireddy et al., 2018).

Many building features, such as shading devices or HVAC systems, will be outdated if they were designed with a past climate in mind (Bravo Dias et al., 2020). The HVAC systems are particularly vulnerable, as their efficiency is derived from proper sizing, and in the process of continual climate change, the system may end up undersized and/or oversized during its life cycle (Y. Sun et al., 2014). The daily shifts, in terms of diurnal temperature range, and the annual shifts, in terms of temperature distribution, will have an impact on the building operation. For example, most of Europe can expect a diminished effectiveness of passive design

strategies. Natural ventilation may become viable only when aided by a wind-driven airflow (Bravo Dias et al., 2020). Future climate will also cause higher concentrations of indoor air pollutants, which are insufficiently tackled in present-day legislation (Zhao et al., 2024).

Climate change is projected to amplify the impact of extreme weather events on power systems, heightening the likelihood of severe power outages, as well as the likelihood of multiple hazards occurring simultaneously or sequentially. The decarbonization of energy supply and reliance on environment-dependent renewables (solar, wind, hydropower) bring an elevated vulnerability of power grids. Renewables faced with accelerating climate change will be challenged with extensive damage to infrastructure, reduced grid inertia and flexibility, and an extended recovery period after a severe weather event.
For example, over 80% of power outages in the United States of America are attributed to extreme events such as hurricanes, wildfires, heat waves, and flooding, many of them attributable to climate change. The previous decade saw an increase of 78 % in weather-related power outages than the decade prior.
The expected severity is also reflected in predictions that by the end of this century, the U.S. East Coast will experience a historical 100-year flooding every year. The risk of power failure is further deepened by the expected rise in energy demand and a likely drop in energy production capacities (L. Xu et al., 2024).

In a disaster event, it is of immense value if the home can continue supplying its residents with all their needs, and even have additional purpose as a shelter for potential neighbors. In a post-disaster situation, poor thermal comfort and excessive dampness should ideally be avoided, as they are common health hazards (such as asthma, allergies, and respiratory and dermatological infections). However, as numerous humanitarian crises have demonstrated, a common notion that energy supply concerns would inevitably and quickly be addressed should be dispelled. This awareness should be retained during the building design process (Li et al., 2024). In that case, any dependence on electric systems is highly unfavorable.

The Nordic region is usually not associated with problems of overheating. However, in Helsinki, almost half of the 6 000 studied apartments during the heatwave of 2021 experienced more than a week of consecutive indoor temperatures above 27 °C. This presents a great health risk and an increase in mortality, especially among the elderly people (Farahani et al., 2024).
Similarly, the growing trend of home offices may cause overheating, as shown in a study of the future climate of Austria (Schaffernicht et al., 2023). Indoor conditions were assessed for a future five-day heat wave of a high-impact (RPC 8.5) scenario by the end of the century. ”Tropical” nights above 25 °C and overheating during heatwaves are expected. Passive cooling strategies will be ineffective due to higher internal loads, and high night temperatures will reduce natural ventilation's cooling potential.

When looking at Nordic households, the residential sector has on average a share of 24 % of the total energy consumption (International Energy Agency, 2022). In the existing buildings, the highest share of energy use belongs to space heating, followed by water heating, lighting, and appliances, as seen in Figure 2. The numbers indicate that the greatest savings could be attained if no energy was used for thermal conditioning.

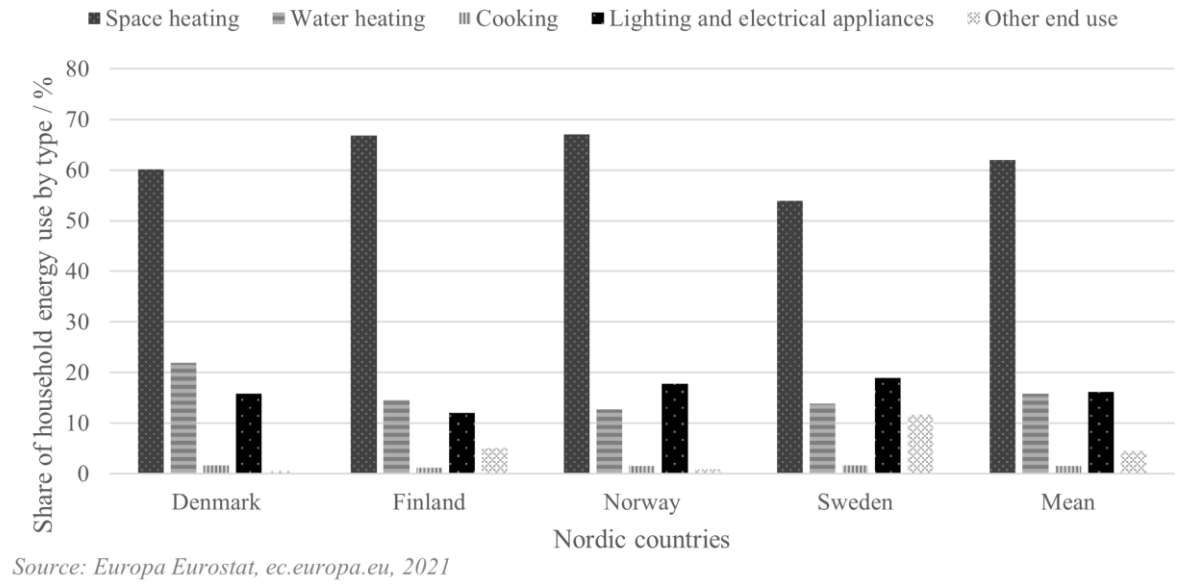

*Figure 2. Final energy consumption in the residential sector by type of end-use in the Nordic countries. Sourced from (*Energy Consumption in Households, *2023)*

However, over the past three decades, housing energy consumption has undergone significant changes, characterized by a decrease in heating, and a notable surge in electricity consumption. Electricity usage predominates in new housing in Denmark. The incremental energy efficiency improvements in household and personal electronic devices have been offset by the widespread ownership and increased usage of appliances (Marsh et al., 2010). These developments are indicative of the rebound effect or Jevons' paradox, which states that gains in energy efficiency result in equal or higher overall energy production and consumption (Sorrell, 2009). Electricity use amounts to around 60 % of the total primary energy consumption for new-build housing. In the second half of the 21st century, more primary energy in Denmark is expected to be used for space cooling than for space heating (Marsh et al., 2010).

2.1.4 Energy Transition

Fossil fuels are indispensable to our civilization. For example, a population of eight billion can only be sustained because synthetic fertilizers are mass-produced by fossil fuels. Oil and petroleum are integral parts of any long-distance transportation. All plastic products, pharmaceuticals, chemical products, most manufacturing processes, and many more cannot be readily separated from fossil fuels.
Around 82 % of global primary energy consumption comes from fossils, while renewables account for less than 8 % (The Energy Institute, 2023). The economic growth is always based on abundant energy (Stern & Kander, 2012), and GDP per capita growth correlates almost linearly with carbon emissions (Our World in Data, 2018). It is almost impossible to decouple global economic growth from its environmental impact. In a study by Vogel & Hickel (2023), it was shown how some high-income countries have slightly decoupled, but at rates more than 10 times lower than necessary for Paris Agreement compliance. Similar results are presented in a meta-analysis by Vadén et al. (2020), where it is shown how economic growth decoupled from environmental impact lacks any empirical evidence; on the contrary, more re-coupling was evident.
This indicates that the current lifestyle and industrial-economic output are incompatible with the goals of a sustainable future. The goal of energy transition away from fossil fuels rests on the development and increase of technology using renewable sources of energy (sunlight, wind, ocean tides, and geothermal heat), as well as increasingly using less-polluting resources (nuclear fuels, biomass, or hydrogen).
The fundamental problems of energy from renewable sources, as described by Arutyunov & Lisichkin (2017), are comparatively low energy density and low conversion efficiency. As long as fossil fuels are available, most countries and companies will opt for them simply because they are usually more profitable. Additionally, the present global energy demand outstrips any realistic maximum achievable with renewable-only energy production (Moriarty & Honnery, 2016). Therefore, any attempt at using energy strictly from the sun, wind, and similar, can only happen if energy use declines extraordinarily, signifying an economic decline.

In a detailed report by Michaux (2021), it is shown how the energy transition is requiring a growing amount of materials, especially metals and rare-earth minerals, which are not as scarce, but impurely spread across the Earth's crust. This means tons and tons of raw ore need to be drilled, excavated, transported, and processed to obtain grams of pure element, all of which is possible only if fossil fuels are used. For example, the global reserves of lithium, cobalt, and nickel are insufficient to produce just the first generation of batteries (life cycle of 10 years) to phase out vehicles with internal combustion engines. The discovery of new mineral deposits has been in decline for years, and the grade of processed ore has had diminishing quality, indicating that in the future more energy would be required to process the same amount of the material. Meanwhile, water consumption and waste production rates in mining are increasing. Biofuels and biomass can also be crossed out as replacements for fossils, as they would require annually more land than is covered in total by the world's forests. Similarly, the analysis demonstrated how nuclear capacity cannot be scaled in time to deliver the same amount of energy as is currently gained from the combustion of fossil fuels.
While gains in potential future energy efficiency should not neglected, they will be offset by the overall growth in energy consumption, as long as energy use is placed within the logic of the market economy. The inability of profit-driven markets to reduce total energy consumption is observed with the gradual introduction of renewable clean technology in the past decades, which acted as an addition, and not a replacement of fossil fuels in the global energy mix (The Energy Institute, 2023).

Although renewables offer significant carbon savings over fossil-based heating/cooling systems, they still have embodied GHG emissions inseparable from their product and end-of-life stages, which should not be overlooked. Moreover, renewables also have higher impacts in some environmental categories beyond global warming potential (Naumann et al., 2022). Heat pumps, for example, demand great amounts of copper, iron, cement, and aluminum (Hertwich et al., 2015), while the production of photovoltaic panels entails water and air pollution, as well as hazardous contaminates, such as SOx, NOx, heavy metals, and various chemical compounds (Tawalbeh et al., 2021), (Rashedi & Khanam, 2020). Recycling these technologies poses significant technological challenges and high costs (Mao et al., 2024).
Fossil fuels are essential for producing and delivering renewable technologies. The depletion of fossil fuels raises concerns about the sustainability of renewables. Manufacturing these technologies requires vast raw materials and fossil fuel-powered machinery, and must be done on a large scale to be cost-effective, leading to high carbon emissions.

Much of the total energy consumption in the Nordic region comes from renewables: 61 % in Norway, 58 % in Sweden, 47 % in Finland, and 40 % in Denmark. These countries are world leaders in heat pump adoption (Rosenow et al., 2022) and in wind power generation (Skjærseth et al., 2023). However, fossil fuels still comprise a large share of the total energy supply: 50 % in Norway, 23 % in Sweden, 37 % in Finland, and 54 % in Denmark (International Energy Agency, 2022). The average Nordic per-capita energy use is among the highest in the world (Our World in Data, 2022).
Nordic countries use up far too many resources than are available. If, for example, everyone on Earth lived like an average Swede, almost four planets would be needed to meet global demands ("Country Overshoot Days," 2024). In buildings, this can be observed in the fact that around 45 % of people in Nordic countries live in under-occupied dwellings (Eurostat, 2022c). Nordic countries have the lowest household size in the EU (Eurostat, 2022a), while boasting some of the largest dwellings by floor area (Eurostat, 2022b). Notably, no country manages to use less resources than the Earth's regeneration capacity. Even if Nordic countries decoupled from fossil fuels, they would remain part of a global economy dependent on complex supply chains, exposing them to global shocks and instabilities.

Survival in the future requires learning to live with less energy, materials, and consumption. Developed economies would have to contract by more than 90 %, according to Trainer (2021). Economic fallout suggests reduced availability of everyday materials. A more sustainable future will have to go beyond the concepts of renewable energy. In construction, this means focusing on local abundant resources that require low energy for extraction, processing, and construction, with minimal environmental and health impacts. Bio-based resources and clay/soil fit these criteria, while passive, resilient design can enhance the success of such buildings, as discussed in the following sections.

2.2 Passive and Resilient Design

The following sections describe and analyze the theoretical design guidelines and practical solutions that may respond well to future conditions.

2.2.1 The Concepts of Resilience and Sustainability

The concept of resilience is subject to varying interpretations, leading to academic debate over its definition. There is a lack of consensus on how resilience should be understood, thereby creating a sense of ambiguity (MacAskill & Guthrie, 2014). Factors such as biosphere destruction, tightly concentrated supply chains with vulnerable chokepoints, global spread of shocks due to hyper-connectivity, increasing inequalities, and governance focused on short-term goals all play a role in undermining the vital characteristics of global resilience (Rockström et al., 2023). As shown by Scheffer et al. (2001), global ecosystems will be more prone to sudden and drastic state shifts, while simultaneously lacking early-warning signals, reducing the probability of adaptation, and increasing the importance of resilient management.
The concept of sustainability in architecture is equally open to discussion and debate, due to various possible interpretations. Sustainability is a constantly evolving set of theoretical and practical approaches seen as the most fit for the occasion, and we can expect the idea of sustainability to keep changing (Villacis-Ormaza, 2024). Generally, while resilience starts from strategic goals of self-organization and risk adaptation, sustainability starts from normative ideals of environmental protection and intergenerational equity. Similarly, while resilience is concerned with response and flexibility to disaster and change, sustainability is concerned with resource efficiency, evolution of complex systems, stability, and mitigation of change. Due to the potential differences between sustainability and resilience, it is questioned whether a common framework combining both is possible (Roostaie et al., 2019).
Risk science should be intertwined with the concept of resilience, as it may enhance and improve the resilience assessment. A resilient system keeps the risk of not achieving a desired functionality sufficiently low (Logan et al., 2022). The risk reduction approach involves preventative control and minimization of negative consequences. If we assume that climate change and resource exhaustion lead to an unpreventable increase in risk sources, what remains is to minimize the consequences through responsive and adaptive measures.
Thermal resilience, crucial for maintaining indoor comfort during extreme events, is gaining attention in research and industry practices. Unlike other types of resilience, such as earthquake or fire resilience, a lack of standardized procedures for thermal resilience is evident in building codes. The key factors that influence the thermal resilience of buildings are the outdoor environment, building characteristics, occupant characteristics, and power grid reliability. Modeling thermal resilience necessitates the consideration of a range of scenarios that encompass different hazards capable of disrupting buildings within a specific geographic/climate area. For example, air pollution or wildfires would limit the opening of windows; power outages would limit the use of HVAC systems; and storms, floods, and other natural disasters would damage structures and systems (Hong et al., 2023).

2.2.2 Bio-based Materials

The link between greater resilience and bio-based materials is evident in the abundance of the resource, its connection to other aspects of the human economy, and the frequent non-harmful environmental/health aspects of such materials. However, as emphasized by Hickel & Kallis (2020), bio-based materials are nonetheless incompatible with the growth-based economy because the infinite growth of any material category conflicts with the environment. The growing demand for timber, for example, has to face a sustainable limit to the supply potential, risking otherwise overharvesting and driving diminishing forest regeneration rates (Vadeboncoeur et al., 2014), (Egenolf et al., 2022).

Bio-based materials offer local availability, thereby improving the logistics and import dependency of the construction sector. Great potential is seen in agricultural byproducts/residues such as hemp, straw, and flax, which are gaining scientific and market interest. Their main building function is as insulation bats or as particle boards (Kanters et al., 2023). Plant-based materials grow rapidly (Shea et al., 2012), and require low amounts of energy in their production, while their disposal poses a low environmental risk, as they easily biodegrade (Bakkour et al., 2024). For example, hemp-lime blocks (hempcrete), consisting of of hemp shives and a lime-based binder, are molded, pressed, hardened, and air-dried, without any thermal treatment (IsoHemp, 2024).

Currently, in the southern Swedish region Scania, straw is mostly procured from wheat and barley, while hemp and flax have a negligible share in straw production. Calculations show that the locally and sustainably harvested straw in Scania could satisfy the total annual building insulation demand for all new residential buildings in the region (Kanters et al., 2023).

The hygrothermal and mechanical properties of these materials vary significantly due to different raw materials, treatment and production processes, and binders/adhesives used (Benfratello et al., 2013). The typical thermal conductivity of crops ranges from 0.04 W/(m·K) to 0.10 W/(m·K) (Kanters et al., 2023). However, thermal conductivity is negatively affected by an increase in relative humidity (Palumbo et al., 2016). There is a deviation in measured against simulated and calculated moisture dependence of thermal conductivity, with the measured results showing significantly higher λ values (Korjenic et al., 2011).
The vapor absorption capacity of bio-based materials (jute, flax, and hemp) is much higher than conventional insulating materials (Palumbo et al., 2016), (Korjenic et al., 2011). Similarly, due to high water content, the heat capacity of hempcrete is considerably higher when approaching 100 % relative humidity (Evrard, 2008). Bio-based materials exhibit high moisture buffer capacities (Rahim et al., 2015), further discussed in the section 2.4, indicating lower measured thermal transmittance against the calculated value (Strandberg-de Bruijn et al., 2019).

In this thesis, much attention was brought to opaque building materials, as there are not any low-tech, bio-based alternatives to modern-day, high-efficiency windows. Practically all low-energy buildings rely on the concept of high-tech windows with optimized glazing and efficiently reduced heat losses/gains. Therefore, the production and sustainability of windows are not further discussed, but their unique status is here acknowledged.

2.2.3 Passive Design Strategies

The main performance-enhancing strategies for buildings are either active or passive. Active strategies aim for improvements in HVAC systems and more efficient control/use of lighting and appliances. They are called active because they consume energy to add or remove heat to the building. Passive strategies aim for improvements in building enclosures, appropriately increasing or decreasing heat gains, thereby reducing energy demand (Verbeke & Audenaert, 2018). They rely on building-based and occupant-driven solutions and include highly insulated building enclosures, high-performance windows, shading devices, evaporative surfaces (green roofs), natural ventilation, passive solar heating/cooling, and thermal mass (Hong et al., 2023). Under future climate uncertainty, when life cycle carbon emissions, life cycle costs, and indoor discomfort hours are considered, the major impact on building performance comes from the thermal transmittance (*U*-value) of the opaque and transparent building enclosure, and wall density (Chen et al., 2024). This means an improvement in building enclosure will most likely contribute the most to the overall building performance.

Passive design strategies (or bioclimatic architecture strategies) are increasingly relevant in the presence of climate change and energy reduction ambitions. Passive heating comprises heat retention and heat admission strategies. Heat retention is achieved by thermal insulation, orientation and space zoning, building size and shape, thermal mass, and convective heat exchange. Heat admission is regulated by orientation and space zoning, convective heat exchange, and direct and indirect thermal gains (glazing, sunspaces/winter gardens/conservatories, Trombe walls) (Bugenings & Kamari, 2022).
Passive cooling comprises heat dissipation, heat exclusion, and heat modulation strategies. Heat dissipation involves evaporative, radiative, conductive, and convective heat exchange, building size and shape, and thermal mass. Heat exclusion relies on thermal insulation, solar shading, orientation, occupancy-related changes, and space zoning. Modulation of heat gains is achieved by thermal inertia (Salvalai et al., 2013). The use of misting fans, ice towels, consumption of cold water, adjustment of activity levels, and layering clothing can further bolster the cooling effect (Hong et al., 2023).

As emphasized by UNEP (2021), it is important to take into account whether the occupants of a building have the ability or inclination to utilize the passive design approaches. The occupants should not just comprehend but actively choose, use, and maintain the identified strategies. Without the awareness, input, and acceptance of the occupants, many of the passive measures may not yield the intended outcomes. In the following sections, thermal inertia and natural ventilation were analyzed in more detail, as they were linked with the performance of the selected case study building.

2.3 Thermal Inertia

Thermal inertia refers to the phenomenon where an initial change in ambient surroundings is not immediately followed within the building interior, but rather delayed and with a reduced effect. It is understood to be a complex phenomenon influenced by climatic conditions, thermal properties of the building enclosure, and occupant behavior. As seen in Figure 3, when diurnal temperature variation is simplified as a sinusoidal curve, the effect of thermal inertia is observed in the amplitude decrease and the peak amplitude time shift, or time lag. The higher mass of the material usually amplifies the effects of thermal inertia (Verbeke & Audenaert, 2018).

Thermal mass and thermal inertia are often used as synonyms, but thermal mass is the material's intrinsic property, while thermal inertia is the outcome of a material accumulating and dissipating heat from and towards the immediate surroundings in a specific context. For example, structures with the same thermal mass can have significantly different thermal inertia, due to layer placement in the building enclosure (Aste et al., 2009). Unlike thermal transmittance of the building enclosure, thermal inertia in Nordic building codes is not properly quantified, or specified with minimum requirements. Norwegian building code mentions exposed thermal mass as a potential passive measure against summer overheating, but it does not provide clearer instructions (*TEK 17*, 2017). Similar status in the U.S. and the U.K. building regulation is reported by L.-S. Wang et al. (2014).

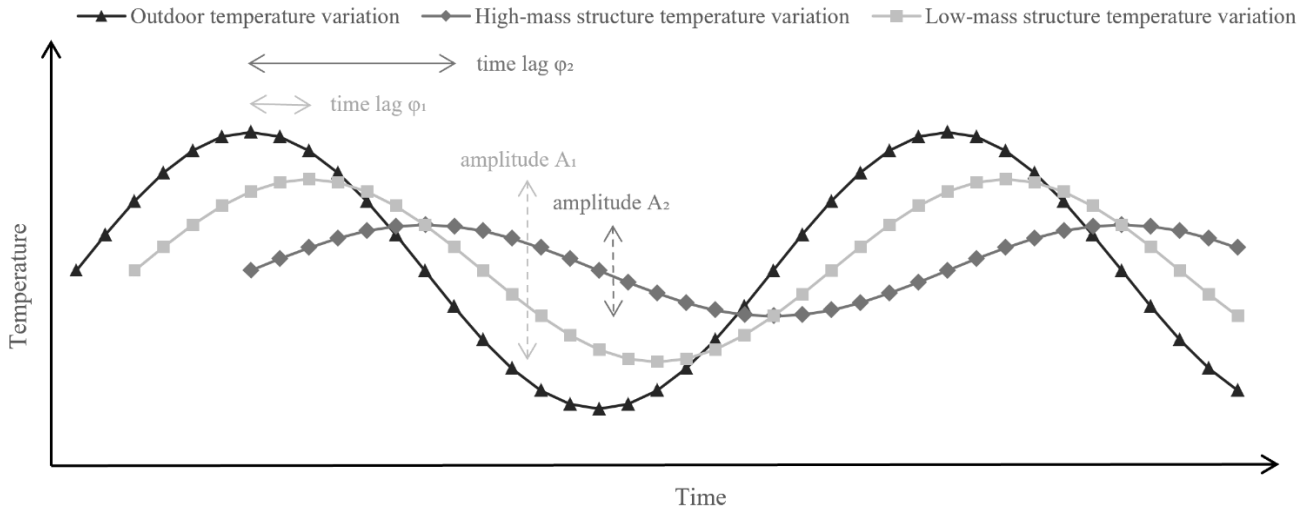

Figure 3. Effects of thermal inertia in a high-mass and a low-mass structure. Based on (Verbeke & Audenaert, 2018).

2.3.1 Categories of Thermal Inertia

Thermal inertia as a scientific term needs to describe or explain heat storage capacity and the speed of the heat storage/release. Heat stored in a material can be either sensible, meaning that the temperature of the material changes, or latent, which is applied with phase change materials (PCMs) (Verbeke & Audenaert, 2018). However, in this study, the focus was on sensible heat storage. The advantages of thermal inertia are also used in part of the thermally activated building systems (TABS), where a hydronic pipe system is embedded in the building structure to lower the heating/cooling load (L.-S. Wang et al., 2014). In this study, however, the focus was on the potential of passive use of this phenomenon.

2.3.2 Physical Metrics

The amount of heat stored/released by the material depends on the temperature difference, density ρ, and specific heat capacity c_p of the material. The rate of heat exchange, on the other hand, depends on the thermal conductivity of the building material λ. High diurnal temperature fluctuation leads to a higher decrease in heat flux, which means that in locations with higher diurnal variability, there is a greater potential for thermal inertia (Verbeke & Audenaert, 2018).
One of the most frustrating facts about this topic is that different authors can define thermal mass differently. The results of their studies can vary because of the lack of a standardized analysis, or a uniform metric. Most of these metrics rely on physics-based equations that are heavily limited with simplified cases and boundary

conditions and cannot account for complex occupant behavior, or effects of solar irradiation (Verbeke & Audenaert, 2018). In the following list, some of the frequently used metrics are described:

a) Thermal capacitance C [J/K] – sometimes it is synonymized with thermal mass (Bergman & Levine, 2019). The same authors mention that thermal mass can also be expressed as a product of mass and specific heat capacity c_p.
b) Volumetric heat capacity – a product of density ρ and the specific heat capacity c_p [J/(m³·K)], it is used to measure the ability of a material to store thermal energy.
c) Thermal diffusivity α [m²/s] – the ratio of the thermal conductivity λ and the volumetric heat capacity ($\rho \cdot c_p$). It is a measure of the speed of temperature change happening through a material. Materials of low thermal diffusivity are characterized by slow reactions to their thermal environment.
d) Thermal diffusivity e [J/(m²·K·s$^{1/2}$)] – it measures the ability of a material to exchange heat with its surroundings. A high thermal diffusivity value means the material can absorb and release heat at a fast pace. Metals are examples of materials of high thermal mass, but low thermal inertia because of their high thermal diffusivity.

There are more similar and related parameters, such as time constant, phase lag, penetration depth, or thermal admittance, which are summarized and briefly explained by Verbeke & Audenaert (2018) and Rüdisser (2018). However, most of these metrics describe properties of a single material, and not for the whole wall/roof/slab assembly.
Standard EN ISO 13786:2017 describes the dynamic thermal performance, including thermal inertia, of building components. Based on the standard, a calculation tool was developed by Rüdisser (2018) to calculate metrics of thermal inertia. According to the tool, the most important metric of thermal inertia is the internal areal heat capacity [J/(m²·K)], a measure of the ability of a material to buffer heat during the diurnal cycle. High internal heat capacity is crucial in avoiding summer overheating, and it has an inverse relationship with indoor temperature variability. The total internal heat capacity is a sum of specific internal areal capacities of materials used in the building, and it is highly dependent on the properties of the innermost building layer. To increase heat capacity, this layer should be characterized by high thermal mass and high thermal conductivity. In other words, dense, uncovered surfaces such as concrete ceilings or stone floors will perform better than suspended ceilings or parquet floors.
With the increase of thermal conductivity, the heat storage capacity increases as well but exhibits diminishing marginal increases. Similarly, there is a maximum critical material thickness until which the heat storage capacity increases, and after which it converges slowly to a constant value (Artmann et al., 2007).

2.3.3 Impacts of Thermal Inertia on Buildings

The benefits of thermal inertia have been used for millennia. For example, in the hot climate of Yemen, vernacular architecture has not changed much over the last centuries, with densely positioned residential towers constructed with thick walls of mudbrick, rammed earth, and stones (Abdallah et al., 2020). The benefits of thermal inertia were studied in the hot semi-arid climate of India (Leo Samuel et al., 2017), and in the tropical climate of Costa Rica (Porras-Salazar et al., 2023). In the Mediterranean climate of Italy, traditional stone houses with walls thicker than 50 cm reach comfortable temperatures during summer and do not require air conditioning, while in winter heating is needed because the indoor temperature is close to the daily maximum outdoor temperature (Cardinale et al., 2013). Recently, technology has been developed where the thermal inertia of water, owing to its great specific capacity, is exploited in window design. Water is filled between two glass panes, and when exposed to the sun, it prevents overheating, while allowing transparent views without the need for shading (Gutai & Kheybari, 2020).

While thermal mass is beneficial for maintaining indoor thermal comfort and reducing energy usage, as evident in historic buildings with thick masonry walls or earth constructions, there are instances where relying solely on thermal mass may lead to undesired outcomes. Such an instance could happen in intermittently used buildings, where it would take some time for the building to reach the desired thermal comfort levels (Karlsson et al., 2013). Similarly, Zhu et al. (2009) warn that although high-mass walls reduce heating demand, in hot desert climates, the cooling demand would increase because of insufficient heat dissipation capacity.
There are conflicting assertions on thermal inertia in the available scientific literature, which is a result of different assessment methods, simulation/calculation assumptions, and climatic conditions. Most authors suggested that high thermal inertia can help achieve indoor thermal comfort. Thermal inertia can exhibit

positive or negative impacts that can be high-pronounced or negligible, depending on the local conditions of ambient air temperature variation, and solar irradiation patterns (Verbeke & Audenaert, 2018).
Buildings with high thermal inertia may reduce heating energy by requiring no heating for several days in a sudden and short cold wave, but only if the stored energy does not need subsequent replenishing. Economically, this could yield savings if heat production is costlier during high-demand cold periods (Karlsson et al., 2013).
One of the issues regarding the residential application of the high thermal inertia concept is that the occupant is not free to rapidly adjust the room temperature, as is possible with active heating and cooling devices (Klein, 2016).

In a study by Feist (2000), it is claimed that the thermal inertia of exterior walls contributes negligibly (less than 0.5 %) to the heating energy reduction, while in interior walls, it is claimed to have a significant influence on temperature stability. Similar results are reported by Long & Ye (2016), where it was determined across various locations in China that thermal conductivity was the key property of exterior walls, whereas thermal inertia was the key property of interior walls.
The thermal inertia of interior finishing materials in Australia and the U.S. was investigated by Taylor & Miner (2014). The study considered thermal mass and price of the material, price of energy, and local climate conditions, combined into a single metric. The results showed that drywall, concrete flooring, and timber paneling were the most effective materials. When only thermal inertia was considered, PCMs, concrete, and clay tiles demonstrated the highest performance. A study by Rodrigues et al. (2016) showed that a super-insulated house in the U.K. had lower overheating hours when mounted with high-density fiberboard and PCMs, in comparison to plasterboard.

In a study by Norén et al. (1999), three simulation tools were used to determine the effect of thermal inertia on the building energy use of a small residential building in Stockholm. Consistently, the results have shown that high-mass exterior wall construction (concrete and brick) led to lower energy use than the low-mass timber-stud exterior wall. In the middle of energy performance, there was a mid-weight wall constructed with solid massive timber panels. The heating energy requirement for the high-mass wall ranged from 59 % to 86 % of the low-mass wall, depending on the simulation tool. In comparison, the heating energy requirement of a massive timber wall was between 75 % and 88 % of the low-mass wall, indicating that increasing the thermal mass on the interior side of the wall could lead to energy savings.
In a simulation of a simplified room model of an office building in China by Yang & Li (2008), it was found that high thermal mass (expressed as a time constant above 400) coupled with night ventilation could reduce cooling load by 60 %. It was also found that the cooling load is decreased the most when the thermal conductivity values of the external and internal wall layers are identical.

2.4 Natural Ventilation and Indoor Climate

Indoor climate, comprising factors such as indoor air quality, temperature, light, and humidity, is both a comfort and a health issue (Kreiger & Srubar, 2019). HVAC systems are often used to achieve indoor climate targets, but at least some factors can be satisfied with natural ventilation.

2.4.1 Natural Ventilation

Energy-intensive air-conditioning is becoming more common in the residential sector. The electrical appliances and insufficiently or poorly scheduled window openings, not the solar gains, are the main driving forces of the total internal heat gains. Effective use of natural ventilation has a great potential to reduce mechanical ventilation use – in Denmark, this was calculated to be up to 90 % during summer (Oropeza-Perez & Østergaard, 2014). Another study in Denmark showed that CO_2 concentration was the most important variable determining the probability of window opening in bedrooms, while indoor relative humidity determined the most whether windows would be opened in living rooms (Andersen et al., 2013).
Ventilation rates above 0.5 air changes per hour in Nordic residential buildings are associated with reduced health risks in children (Sundell et al., 2011). Relative humidity above 40 % is vital for the functioning of mucous membranes in human bodies, as dry air is associated with irritations of the eyes, nose, and throat (Wolkoff, 2018a).

A study by Salvalai et al. (2013) analyzed cooling strategies in representative European climates. The conclusions were that in Northern Europe, natural ventilation ensures high comfort levels; in Central Europe, there is a potential for improvement, e.g. by increasing the air change rate, or by formulating a different algorithm for window opening; and in Southern Europe, there is a low cooling potential by natural ventilation because the ambient temperature is too high, while the diurnal temperature variation is too low. The authors suggested a certain viability threshold of natural ventilation, defined as when the mean ambient temperature is below 18 °C for at least 70% of the overall hours, from May to September.
Based on the investigations of three dwellings in Denmark, Germany, and Austria, window opening was crucial in maintaining indoor thermal comfort. Night cooling was a sufficient strategy to counter the risk of overheating in rooms with the highest solar gains. Overheating episodes during summer afternoons were exceptionally rare, yet their infrequency led to them being considered insignificant. The authors advised that concerns with privacy, safety, and noise should be taken into design consideration, as it may affect the willingness of the occupants to open the windows/doors (Foldbjerg et al., 2014). In Nordic regions, the outdoor pollution and noise levels pose no constraints to window opening (Andersen et al., 2013).

2.4.2 Indoor Climate

Carbon dioxide concentrations that are less than 700 parts per million (ppm) higher than the ambient outdoor air (currently around 420 ppm) result in around 80 % of occupants judging the air odor as acceptable (Persily, 2022). Although a CO_2 concentration metric for assessing indoor air quality may seem appealing due to its simplicity, numerous other indoor air pollutants have greater health and comfort implications (World Health Organization, 2010). Some of them include mold, particulate matter, radon, nitrogen dioxide, and volatile organic compounds (Cony Renaud Salis et al., 2017). Additionally, many of these pollutants correlate poorly with indoor CO_2 concentrations (Persily, 2022).

Moisture safety, often associated with resistance to the growth of mold and other microorganisms, is an important aspect of building design. Careful design prevents air-transported moisture as the main type of moisture transport. Other types include capillary action, bulk movement, and vapor diffusion through the building enclosure. Hygrothermal properties of materials, such as thermal conductivity or diffusion resistance, are both temperature and moisture-dependent (Medved, 2022). The values used in many building performance simulations are static, but in reality, their nature is dynamic.

Moisture storage, or moisture buffer capacity, denotes behavior in hygroscopic building materials where moisture is adsorbed when ambient air humidity levels are high, whereas it is released when relative humidity is lower (Zu et al., 2020). This phenomenon is useful because it regulates excess or deficient moisture levels without the need for mechanical (de)humidification. The moisture buffer value of a material depends on its density, hygroscopicity, and vapor permeability. The moisture buffering capacity can be negligible, limited, moderate, good, or excellent, based on the NORDTEST method (Peuhkuri et al., 2006). According to this classification, hemp-lime concrete and flax lime concrete display ”excellent” moisture buffer values (above 2.0 g/($m^2 \cdot \%_{RH}$)), unlike plaster, brick, or concrete, which all have reduced buffering capacities (Rahim et al., 2015). It needs to be emphasized that the buffering value is significantly diminished (by around 60 %) when hemp is covered with plaster, plasterboard, or paint unless lime plaster is applied (10 % reduction). This means that the moisture buffer value of such assemblies is reduced to the ”good” category (Latif et al., 2015). Moisture accumulation in hygroscopic materials during the heating season leads to the release of energy via condensation, which can yield lower heating energy requirements if a control strategy is provided. Similarly, in the cooling season, evaporation of water from the hygroscopic material can reduce cooling energy by 10 % to 30 %, depending on occupancy and building location (Osanyintola & Simonson, 2006). Energy saving potential is more pronounced in colder and drier climates (Zhang et al., 2017).

2.5 Thermal Comfort

Human thermal comfort is reached when in thermal equilibrium, which can be defined by a general comfort equation (Fanger, 1973). Fanger’s work was the base for the development of standards ISO 7730-1984 and ASHRAE 55-1992, where it was stated that the operative temperature range should be between 20 °C and 24 °C during the heating season, and between 23 °C and 26 °C during the cooling season. The proposed steady-state thermal comfort model is described by indoor air temperature, air velocity, humidity, mean radiant temperature, occupants' clothing, and activity level. It accurately predicts comfort in predictable, mechanically

conditioned spaces. However, it cannot take into account variable occupant behavior, and the transient state of naturally ventilated spaces (J. F. Nicol & Humphreys, 1973). Nicol and Humphreys found that indoor thermal comfort in free-running buildings is a function of indoor operative temperature. They proposed the adaptive thermal comfort model (J. F. Nicol & Humphreys, 2002).

2.5.1 Adaptation to the Environment

The adaptive model is used because people are capable of adapting to the variable environment. There are three thermal adaptive principles: physiological, behavioral, and psychological (IEA EBC Annex 69, 2020). Physiological adaptation is the unconscious adjustment to fluctuations of the ambient environment, including vasoconstriction/vasodilation, sweating, and shivering. The human body acclimatizes when repeatedly exposed to conditions outside the comfort range. Extreme and rapid temperature changes can be potentially dangerous to humans, whereas slow and gradual change is perceived naturally. Behavioral adaptation includes adjustments of activity level, clothing, and the indoor environment (opening windows), thereby regulating the rates of indoor heat generation and bodily heat loss.
Psychological adaptation, the least researched of the three mechanisms, shows that perception of a higher degree of control leads to a higher degree of satisfaction with the conditions and an acceptance of a wider range of indoor temperatures. There are also social factors and factors related to expectations and environmental attitudes, that may determine the adaptive potential of an individual. Apart from potential energy savings from accepting a varied indoor temperature range, a benefit to overall health and well-being is reported in contrast to thermal monotony associated with HVAC systems (IEA EBC Annex 69, 2020).

2.5.2 Adaptive Thermal Comfort Model

The European standard EN 15251 (withdrawn, today replaced by EN 16798-1:2019), encompassing thermal comfort in free-running buildings, was derived from the work by F. Nicol & Humphreys (2010). Free-running buildings were defined as those where no energy is being used either for heating or for cooling. The use of ventilating ceiling fans was still considered to be a free-running building. In a free-running building, the indoor temperatures are subject to change, and so the comfortable temperature is also dynamic.
In the standard, comfortable/neutral temperature is the operative temperature at which the largest share of occupants is at comfort, which is defined as persons who are "slightly cool", "neutral", or "slightly warm". The daily, exponentially weighted running mean temperature is used for calculating the neutral temperature. When compared to ASHRAE 55, it is shown that, while similar, they are in the end different for many reasons, whether by approach, databases used, or building classifications, and therefore not commensurate. The authors believe the procedure for derivation of the neutral temperature is more accurate and advanced than the one used in ASHRAE 55. Since European case studies were analyzed in the making of the standard, EN 15251 was deemed more appropriate for European buildings (F. Nicol & Humphreys, 2010).
In the adaptive thermal comfort model from the standard EN 16798-1:2019, there are three categories of thermal comfort (I – III, I being the highest level of comfort, and III being the lowest).
The limits of the categories are defined by the exponentially weighted running mean of the daily outdoor temperature, as formulated in Equation 1:

$$\Theta_{rm} = (1 - \alpha) \cdot (\Theta_{ed-1} + \alpha \cdot \Theta_{ed-2} + \alpha^2 \cdot \Theta_{ed-3}) \quad (1)$$

where

Θ_{rm} is the outdoor running mean temperature for the considered day [°C],
Θ_{ed-1} is the daily mean outdoor air temperature for the previous day [°C],
Θ_{ed-i} is the daily mean outdoor air temperature for the previous day i [°C], and
α is a constant between 0 and 1 (the recommended value is 0.8).

In Table 1, the limits of the categories are described as formulations of indoor operative temperature, Θ_o.

Table 1. Categories of thermal comfort as defined in the standard EN 16798-1:2019.

Category I	Upper limit	$\Theta_o = 0.33 \cdot \Theta_{rm} + 18.8 + 2$
	Lower limit	$\Theta_o = 0.33 \cdot \Theta_{rm} + 18.8 - 3$
Category II	Upper limit	$\Theta_o = 0.33 \cdot \Theta_{rm} + 18.8 + 3$
	Lower limit	$\Theta_o = 0.33 \cdot \Theta_{rm} + 18.8 - 4$
Category III	Upper limit	$\Theta_o = 0.33 \cdot \Theta_{rm} + 18.8 + 4$
	Lower limit	$\Theta_o = 0.33 \cdot \Theta_{rm} + 18.8 - 5$

It should be noted that the categories in the standard are prescribed only for the running mean outdoor air temperature in the range of 10 °C to 30 °C. When plotted on a chart, the limits of the categories are shown in Figure 4.

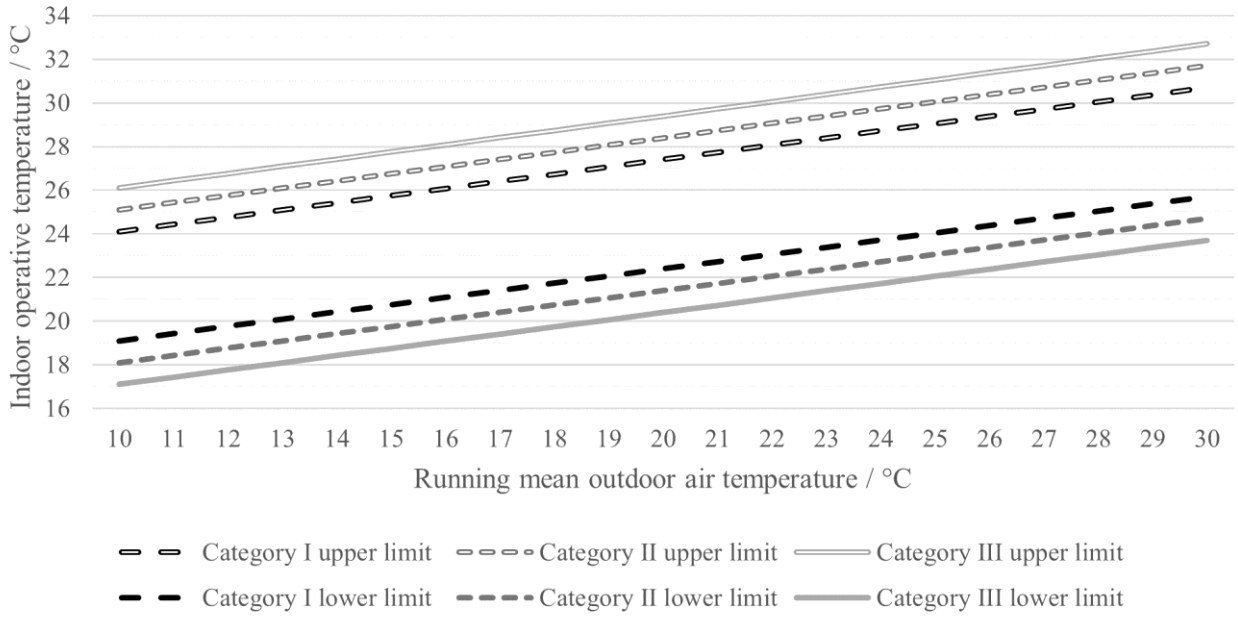

Figure 4. Limits of thermal comfort categories of the adaptive thermal comfort from the standard EN 16798-1:2019.

2.6 Future Climate Weather Files

Not considering the effects of future climate can result in overlooking the opportunity for significant improvements during the building design optimization (Zou et al., 2021) When more future climate scenarios are considered, a more robust solution is provided. It was demonstrated that those design options that considered only one weather file were not close to the Pareto optimum front, meaning that they showed a higher risk of maladaptation to potential unforeseen vulnerabilities of the future climate (Chen et al., 2024). Relying solely on typical or observed extreme conditions may fail to anticipate critical peak load increases, posing risks to the climate resilience of buildings and energy systems, as the production capacity of power plants can be significantly affected in the extreme period. Peak cooling loads during near-future extreme conditions can be significantly higher compared to typical conditions, up to 28.5% in some of the representative building cases (Moazami et al., 2019).

The synthetization of future weather files starts from complex climate models. General Circulation Models (GCMs) are modeled based on the Representative Concentration Pathways (RCPs) introduced by the IPCC in 2011 (Van Vuuren et al., 2011). The GCMs are characterized by a low spatial and long temporal resolution. To generate local, hourly values for building performance simulation, the GCMs need to be downscaled. The

downscaling process can be either static, dynamic, or hybrid.
Uncertainties can easily proliferate in this process, as GCMs are generated under various climate assumptions and modeled independently in many government and university institutions (Moazami et al., 2019). The limited value of GCMs is also raised by Hansen et al. (2023), where it is shown how overreliance on GCMs in IPCC reports results in understated effects of human-made climate change. Usually, GCMs based on IPCC reports assume linear instead of accelerated global warming. Similarly, the issues of scientific reticence in climate science and hesitant communication about outcomes worse than initially imagined are provided by Hansen (2007) and Anderson (2015).

Morphing is a deterministic statistical downscaling method, whereby hourly values of weather variables are either shifted, stretched, or both, depending on the type of the variable. Shifting and stretching are additive or multiplicative algorithms. CCWorldWeatherGen and WeatherShift are two common morphing tools.
While morphing is the simplest option, it also has drawbacks in accuracy and consistency caused by the independent statistical changes of the variables that are mutually interconnected. Future weather extremes cannot be modeled with this method.
Stochastic generation is a statistical downscaling method, whereby future weather data is interpolated based on a few weather variables stemming from historic climate data. Meteonorm is a commonly used tool that applies the stochastic method. The advantages of stochastic models are a simulation of a wide range of possible climate conditions and a simulation of future extreme weather conditions. The disadvantage of stochastic models is that it is inherently constrained by the available historical data.
Dynamic downscaling provides physically consistent data across all changed weather variables but comes at a cost of high computing power, large datasets required, and high expertise to generate and understand the model. Weather files generated through dynamic downscaling, accounting for both typical and extreme conditions, are deemed the most reliable for assessing energy resilience under future climate uncertainties.

3 Case Study Building: 2226

In the following sections, the case study building was explored. Named “2226”, and located in the Alpine region of Austria, it was regarded as an interesting and suitable case study, since it is a well-known and well-publicized project, meaning that detailed information about it is readily available; it is located in a temperate climate that is comparable to the southernmost parts of Scandinavia; it is the first well-researched and successfully operated free-running building in such a climate; and it lays claims on being resilient and sustainable.

3.1 General Information

The first building designed and built under the 2226 concept by the architectural studio Baumschlager Eberle stands completed and in operation since 2013 in Lustenau, Austria, near the border with Switzerland. The name is derived from the idea that indoor air temperature can always be within the range of 22 °C and 26 °C, without conventional heating, cooling, and mechanical ventilation. Instead, the building is equipped with sensors that track temperature and CO_2 levels and are connected to an automated building ventilation system (Junghans & Widerin, 2017).
To achieve that goal, the design team utilized high thermal inertia of building components, low transmittance building enclosure, and automated natural ventilation through window opening vents as main passive design strategies.
The building is used mainly as the studio’s open-plan office, but it also houses a café bar, a library, and an art gallery, with potential residential spaces on the highest floors (Klein, 2016). It is a six-story building of compact, cubic shape, with dimensions of approximately 24 m × 24 m × 24 m, as shown in Figure 5.

Figure 5. Building 2226 in Lustenau, Austria. Photograph by Eduard Hueber/archphoto. ©Baumschlager Eberle

3.2 Site and Local Climate

Lustenau is a small town in the Austrian state of Vorarlberg, located in the Austrian Alps, in the valley of the river Rhine, as shown in Figure 6. The 2226 building lies in the town outskirts, surrounded by commercial buildings and single-family houses.

Figure 6. Location of 2226 office building by Baumschlager Eberle in Lustenau, Austria.

The closest available climate data is from the nearby town of Dornbirn, less than 10 km from Lustenau. As depicted in Figure 7, there is a pronounced seasonality, with cold winters and warm summers. The average annual air temperature is 9.6 °C, and the average air relative humidity is 78.4 %. February is the coldest month, with the average temperature just above 0 °C, and the warmest month is July, with the average temperature of 18.7 °C. Cold months are the most humid, and the least humid are the transitional months, although the monthly average never drops below 68 %.

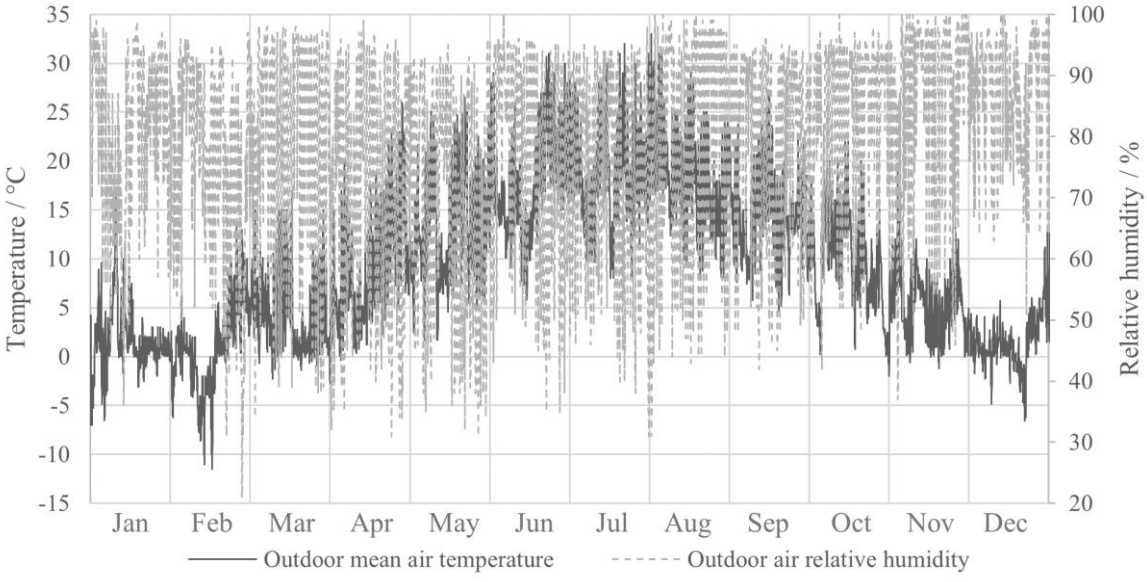

Figure 7. Typical Meteorological Year (TMY) of Dornbirn, Austria, based on climate data 2007 – 2021.

3.3 Building Design and Materials

The floors are organized in a pinwheel shape, with four equally sized rooms occupying corners on each floor. Internal cores contain an elevator, toilet, and staircase. Figure 8 depicts a typical floor plan and a vertical section. The ground floor has a floor-to-ceiling height of more than four meters, while other floors have a floor-to-ceiling height of 3.4 m. That has proven beneficial for natural ventilation, as further explained in the section 3.5.

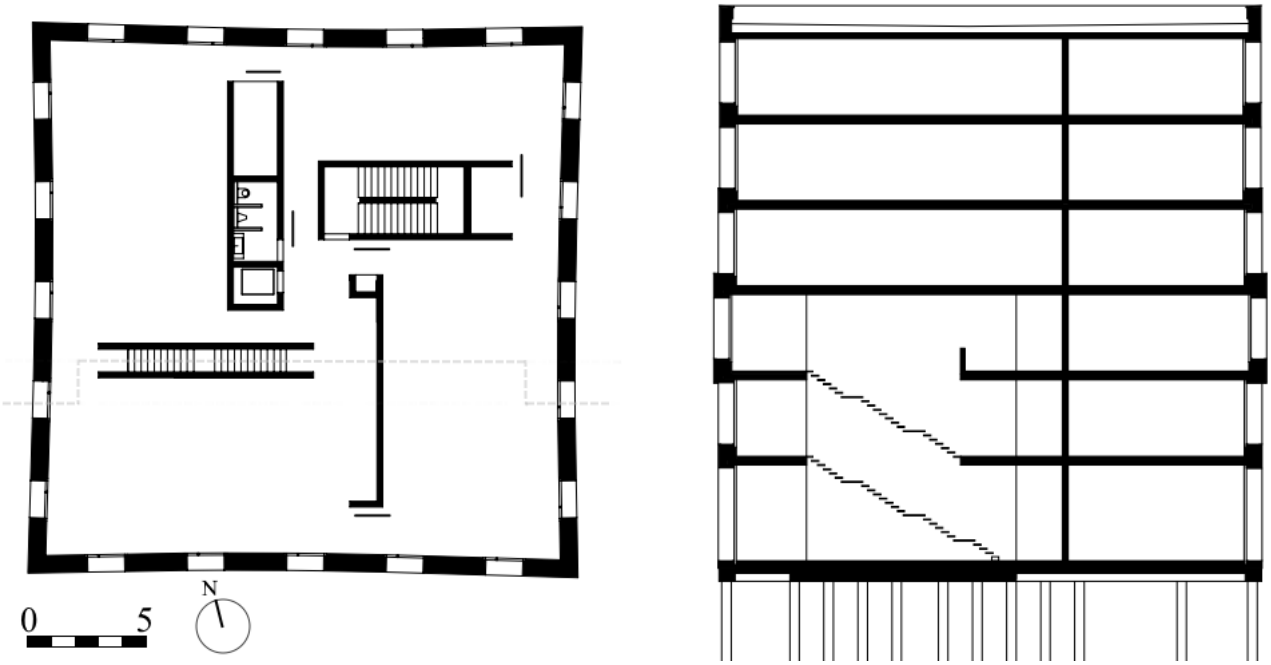

Figure 8. Typical floor plan (left) and vertical section (right) of the 2226 building in Lustenau, Austria. Sourced from (Klein, 2016).

In Table 2, the dimensions of the building are listed.

Table 2. Area and volume metrics of the 2226 building in Lustenau, Austria. Sourced from (Klein, 2016).

Gross floor area / m²	3 201	**Gross ground floor area / m²**	532
Net floor area / m²	2 700	**Enclosed space volume / m³**	13 158

The materials used in the building have a high thermal mass and a high thermal resistance. Two main construction materials are extruded masonry bricks in walls, and concrete in floor slabs. Concrete is not used in walls, which is made possible by thick and high load-bearing brick blocks with great compressive load resistance. The total thickness of the external walls is 81 cm.
Typical thermal insulation materials are only used beneath the ground floor slab and the foundations, as well as on top of the roof slab.
Windows are regularly and identically placed on every floor and every facade. Each room has the same number of windows. Window-to-wall ratio is around 16 % (Junghans & Widerin, 2017). Although that may cause sufficient daylight levels in the Austrian context, it would have to be further examined how well-lit the rooms would be in the Nordic locations. On the one hand, daylight illuminance is more important in the working environment, which implies that perhaps this window-to-wall ratio would still be adequate for residential purposes. On the other hand, a simple calculation shows that the glass-to-floor ratio is on average around 12 %, achieving compliance with the Swedish *Boverket* regulations of above 10 % (Bournas, 2021). Nonetheless, daylight performance can be of importance because it can significantly affect electric lighting use. Each window is deeply recessed on the interior side of the external wall. No shading devices were constructed, as the windows are adequately shaded by the wall's thickness (Junghans, 2016).

In Table 3, the thermal properties of the building enclosure are listed. The value of the thermal bridge is a provisional one used by Baumschlager Eberle in their simulations.

Table 3. Thermal properties of the building opaque and transparent assemblies. Sourced from (Junghans & Widerin, 2017).

External wall *U*-value / W/(m²·K)	**Roof *U*-value / W/(m²·K)**	**Window glazing *U*-value / W/(m²·K)**
0.127	0.109	0.700
Infiltration $ACH_{50\ Pa}$ / 1/h	**Thermal bridge / W/(m²·K)**	**Window *g*-value**
0.510	0.030	0.550

A detailed look into the section offers insight into the wall: it is composed of two vertical layers of extruded brick, a layer of mortar in between (10 mm), and lime plaster on the interior and exterior side finishing (both 20 mm). As seen in Figure 9, the two layers of brick blocks are offset vertically by half a block module, as it significantly minimizes the thermal bridging caused by the more conducting mortar joints (Fannon et al., 2021). The interior layer of bricks has higher load-bearing properties, whereas the exterior layer has more insulating properties.

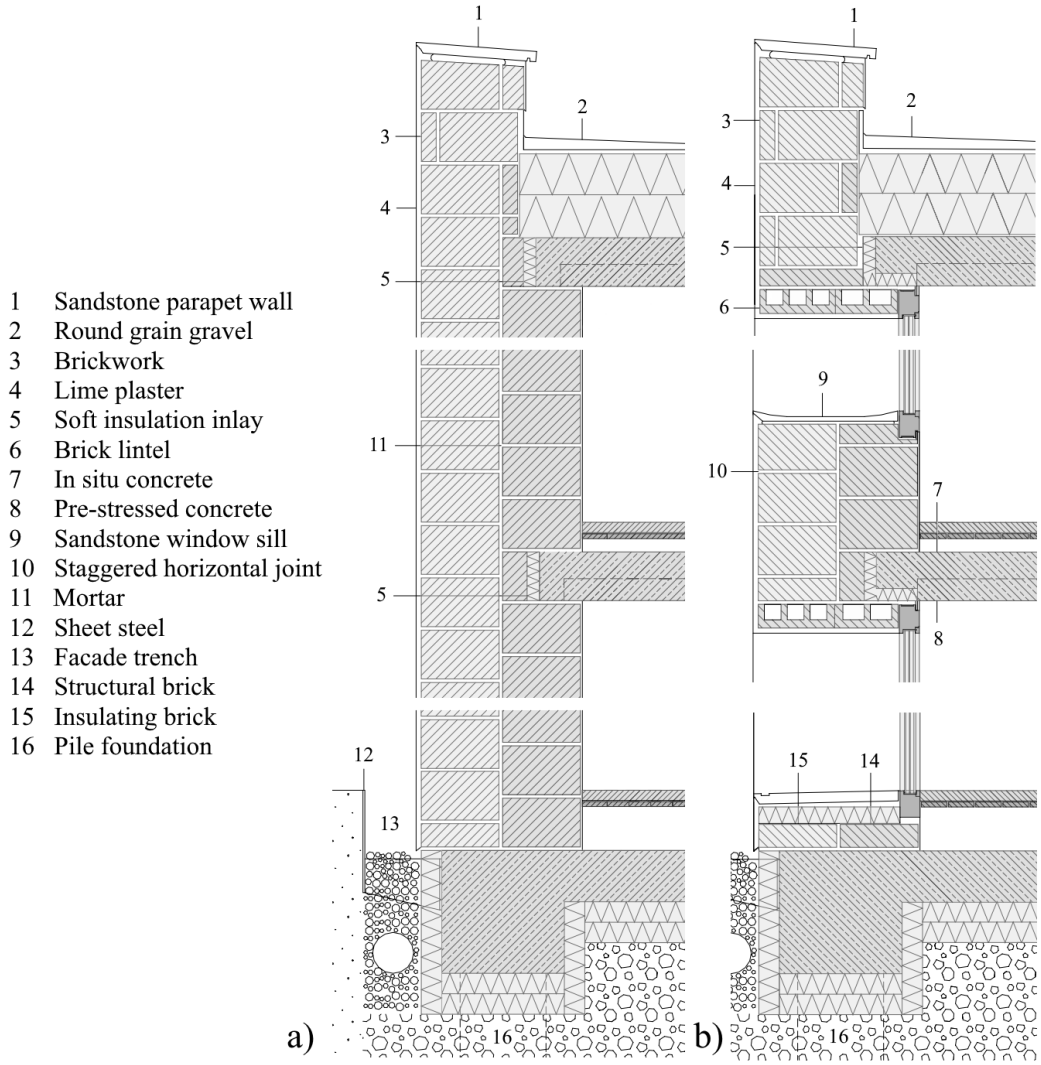

Figure 9. Detail of the external wall and window. Sourced from (Klein, 2016).

Both types of brick blocks are mass-produced by Wienerberger, one of the world's largest clay brick and clay tile manufacturers (Fannon et al., 2021). The load-bearing type is a model Porotherm 38 Plan (*Porotherm 38*

Plan, 2023), and the insulating type is a model Porotherm 38 H.i Plan (*Porotherm 38 H.i Plan*, 2023). They are equal in size, having a thickness of 38 cm. Figure 10 depicts the two block types.

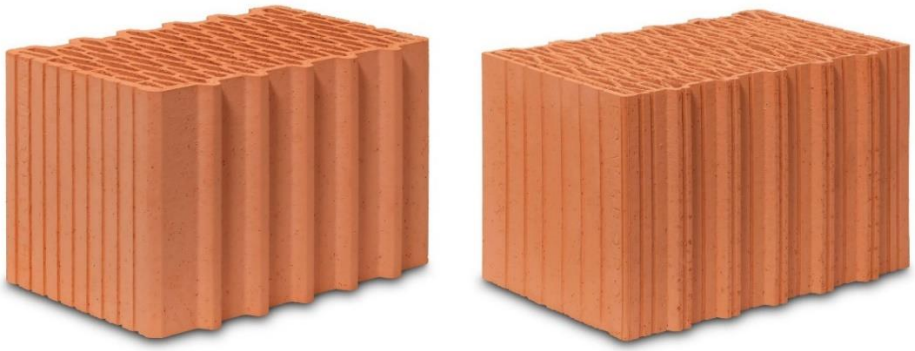

Figure 10. Porotherm 38 Plan (left), Porotherm H.i 38 Plan (right). © Wienerberger Österreich GmbH

The vertical perforations inside the bricks contribute to the lower overall mass while increasing thermal resistance by trapping air inside them (Fannon et al., 2021). Table 4 provides an overview of the thermal properties of the materials in the exterior wall.

*Table 4. Thermal properties of the exterior wall layers, starting from the interior towards the outdoors. Sourced from (*Porotherm 38 Plan*, 2023), (*Porotherm 38 H.i Plan*, 2023), and (MASEA, 2024).*

Layer	**Thermal conductivity / W/(m·K)**	**Density / kg/m³**	**Specific heat capacity / J/(kg·K)**
Lime gypsum plaster	0.490	1200	790
Porotherm 38 Plan	0.112	745	1000
Mortar	0.800	1800	790
Porotherm 38 H.i Plan	0.090	650	1000
Light mortar plaster	0.400	800	790

3.4 Thermal Inertia of 2226

In a study by Hugentobler et al. (2016), the thermal inertia of the 2226 building is explained through metrics of thermal diffusivity α, and thermal phase lag φ. The indoor concrete slab of 24 cm and the anhydrite floor are uncovered to facilitate their great thermal mass (Junghans & Widerin, 2017). In Table 5, the thermal diffusivity and thermal time lag of the external wall layers are presented.

Table 5. Properties related to thermal inertia in the external wall layers, starting from the innermost one.

Layer	**α / Mm²/s**	**φ / h**
Lime gypsum plaster	0.52	0.2
Porotherm 38 Plan	0.15	266.8
Mortar	0.46	0.1
Porotherm 38 H.i Plan	0.14	289.7
Light mortar plaster	0.63	0.2

As shown in Figure 11, the heat storage rate is observed in the same room, once on a typical winter day, and once on a typical summer day. It is noticeable how in cold months less heat is stored and dissipated, but in both periods the storage takes place during the day, and heat dissipation occurs during the night.

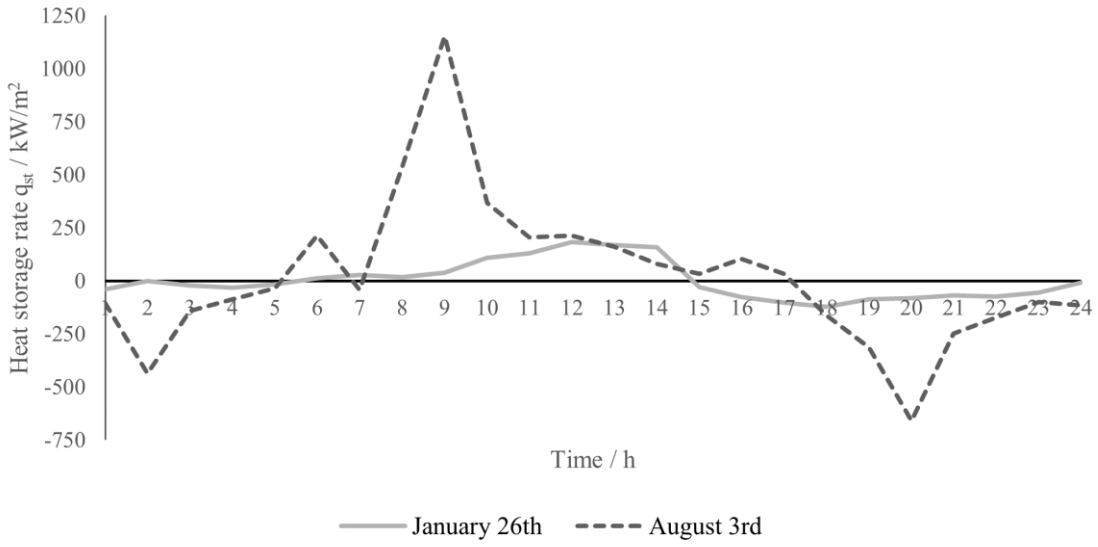

Figure 11. Daily heat storage rate of a room in the 2226 building in Lustenau, Austria, shown in two seasons, based on a recreated simulation model of the building.

The internal areal heat capacity of the exterior wall, calculated by the tool provided by Rüdisser (2018), is 35.6 kJ/(m²·K). The value could have easily increased to more than 40 kJ/(m²·K) just if a slightly different plaster were applied. This indicates that further improvements to the 2226 concept are possible.
The internal areal heat capacity of the interior wall is 33.4 kJ/(m²·K), for the floor slab it is 42.5 kJ/(m²·K) as a floor, and 78.7 kJ/(m²·K) as a ceiling, while for the roof it is 78.3 kJ/(m²·K).

3.5 Natural Ventilation and Sensor-based Controls

There is an obvious concern about balancing the need for fresh air and conserving indoor heat. Optimized natural ventilation allows for minimal heat losses (or undesired gains during summer) as the ventilation period is kept as brief as possible, around 15 – 20 minutes at a time, due to the vertically arranged window openings that were found to have the greatest ventilation efficiency. The computer system controls the natural ventilation openings via sensors, in response to the indoor carbon dioxide concentration, indoor and outdoor temperature levels, and occupant demands. An on-off controller with a death band (DB), or a hysteresis controller, actuates the natural ventilation openers (Junghans & Widerin, 2017). The control system consists of room sensors, motorized actuators at the window openings, a weather station on the roof, and a facility server gathering and evaluating sensor data (Klein, 2016). The system setup allows for separate room treatment, as well as user override, further enhancing indoor comfort potential. Figure 12 shows natural ventilation openings integrated with windows.

Figure 12. Interior of the architecture office in the 2226 building in Lustenau, Austria. Photograph by Eduard Hueber/archphoto. ©Baumschlager Eberle

The system is activated when the CO_2 level exceeds 1 200 ppm, or when the room air temperature exceeds 26 °C (as long as it is lower than the outdoor air temperature). The system is closed if the CO_2 concentration falls below 800 ppm, or when the room air temperature does not meet at least 22 °C. The simplified full depiction of the automated opening/closing algorithm is shown in Figure 13.

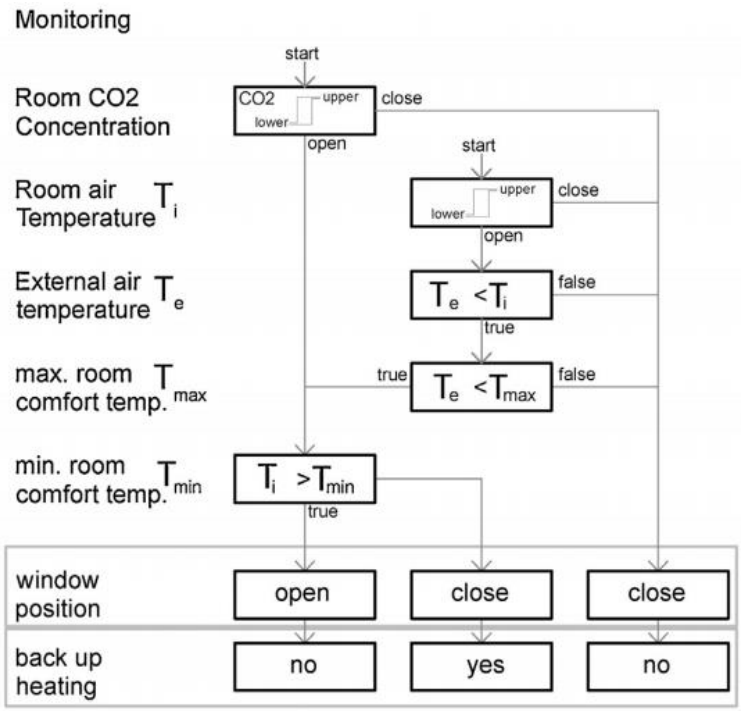

Figure 13. Automated natural ventilation algorithm in 2226 building. Sourced from (Junghans & Widerin, 2017).

Measurements of CO_2 levels are important as they prevent unnecessary window openings when the occupants are not present, thereby accounting for their dynamic behavior (Klein, 2016). In the cooling season, night ventilation is used. The system is activated if the external temperature is below 26 °C, or if a high indoor temperature is expected for the next day.

Significant room height is also essential, as it allows for less frequent window openings while maintaining fresh enough air. The stratification effect of the accumulated carbon dioxide is exploited, as the CO_2 concentration does not increase uniformly in the room (Klein, 2016), (Bulińska et al., 2014). It acts much like warm air, concentrating primarily towards the ceiling, as shown in Figure 14.

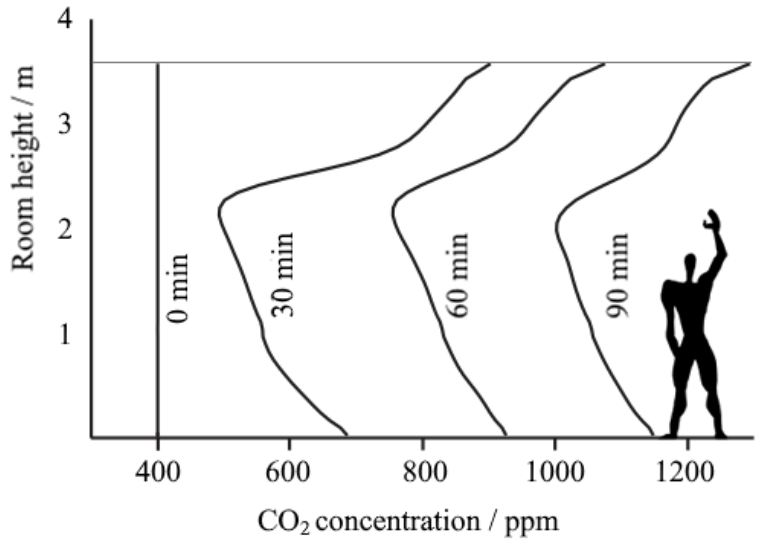

Figure 14. CO_2 concentration at different room heights as a function of time. Modified graphic from a computational fluid dynamics simulation by (Klein, 2016).

That means that the CO_2 concentration in the occupied area (lower part of a room) increases more slowly than the overall room CO_2 concentration, which is conventionally calculated with the assumption of a uniform distribution. The real threshold value is then exceeded later, saving more indoor heat.
Geometry and design of natural ventilation openings significantly influence CO_2 distribution. A computational fluid dynamics simulation may be necessary for each case if one wants to determine the exact distribution scenario (Bulińska et al., 2014).

3.6 Energy Performance of 2226

The annual total energy consumption by the 2226 building is around 38 kWh/m² (Klein, 2016), while Maierhofer et al. (2022) report a similar value of 41.1 kWh/m² of the gross floor area. During winter vacations, it was observed that the room temperature dropped to below 21 °C, due to decreased internal gains from the appliances (Hugentobler et al., 2016). This period and similar occurrences of extremely cold waves were countered by leaving the lighting switched on overnight (Junghans & Widerin, 2017).

3.7 Thermal Comfort and Indoor Climate of 2226

An empty 2226 building set in Lustenau, Austria, would still follow the external temperature fluctuations, but with a temporal offset, due to the high thermal inertia of its materials. The indoor temperature amplitude did not decrease as much compared to the outdoor temperature amplitude. This time lag may be up to two months in duration. The temperature fluctuation indoors was approximately ± 10 °C (Klein, 2016).
With internal gains from occupants, lighting, and appliances included, but without a control system, the room temperature range was steadily between 18 °C and 28 °C. The remaining temperature fluctuation was still approximately ± 5 °C. When the ventilation/cooling automated control system was introduced, the range between 22 °C and 26 °C was successfully achieved, with a fluctuation of just ± 2 °C.

The adaptive thermal comfort model was used for the evaluation of the indoor climate (Junghans & Widerin, 2017). The results for the cold season showed that the room temperature never went below the required minimum of 20 °C. The carbon dioxide levels shortly exceeded 1 200 ppm. It was claimed that this, however, was in line with the ASHRAE 62.1-2010 standard. Internal gains of around 8 W/m² for lighting and 12 W/m² for appliances were found to be sufficient in increasing the indoor temperature to the required level (Klein, 2016). In summer, during limited periods of extremely warm weather (temperatures above 35 °C), the

maximum room temperature of 26 °C was exceeded. Room temperature stayed above 26 °C even after a drop in outdoor air temperature in the following days. This was explained as a result of the high internal mass in the concrete ceiling. However, for the majority of the cooling season, the room temperature was within the required limits. The carbon dioxide levels during summer were always below 1 000 ppm.

It was shown that in the adaptive thermal comfort model, only for an inconsiderable amount of time has there been an exceedance of the upper-temperature limit for 80 % satisfaction (4 hours in a year), and around 30 hours of upper limit exceedance for 95 % predicted satisfaction. When surveyed, the occupants reported the room temperature was either "ok" or "slightly too cold" in winter, the latter being usually in the morning. One of the responding occupants said they had used a personal heater.
During summer, more occupants reported room temperature as "ok" than as "slightly too warm". On the warmest days of the year, the majority reported "slightly too warm", meaning that the room temperature was suboptimal in that period. There had been no occupant complaints about the indoor air quality, indicating that the short periods of increased CO_2 concentration were acceptable. The overheating could have been prevented with a higher degree of window opening, and placement of shading devices (Junghans & Widerin, 2017).

Radiant temperature asymmetry was measured, and reported as practically non-existent, owing to the great thermal inertia of the walls. During summer, it was observed that the rooms facing west registered a 1 °C higher air temperature (Hugentobler et al., 2016). After the building's completion, curtains were added to certain windows to prevent overheating during the summer. No occupants have experienced discomfort due to the cold air draft at either the ventilation openings or the large windows (Junghans, 2016).

Indoor relative humidity was always maintained in the range of 35 % – 60 %, as measured over two years of building operation (Hugentobler et al., 2016). This is close to the ideal range of 40 % – 60 %, where respiratory issues, microbial growth, and allergic reactions are least likely to occur.
The authors emphasized this as one of the most noteworthy qualities of this building, unlike in many other energy-efficient buildings, where occupants reported chronic problems with dry air that often had to be balanced with active humidification systems (SECO, 2010), (Wolkoff, 2018b). The explanation for this behavior is twofold: on the one hand, the building layers are permeable and allow for indoor-outdoor moisture transport. On the other hand, bricks were highlighted as a high moisture capacity material, meaning that they could delay and regulate humidity change. The simplified behavior of relative humidity in hygroscopic materials exhibits an inverse sinusoidal relationship with temperature observed in the same material (Cascione et al., 2021), as shown in Figure 15.

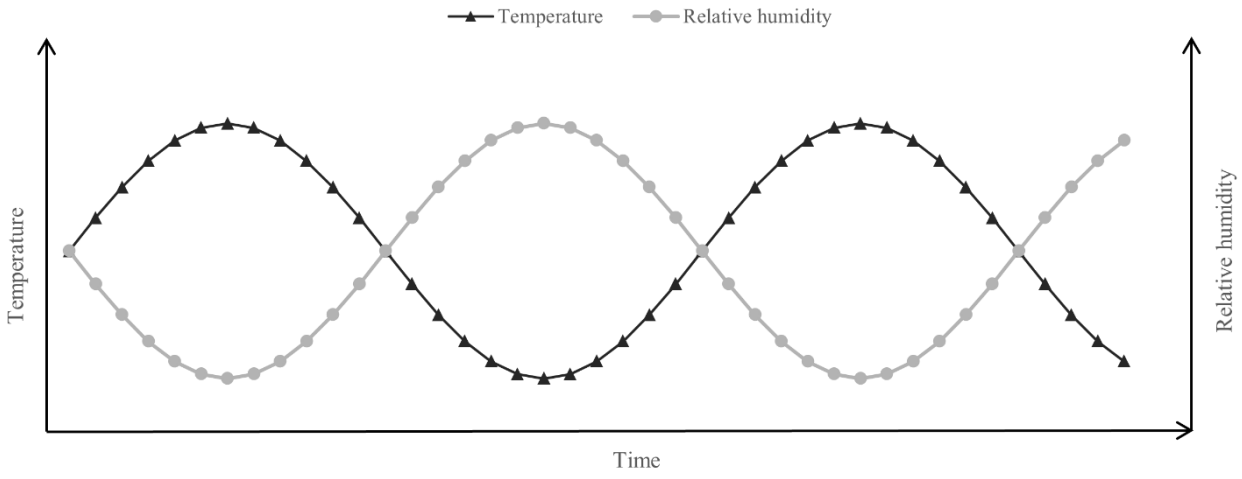

Figure 15. The simplified sinusoidal behavior of indoor temperature and indoor relative humidity in assemblies with thermal inertia and moisture buffer capacity. Based on the study by (Cascione et al., 2021).

The measurements conducted by Hugentobler et al. (2016) demonstrated the impact of moisture inertia between outdoor and indoor air humidity, persisting for several weeks between their peaks. Additionally, the total bacterial count (bacteria, mold, and yeast) was sampled and measured. The results showed a remarkably low bacterial count, but no explanation for such a good performance was offered.

3.8 Environmental Aspects of 2226

A life cycle assessment of the 2226 building was conducted in 2022, according to the EN 15978–1:2021 standard (Maierhofer et al., 2022). For modules A1 – A3, B4, C1, C3, and C4 (which are related to product stage, use stage, and end-of-life stage, respectively), quantities were obtained by the BIM model of the building. The operational energy had been evaluated according to modules B6.1 – B6.3, with the functional unit being 1 m² of the gross floor area of an office building. Construction stage modules A4 and A5 used data obtained from other literature sources.
The reference study period was 60 years, with the assumption of constant energy demand and a constant energy mix throughout the observed period. However, the architects claim the building will stand for 200 years (Klein, 2016), indicating that the share of operational energy in total environmental impact would significantly increase.

Two-thirds of embodied GHG emissions were found to be caused by modules A1 – A3, the majority of which were caused by brick and concrete production. However, when total GHG emissions were analyzed, it was calculated that operational energy use was responsible for 67 % of emissions during the whole life cycle.
The authors of the study compared the 2226 building with high-performance, nearly zero-energy (nZEB) buildings studied earlier (Röck et al., 2020). It was concluded that the 2226 building was close to the median of the studied group in regards to the embodied GHG emissions.
Despite eliminating HVAC systems, there was no reduction of embodied emissions compared to concepts with similar ambitions, as the savings from HVAC abandonment appeared offset by additional emissions from the high-mass structure.
However, a major caveat is that in the previous study, module B6.3 had not been considered. That module encompasses the non-integrated systems, such as plug-in appliances, which are known to have a high impact on the total lifecycle GHG emissions. This means that the comparison, as noted by the authors, did not provide a real and clear picture. The study authors nonetheless discouraged building with carbon-intense materials used in 2226 building – fired clay brick, concrete, and steel rebar – as it is a major hindrance in achieving a carbon-neutral built environment.
The environmental footprint of the building could be significantly lowered if unfired clay bricks were used in all non-bearing walls, as they maintain high hygrothermal properties (McGregor et al., 2014).

3.9 Economic Aspects of 2226

Mechanical spaces are absent in the building plan, which might have positive consequences regarding the amount of (rentable) space gained in the building (Fannon et al., 2021). However, that may be to some extent negated by the large surface area footprint of the thick walls. In comparison to another standard building, the 2226 building was shown to be more area-efficient, meaning that the thick walls were offset by freed-up space (Pelzeter, 2017). There was also no need for suspended ceilings since they contained no building services, and covering the ceiling would anyway deter heat transfer with thermal storage. A potential disadvantage of such a building concept might be that planners, builders, and designers could find some obstacles in the bureaucratic process of construction approvals (Klein, 2016).

Compared to contemporary high-performance buildings, the 2226 building had lower initial costs by not having many upfront sophisticated technical systems, and lower operational costs by not requiring much maintenance and electricity use of those systems (Junghans & Widerin, 2017). It was estimated that the construction and investment costs were 25 % lower when compared to standard buildings (Wienerberger, 2023). In a study by Pelzeter (2017), the following costs were listed: € 1200/m^2_{net} (excluding VAT) of construction costs in 2013, and € 0.47/ m^2_{net} monthly of operational costs at 20 % vacancy for wastewater, electricity, and cleaning (when the electricity price is € 0.1/kWh). The automated window opening system will need to be replaced after 15 – 20 years, the electricity wiring after 25 – 30 years, and the sanitary installations after 35 – 40 years.
For a study period of 50 years, it was calculated that life cycle costs would amount to between € 2099/m^2_{gross} and € 3071/m^2_{gross} (prices in 2012), depending on the assumed interest rates and price increase. The highest share in life cycle costs belonged to construction and electricity. In comparison to a standard building, the 2226 building had 63 % lower maintenance and repair costs and 43 % lower total life cycle costs (Pelzeter, 2017).

4 Method

To test the viability of passive design strategies in the Nordic context, the 2226 building was recreated in the energy modeling software IDA ICE 4.8. After verification of the model (compared to existing data), the location and climate data were moved to selected places in the Nordic region, where further simulations were performed. The building enclosure, internal gains, and climate scenarios were parametrically simulated and assessed in the two critical zones, as determined by the results of the simulation.

Geometry of the building 2226 was determined as appropriate and suitable for the simulation of residential types, as the size and shape of the floor levels could be easily divided into a range of apartments of varying sizes. Additionally, since the windows of the 2226 building are placed equally in number, size, and shape on each façade, it was considered that by simulating this building, an important understanding of the effect of the window orientation could be examined as well.

4.1 Recreation, Calibration, and Verification of the Case Study

The first step in the exploration of resilient passive design strategies was to recreate and verify the energy model of the 2226 building. When successfully verified, the model could be transferred to different locations in the Nordic countries to see how well it would behave under different climatic conditions.
The building was modeled in IDA ICE, using sources in literature as input data. Four zones per floor were modeled, in the same pinwheel spatial organization and room size as in the real building. The results of the recreated model were compared to a graph of the indoor temperature of the 2226 building measured in 2015, as provided by Junghans & Widerin (2017).
Afterward, building elements of the model were parametrically changed to arrive at potential design improvements. The following charts present the work undertaken in calibrating and verifying the energy model.

Firstly, the building was simulated without occupants, lighting, and appliances, with windows constantly closed, as shown in Figure 16. Note that there were great differences between rooms of different orientations, as well as a difference between floors.

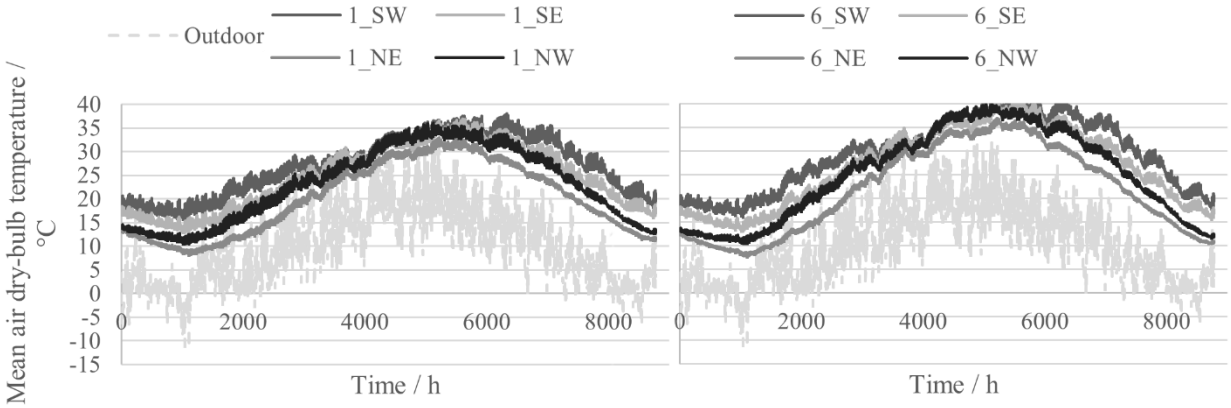

Figure 16. Comparison of outdoor air temperature and indoor air temperatures in the empty ground floor (left) and in the empty fifth floor (right) of the recreated 2226 building in Lustenau, Austria. The zone names are coded as Floor number_Orientation.

The relative humidity charts were irrelevant, as there were yet no occupants. However, a notable insight so far was that the temperature time lag was significant, but the temperature amplitude had not decreased, leading to significantly high indoor temperatures in summer. This signified that natural ventilation was essential in lowering indoor temperatures.

Secondly, a building was simulated without occupants, lighting, and appliances, while windows were controlled by PI temperature control. Here, there was not much variation between the floors, but still significant variation between room orientations. It was concluded that PI control effectively opened windows during the warm months, although in summer months the temperatures often exceeded 30 °C, as shown in

Figure 17. However, the PI controller responded to temperature set points, which meant that windows were not opened for almost the whole winter when the outdoor temperature was lower than the minimum indoor target.

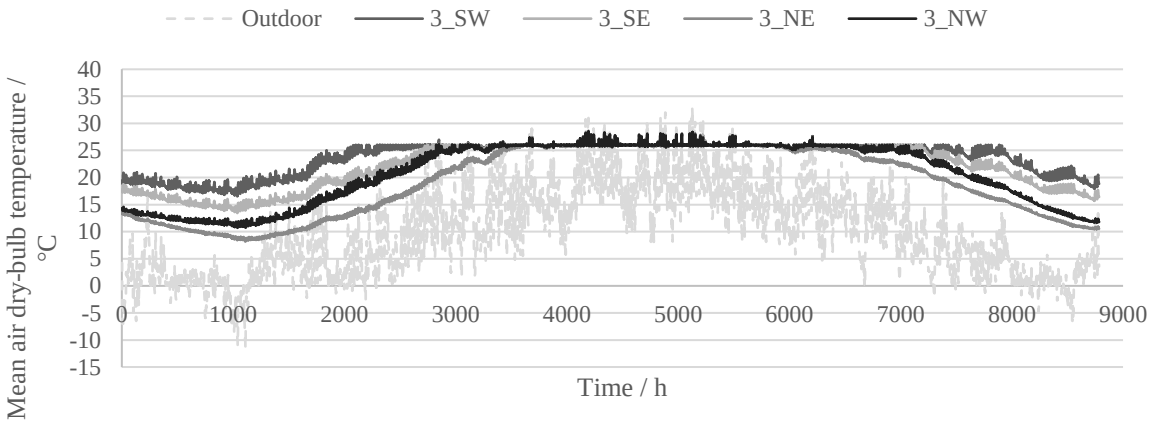

Figure 17. Comparison of outdoor air temperature and indoor air temperatures in the empty second floor with PI-controlled windows of the recreated 2226 building in Lustenau, Austria. The zone names are coded as Floor number_Orientation.

Thirdly, the building was simulated with occupants, lighting, and appliances (values assigned for an office building based on EN 16798-1:2019). Windows were controlled by PI temperature control. The results showed well-accomplished temperature control, as the temperature range throughout most of the year was within the desired range, as seen in Figure 18. In comparison to the previous simulation step, this denoted that internal gains significantly affected the indoor temperature. There was still an overheating issue during summer.

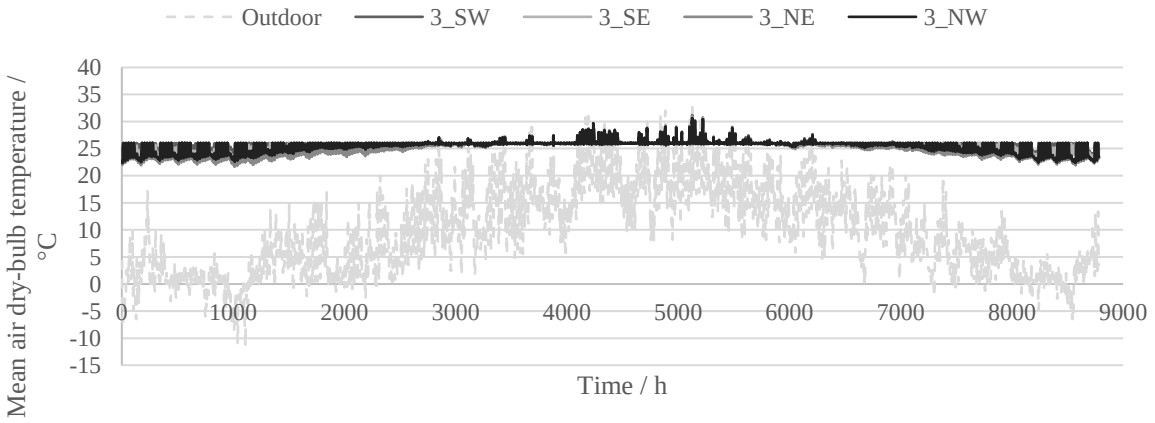

Figure 18. Comparison of outdoor air temperature and indoor air temperatures in the occupied second floor with PI-controlled windows of the recreated 2226 building in Lustenau, Austria. The zone names are coded as Floor number_Orientation.

However, when relative air humidity is observed, it can still be said that PI controllers did not respond well during winter, as depicted in Figure 19. Several months were simulated with windows never being opened, which would mean unbearable air quality conditions for the occupants. This is also seen in critical (north-facing) zones where excess moisture from breathing occupants created 100 % relative humidity conditions. In south-facing rooms, relative humidity during winter was too low as well.

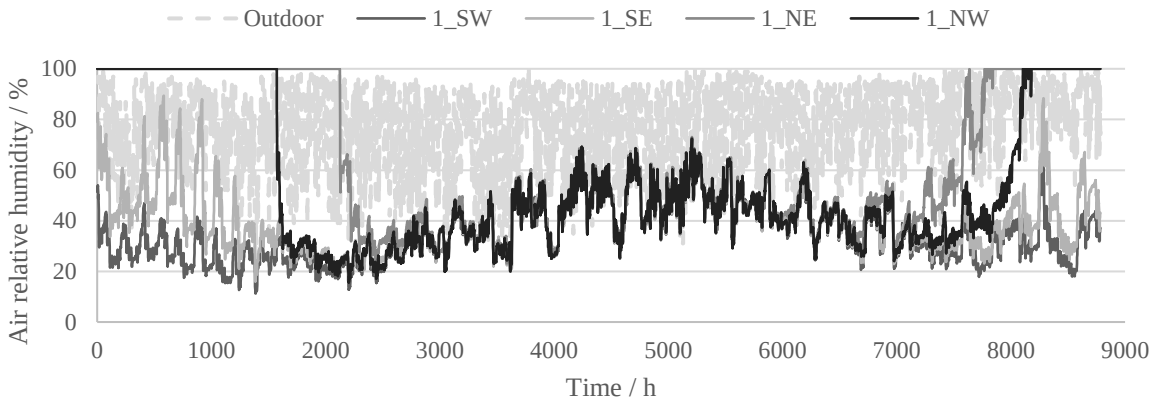

Figure 19. Comparison of outdoor and indoor air relative humidities in the occupied ground floor with PI-controlled windows of the recreated 2226 building in Lustenau, Austria. The zone names are coded as Floor number_Orientation.

Fourthly, the building was simulated with occupants, lighting, and appliances, while windows were controlled by simultaneous PI temperature control and a default "always open" schedule. It was concluded that the same issues pertained. Further improvement steps were analyzed, such as incorporating shading devices or changing the set points for the PI controller, but no significant improvement was noticed.

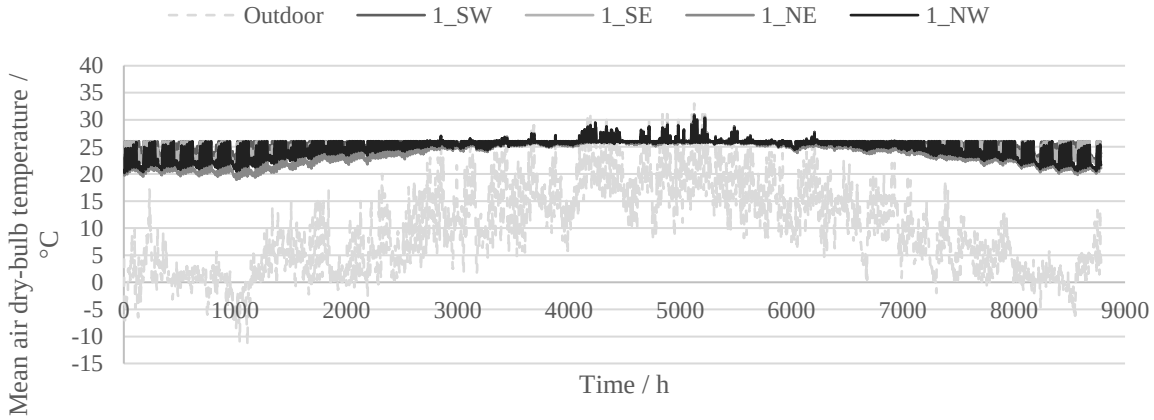

Figure 20. Comparison of outdoor air temperature and indoor air temperatures in the occupied ground floor with PI-controlled windows and a default schedule of the recreated 2226 building in Lustenau, Austria. The zone names are coded as Floor number_Orientation.

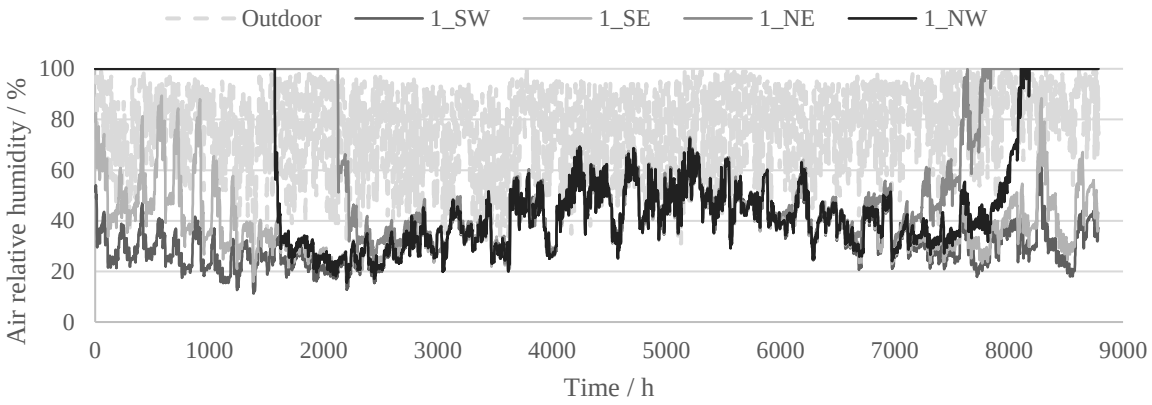

Figure 21. Comparison of outdoor and indoor air relative humidities in the occupied ground floor with PI-controlled windows and a default opening schedule of the recreated 2226 building in Lustenau, Austria. The zone names are coded as Floor number_Orientation.

Fifthly, several options were simulated where the PI controller was omitted, and the windows were regulated only by the predefined opening schedule. The results shown in Figure 22 and Figure 23 are the best-performing among the attempted ones, but they all had in common excessively high gradients of indoor temperature and relative humidity. This indicated that natural ventilation had not been optimized at all, as the effect of thermal inertia was not noticeable in either time lag or amplitude decrease.

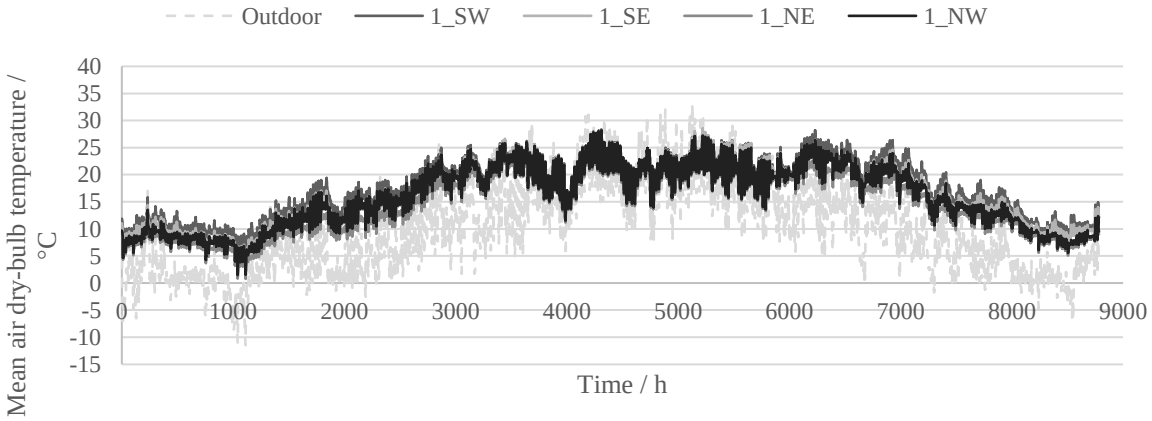

Figure 22. Comparison of outdoor air temperature and indoor air temperatures in the occupied ground floor with a predefined opening schedule of the recreated 2226 building in Lustenau, Austria. The zone names are coded as Floor number_Orientation.

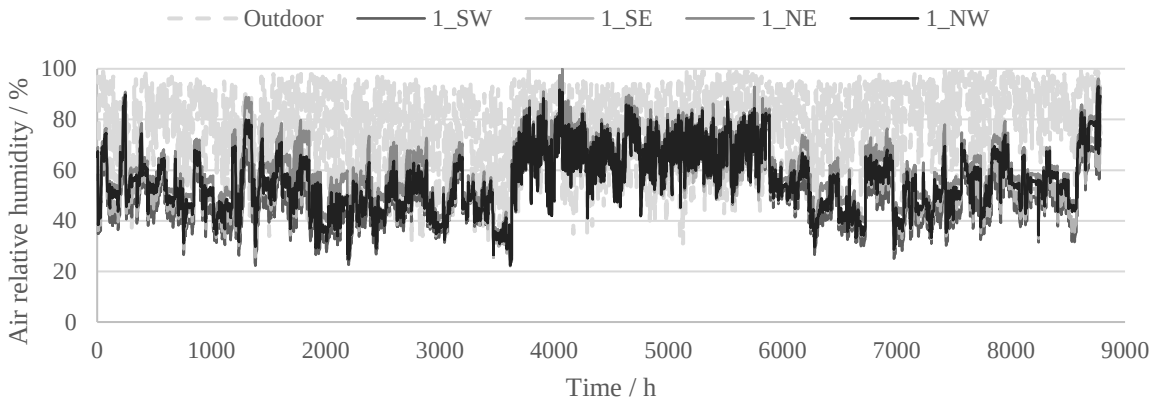

Figure 23. Comparison of outdoor and indoor air relative humidities in the occupied ground floor with a predefined opening schedule of the recreated 2226 building in Lustenau, Austria. The zone names are coded as Floor number_Orientation.

Finally, it was deduced that trying to create a predefined opening schedule or using the PI controller could not yield realistic results. A scripted algorithm was created and simulated, similar to the original described by Junghans & Widerin (2017), where the weather is not assumed, and the model responds to real indoor and outdoor conditions. The window-opening algorithm was applied to all windows in the building and subsequently used in all the following building design proposals.

In Figure 24, it is shown how the algorithm was modeled in IDA ICE, with the help from customer support by the software developers. Independently, the windows open either when the indoor air temperature in the zone exceeds 26 °C (while also being below outdoor air temperature), or when the indoor CO_2 concentration is above 1200 ppm (as long as the indoor air temperature is above 18 °C).
The windows close either when the indoor air temperature in the zone is below 22 °C, or when the indoor CO_2 concentration drops below 800 ppm.

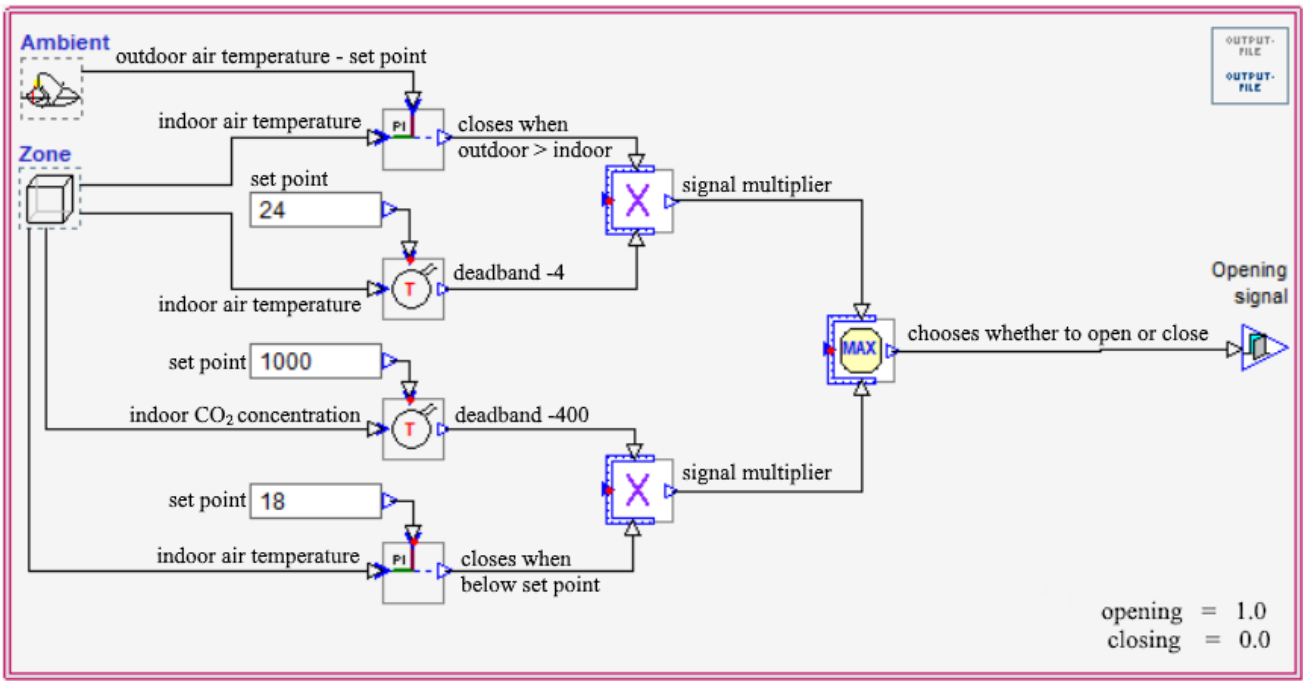

Figure 24. Natural ventilation algorithm for opening the windows in the building. The algorithm is based on sensors of air temperature and CO_2 level, with the deadband thermostat and the PI controllers.

Figure 25 depicts the indoor air temperature over the year being within the range of 20 °C and 26 °C for the majority of the time. Only on the ground floor was there a substantial amount of time with temperatures below

20 °C, but the assumption was that the internal gains were not modeled properly on the ground floor (office instead of multi-purpose zones). The differences between the model and the actual building may stem from the zone simplification of the model, as well as the complex occupant behavior that could not be modeled without additional advanced occupant modeling. Similarly, indoor relative humidity levels should be approached with suspicion, as the hygrothermal properties of the building materials, such as the moisture storage/buffer capacity, were not taken into consideration. The simulation results for the indoor relative humidity are shown in Figure 26. Most of the time, relative humidity was in the range of 30 % – 70 %, with occasional and periodic fluctuations exceeding these values.

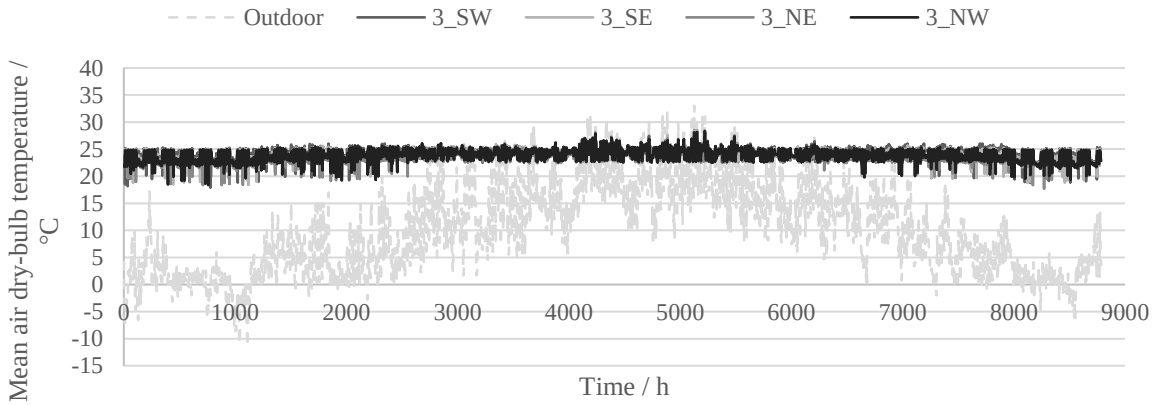

Figure 25. Comparison of outdoor air temperature and indoor air temperatures in the fully occupied second floor with a window-opening algorithm of the recreated 2226 building in Lustenau, Austria. The zone names are coded as Floor number_Orientation.

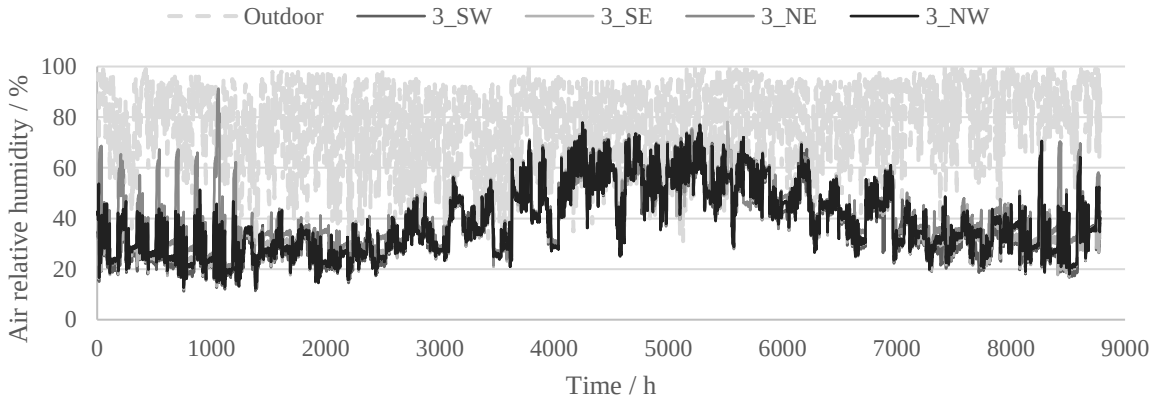

Figure 26. Comparison of outdoor and indoor air relative humidities in the fully occupied second floor with a window-opening algorithm of the recreated 2226 building in Lustenau, Austria. The zone names are coded as Floor number_Orientation.

The model can be compared to actual measured data, as shown in Figure 27. The reasons why the simulated data did not perfectly correspond to measured data can be explained by many assumptions undertaken during the energy modeling (such as the specific internal loads and occupancy schedules), and the difference between the climate of the specific year and the climate file used in the simulation. However, since the similarities are evident in the Figure 27, and to the available knowledge of the author of the thesis, no other sources relevant to the energy model could have been found, it was concluded that the model had been successfully recreated and verified to continue using it in further simulations.

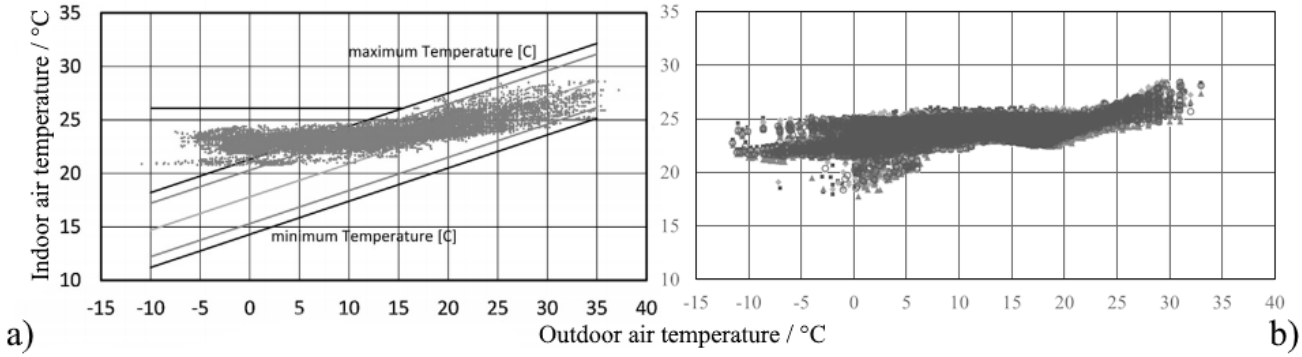

Figure 27. Indoor air temperature in relation to the outdoor air dry bulb temperature. On the left, measured data of the 2226 building, performed in 2015. On the right, a simulation of the recreated model of the building, with plotted hourly results of zones on the second floor.

The only change regarding the building geometry before simulations in the Nordic regions was applied to the ground floor, where ceiling height was adjusted to be the same as on other floors, as the height of more than four meters was deemed too high for residential function. Similarly, ground-floor windows were changed to be identical to the rest of the windows on other floors.

The sensor-based automatic window-opening system as used in the 2226 building remained in the studied simulations, although it is not in line with the building philosophy sans high-tech indoor conditioning. However, during the creation of the simulation model, no pre-determined schedule could adequately satisfy the requirements of the indoor climate and thermal comfort.
Therefore, the automatic system played the role of a surrogate for a more advanced occupant model, assuming that the occupant would also take into account the outdoor and indoor conditions, and appropriately respond. For the sake of simplicity in simulations, truly advanced occupant models were not used, so this approach is deemed as something in the middle of the potential simulation accuracy. It is still acknowledged that in reality, the occupant may respond in widely different ways that are not similar to the automated ventilation algorithm. The reasons for this are varied, and include the human inability to detect exact temperature and CO_2 levels, the slower response, unawareness of the situation, absence from home at a particular time of day, personal preferences, or outdoor noise/pollution levels.

4.2 Generation of Future Climate Weather Files

In this study, Meteonorm was used to generate future weather files because of the substantial number of available weather data locations and data outputs, its ability to create future extreme weather conditions, simplicity of use, and the low required computing power during the process.

Meteonorm 8.2 is a climate database and a tool that generates stochastic typical weather based on interpolated long-term monthly means. Ground station and satellite-obtained data are used from the periods 2001 – 2020 for eight radiation parameters and 2000 – 2019 for 26 meteorological parameters. Data from different sources is combined to optimally represent a typical year or a time series (Meteotest, 2023). In addition, future data is generated from CMIP5 data models, based on ten GCMs created for scenarios RCP2.6, RCP4.5, and RCP8.5 from the IPCC Fifth Assessment report.
After selecting one of the three RCP scenarios, the user can select a future decade for which they want to see the interpolated data. Available decades are up to the year 2100. In calculation settings, one can also modify the radiation, temperature, and sky model, as well as monthly extreme values for temperature and radiation. As output files, various formats can be selected at a scale of hourly or even minute data. Currently, the software predicts only a small change in radiation in the 21st century, whereas temperature is expected to change more significantly. However, it is noted that previous predictive models underestimated already observable radiation anomalies.

Six Nordic locations representing different climatic conditions were selected for the analysis, due to their varying latitudes, altitudes, proximity to sea (continental/maritime effect), and other local particularities.

According to the Köppen climate classification, they range from oceanic (Cfb) and humid continental (Dfb) to subarctic (Dfc and Dfb) climates. As seen in Figure 28, the selected locations are:

a) Copenhagen (Airport) 55.6°N, 12.6°E, elevation 5 m.
b) Karlstad 59.4°N, 13.5°E, elevation 55 m.
c) Helsinki (Kaisani) 60.2°N, 25.0°E, elevation 9 m.
d) Bergen (Florida) 60.4°N, 5.3°E, elevation 12 m.
e) Jyväskylä 62.4°N, 25.7°E, elevation 145 m.
f) Östersund 63.2°N, 14.5°E, elevation 376 m.

Subsets of EPW file outputs were created for each location, to be used in IDA ICE simulations.
Each weather station had four associated weather files: historic climate data (1961 – 1990), contemporary climate data (2000 – 2019), future climate data under the RCP 8.5 in the year 2100, and future extreme climate data (higher temperature and radiation in summer, lower in winter), also under the RCP 8.5 in the year 2100. By doing so, the impact assessment of climate change could be analyzed. Weather stations north of the polar circle could not be used in this assessment, as future climate data was available only south of the 65° parallel. Historic weather files were obtained because they were closest to a future cooling scenario caused by the AMOC collapse, as discussed previously in section 2.1.2.
The choice of creating two future climate files for each location is due to fundamental uncertainty in future projections. Therefore, even in the most impactful scenario, an extreme year comprising less likely/frequent heat waves and cold waves could yield significantly different performance results. This is in line with the method described by Nik (2016), where next to a typical downscaled year, two files for an extremely warm and an extremely cold year are created. However, if extreme cold is usually expected during winter and extreme heat during summer, it was assumed that such extremes could be modeled seasonally into one file.

Figure 28. Positions of selected weather stations spanning the variations of the Nordic climates.

In the Appendix B, figures (Figure 37 – Figure 42) of generated weather files are provided, presenting values of the changing outdoor air dry bulb temperature, outdoor air relative humidity, and direct normal irradiation for four climate scenarios for each location, as obtained from Meteonorm.

Generally, there was no significant difference between the historic and contemporary files. In the presented future climate scenarios, temperature will increase significantly. Direct normal radiation is increased as well, but most notably in the extreme future scenario during the summer. Conversely, relative humidity in warm months is universally expected to be lower than today, while being higher in the cold months, except for Helsinki and Östersund, where future relative humidity will be lower than today throughout the whole year.

4.3 Parametric Simulation

In the parametric simulation, parameters of building enclosure and internal gains were combined with the four different climate files for each Nordic location. For building enclosure, the wall from the 2226 building was analyzed, and possible alternatives were examined: ten high-mass walls, where the intention was to see if thermal inertia could be better exploited; and two low-mass walls constructed from bio-based materials, as discussed in the section 2.2.

4.3.1 Parameters of Building Enclosure

Various wall assemblies were analyzed: the 2226 original wall, other high-mass walls, and walls made from bio-based materials. The high-mass walls followed the same construction logic as the 2226 wall but with a few modifications of wall layers in hopes of improving thermal inertia.
The walls were categorized in three ways relating to the 2226 original wall:

a) Other Wienerberger monolithic clay blocks were used instead of Porotherm 38 Plan and Porotherm 38 H.i Plan.

These blocks were split into load-bearing ones that were placed on the interior side of the wall in every combination, and insulating ones that were placed as the exterior layer. All block combinations were then analyzed, and some combinations were selected for simulation based on principles as stated below in the text. In Table 6 and Table 7, properties of the studied Wienerberger blocks are described. The densities of the blocks containing perlite infill in the vertical cavities have been approximated based on the known densities of the brick and the perlite.

Table 6. Wienerberger load-bearing monolithic clay blocks analyzed in the parametric study. Sourced from the Wienerberger website catalog.

Block name	Thickness / mm	λ / W/(m·K)	ρ / kg/m³	c_p / J/(kg·K)	α / Mm²/s
Poroton S8 Perlit	365	0.080	750	868	0.12
	425	0.080	750	868	0.12
	490	0.080	750	868	0.12

Table 7. Wienerberger insulating monolithic clay blocks analyzed in the parametric study. Sourced from the Wienerberger website catalog.

Block name	Thickness / mm	λ / W/(m·K)	ρ / kg/m³	c_p / J/(kg·K)	α / Mm²/s
Porotherm 50-20 Plan	500	0.116	720	1000	0.16
Poroton T6,5 Perlit	425	0.065	498	868	0.15

b) Exterior and interior finishing was changed (unventilated brick façade). The properties of the solid brick are presented in Table 8.

Table 8. Alternative finishing material used in the design of high-mass walls. Sourced from the WUFI/MASEA database.

Material	Thickness / mm	λ / W/(m·K)	ρ / kg/m³	c_p / J/(kg·K)	α / Mm²/s
Solid façade brick	60	0.544	1744	889	0.35

c) The exterior block layer was replaced with insulation materials. All insulating materials were placed on the exterior side of the load-bearing brick, with properties described in Table 9.

Table 9. Thermal insulation materials used in the design of high-mass walls. Sourced from the WUFI/MASEA database.

Material	λ / W/(m·K)	ρ / kg/m³	c_p / J/(kg·K)	α / Mm²/s
Hemp-lime brick	0.070	300	1870	0.12
Straw bale	0.067	85	1800	0.44

All of the proposed new high-mass walls were first designed to have, as a control parameter, identical or similar *U*-value to the 2226 original wall (with a margin of error of ± 1 %), so that the relative impact of thermal inertia could be better studied. After, a wall assembly with the lowest *U*-value was simulated as well.

Similarly, walls made from bio-based materials were designed with the principles of minimum environmental footprint, low-tech design, and circular construction, as evident in the abstention from plastic film foils, plastic insulation, and industrial manufacture of load-bearing timber. These principles are described in detail by Ejstrup et al. (2019), where timber-frame wall design is provided for straw-bale insulation. The insulation thickness has been adjusted just so the wall assembly reaches the desired *U*-value similar to the *U*-value of the 2226 wall.

Likewise, construction assembly with hemp-lime brick was provided. Although having a relatively high conductivity for insulating material, hemp-lime brick has a relatively high density, a high specific heat, and the lowest thermal diffusivity among insulating materials, as seen in Table 10. This boosted hopes that it could have a noticeable effect on thermal inertia.

Table 10. Thermal diffusivity α for a range of insulating materials. Sourced from the WUFI/MASEA database. Italicized materials can be considered bio-based.

Insulation material	α / Mm²/s
Cellular glass	0.400
Cellulose fibre	0.408
Cork	0.181
Expanded polystyrene (EPS)	0.889
Extruded polystyrene (XPS)	0.500
Fisolan sheep's wool	0.733
Hemp-lime brick	0.125
Mineral glass wool	1.429
Straw bales	0.438
Wood fiber (Pavatex Diffutherm)	0.125

In the following tables (Table 11 – Table 14), the high-mass wall assemblies are presented in detail. Each wall is listed with the internal areal heat capacity, as it was the only metric found in the literature review that could be used to assess the thermal inertia of the whole building assembly and not just one particular material.

Table 11. High-mass walls with Wienerberger monolithic clay blocks, starting from the innermost layer.

Wall	Layers	Thickness / mm	*U*-value / W/(m²·K)	Internal areal heat capacity / kJ/(m²·K)
01	Solid façade brick	60	0.1255	60.24
	Mortar	10		
	Porotherm 38 Plan	380		
	Mortar	10		
	Porotherm 38 H.i Plan	380		
	Light mortar plaster	20		
	Total	*860*		
02	Lime gypsum plaster	20	0.1254	35.57
	Porotherm 38 Plan	380		
	Mortar	10		
	Porotherm 50-20 Plan	500		
	Light mortar plaster	20		
	Total	*930*		
03	Light gypsum plaster	20	0.1256	35.57
	Porotherm 38 Plan	380		
	Mortar	10		
	Porotherm 38 H.i Plan	380		
	Mortar	10		
	Solid façade brick	60		
	Total	*860*		

Table 12. High-mass walls with hemp-lime brick, starting from the innermost layer.

Wall	Layers	Thickness / mm	*U*-value / W/(m²·K)	Internal areal heat capacity / kJ/(m²·K)
04	Lime gypsum plaster	20	0.1258	35.57
	Porotherm 38 Plan	380		
	Mortar	10		
	Hemp-lime brick	300		
	Light mortar plaster	20		
	Total	*730*		
05	Lime gypsum plaster	20	0.1278	32.53
	Poroton S8 Perlit	490		
	Mortar	10		
	Hemp-lime brick	100		
	Light mortar plaster	20		
	Total	*640*		
06	Solid façade brick	60	0.1264	60.71
	Mortar	10		
	Poroton S8 Perlit	490		
	Mortar	10		
	Hemp-lime brick	100		
	Light mortar plaster	20		
	Total	*690*		

Table 13. High-mass walls with straw bales, starting from the innermost layer.

Wall	Layers	Thickness / mm	*U*-value / W/(m²·K)	Internal areal heat capacity / kJ/(m²·K)
07	Solid façade brick	60	0.1265	60.72
	Mortar	10		
	Poroton S8 Perlit	365		
	Mortar	10		
	Straw bale	200		
	Light mortar plaster	20		
	Total	*665*		
08	Light gypsum plaster	20	0.1267	32.53
	Poroton S8 Perlit	365		
	Mortar	10		
	Straw bale	200		
	Mortar	10		
	Solid façade brick	60		
	Total	*665*		
09	Light gypsum plaster	20	0.1266	32.54
	Poroton S8 Perlit	425		
	Mortar	10		
	Straw bale	150		
	Mortar	10		
	Solid façade brick	60		
	Total	*675*		

Table 14. High-mass wall with the lowest U*-value, starting from the innermost layer.*

Wall	Layers	Thickness / mm	*U*-value / W/(m²·K)	Internal areal heat capacity / kJ/(m²·K)
10	Solid façade brick	60	0.0768	60.72
	Mortar	10		
	Poroton S8 Perlit	490		
	Mortar	10		
	Poroton T6,5 Perlit	425		
	Light mortar plaster	20		
	Total	*1015*		

The two walls from bio-based materials are detailed in Table 15.

Table 15. Wall assemblies constructed from bio-based materials, starting from the innermost layer.

Wall	Layers	Thickness / mm	*U*-value / W/(m²·K)	Internal areal heat capacity / kJ/(m²·K)
11	Gypsum plaster	20	0.1282	34.85
	Hemp-lime brick between timber joists	520		
	Gypsum plaster	20		
	Total	*560*		
12	Mud plaster	50	0.1282	56.49
	Straw bale between timber joists	500		
	Mud plaster	50		
	Total	*600*		

It would be unreasonable to construct a building with these materials while carrying massive concrete slabs or to use the same materials for indoor walls, due to their thickness (Minke & Krick, 2020). Therefore, for the

two walls, 11 and 12, a new floor slab, interior walls, and roof slab were introduced, as regarded as more appropriate to the lightweight design. The design of these assemblies was sourced from the online catalog of timber constructions by the Austrian Forest Products Research Society (HFA-ÖGH, 2024).
In the parametric simulation, high-mass walls were simulated with the 2226 original slabs, interior walls, and roof, while the lightweight assemblies were only paired with walls 11 and 12. The insulation thickness in the roof assembly was adjusted to achieve the same *U*-value as the 2226 roof. The interior wall was designed as a compartment wall with a fire resistance (REI) of 60 minutes. Oriented strand board was used as a vapor barrier. In Table 16, the characteristics of the lightweight floor slab, interior wall, and roof slab are presented. As an interior insulation material, wood fiber was used, as it is a bio-based material with low environmental impact and great applicability in circular construction (Ejstrup et al., 2019).

Table 16. Thermal characteristics of the lightweight timber construction assemblies paired with exterior walls 11 and 12. Sourced from (HFA-ÖGH, 2024), with insulation materials values from the WUFI database. The horizontal layers are listed from top to bottom.

Type	**Layers**	**Thickness / mm**	**λ / W/(m·K)**	***U*-value / W/(m²·K)**	**Internal areal heat capacity /kJ/(m²·K)**
Floor slab	Dry screed	25	0.210	0.1187	Floor: 26.45 Ceiling: 27.20
	Wood fiber Pavatex Diffutherm	40	0.044		
	Perlite filling	30	0.700		
	Oriented strand board (OSB)	15	0.130		
	Wood fiber between timber joists (22 cm)	100	0.044		
	OSB	15	0.130		
	Gypsum board	12.5	0.200		
	Total	*357.5*			
Interior wall	Gypsum board	12.5	0.200	0.170	24.18
	OSB	15	0.130		
	Wood fiber between timber studs Pavatex Diffutherm	100	0.044		
	OSB	15	0.130		
	Gypsum board	12.5	0.200		
	Wood fiber Pavatex Diffutherm	20	0.044		
	Gypsum board	12.5	0.200		
	OSB	15	0.130		
	Wood fiber between timber studs Pavatex Diffutherm	100	0.044		
	OSB	15	0.130		
	Gypsum board	12.5	0.200		
	Total	*330*			
Roof slab	Spruce cladding boards	25	0.120	0.108	21.33
	Ventilated air gap with spruce counter battens	80	-		
	Softwood fiberboard	15	0.045		
	Wood fiber between timber rafters Pavatex Diffutherm	320	0.044		
	OSB	15	0.130		
	Wood fiber Pavatex Diffutherm	50	0.044		
	Gypsum board	25	0.120		
	Total	*530*			

4.3.2 Parameters of Internal Gains

The internal gains were simulated in two cases, once where internal gains (including occupants, lighting, and appliances) were assigned based on the values for residential buildings in EN 16798-1:2019. This meant that the simulated values corresponded fully, or 100 % to the standard values. Then, similarly to the proposal by K. Sun & Hong (2017), a higher occupancy (200 % of standard internal gains) was applied for sensitivity analysis. Here, the occupancy per net floor area was doubled from 0.035 residents/m² to 0.07 residents/m². The internal gains from appliances were also doubled from 3 W/m² to 6 W/m². The lighting remained unchanged at 6 W/m², as it was deemed unlikely for it to follow linearly the increase in occupancy, as well as because of the expected gains in near-future lighting energy efficiency (Morgan Pattison et al., 2018). Occupancy lower than the standard was not considered, as it was judged already relatively low, as discussed previously in section 2.1.4.
The increase in gains from appliances followed the increase in occupants, so it cannot be regarded as a change in behavior style. Of course, many more behavior and occupancy combinations could have been investigated and simulated, but for the sake of understanding building behavior, here it was investigated how an overall increase in internal gains affected the indoor thermal comfort and the indoor climate.

In total, 13 external walls were simulated twice for each weather file, and six Nordic locations were each simulated with four weather files, which gave a total of 624 simulation outcomes.

4.3.3 Performance Metrics

The obtained results from IDA ICE were categorized into annual energy use, and hourly datasets of temperature, relative humidity, and indoor carbon dioxide.
The results of the thermal comfort were measured by the indoor operative temperature, as described in the EN 16798-1:2019 standard for adaptive thermal comfort. Category III was selected as the maximum/minimum limit that should not be exceeded.
As described by Sicurella et al. (2012), thermal comfort can be assessed with an approach where the only required input data is the hourly operative temperature. Namely, the thermal discomfort needs to be measured both in its frequency and in its intensity. Depending on the fluctuation of thermal discomfort, four discomfort options can therefore be identified:

a) Light and temporary thermal discomfort.
b) Frequent but not intense thermal discomfort.
c) Temporary but intense thermal discomfort.
d) Frequent and intense thermal discomfort.

The performance target for relative humidity was to be between 40 % and 60 % (± 10 %), while the target for indoor carbon dioxide was to be below the room average of 1200 ppm.

4.4 Limitations

Since the simulations were based on the design of the single case study building, the universal conclusions on the viability of free-running buildings in the Nordic context cannot be reached, as perhaps a different set of materials, passive design strategies, building geometry, etc. could provide better building performance.

The generated weather files were based on the extrapolation of past and present climate observations. Far-future predictions are generally bound with increased uncertainties, meaning that the confidence about the accuracy of the prediction is reduced (de Wilde & Tian, 2012). Additionally, as discussed in sections 2.1.1 and 2.1.2, the future climate may bring unforeseen escalation that does not fit the observed (linear) patterns, most likely by exceeding tipping points and planetary boundaries. This means that the obtained results do not necessarily conclusive predictions, but they do provide indications of potential future building performance. Another important aspect is that the generated weather files did not take into account the urban heat island effect, which can considerably affect the built environment (Palme et al., 2017).

The results of the relative humidity cannot be considered fully accurate, as the software tool did not calculate the dynamic hygrothermal nature of the building materials. For a complete heat, air, and moisture transfer simulation, the following parameters are needed: bulk density, porosity, specific heat capacity, moisture-

dependant thermal conductivity, moisture storage function, liquid transport coefficients for suction and redistribution, and water vapor diffusion resistance factor (Barclay et al., 2014). In IDA ICE, only density, specific heat capacity, and static thermal conductivity are considered. In reality, it is assumed that the high moisture buffer capacity of some materials would help in the regulation and modulation of indoor moisture levels. However, the relative humidity results can still be useful in determining when the potential moisture risks occur, and in identifying building behavior trends.
Although emphasized by Persily (2022) and discussed in the section 2.4 how it is neither the only nor the best representative metric for indoor air quality, CO_2 was still assessed because other concentrations of gas/particulate matter were not provided in the simulation software.

Another limiting effect of the performed parametric simulation was that the modeled occupant was too static: for example, the occupancy schedule was temporally not changed, and the clothing level (clo) remained the same throughout the year. It was assumed that the occupant of the late 21st century would behave and dwell similarly to the present. The transient, seasonal, and adaptive behavior of humans in their dwellings, emphasized by Khovalyg et al. (2023), was not modeled in this study.

The building model also exhibited a preference for regulation of indoor temperature over other parameters. This means that the model would try to keep the temperature within the limits, even if thereby sacrificing the indoor climate. Therefore, no temperature result can be assessed separately from the results of relative humidity and carbon dioxide concentrations. It is the inherent and fundamental flaw of the simulation setup, as it does not accurately reflect real-life behavior. In reality, the occupant would try to balance the temperature and the fresh air. Nonetheless, these results indicate clearly if/when the outdoor temperature is simply too low or high to consider opening the windows, thereby signaling the viability of a free-running building.

5 Results and Discussion

In the following sections, results and discussion of simulations are provided for delivered energy, indoor temperature, relative humidity, and CO_2 concentrations. Observations are exemplified with one or more figures representing universal phenomena, as the results for all locations follow certain patterns, only with varying values on *x*-axes and *y*-axes.
The full results of the simulations in the form of graphic figures are openly available in the digital repository Zenodo (Ljubas, 2024).
The two critical identified zones in all cases were the northeast-facing one on the ground floor, and the southwest-facing one on the top floor. Therefore, all figures depict the results for those two zones.

5.1 Delivered Energy

The delivered energy from simulated models depends on the internal gains. Hence, the detailed breakdown of the two energy cases is shown in Table 17 below.

Table 17. Annual delivered energy in kWh/m² of net floor area for the simulated cases, depending on the internal gains.

Internal gains	Appliances / kWh/m²	Lighting / kWh/m²	Domestic hot water / kWh/m²	Total / kWh/m²
100%	15.70	5.27	14.91	35.88
200%	31.41	5.27	14.91	51.60

5.2 Temperature

There were significant differences in temperature results between the two internal gains scenarios, the room orientation/story height, and the weather files used for the certain location. The described and observed phenomena are exemplified in the selected figures (Figure 29 – Figure 32).

In most cases, more than 97 % of the time the indoor operative temperature stayed within the bounds of category III of the thermal adaptive model. However, the best temperature control was observed in wall 10 in all simulated cases, meaning that the indoor operative temperature distribution was narrow and close to the median value of around 25 °C. The worst temperature control was observed in low-mass walls in all simulated cases, where the standard deviation was larger, even when the mean or median value was the same as for high-mass walls. The difference between wall 11 and wall 12 was almost negligible in all simulated cases. An example of this can be seen in Figure 29, where the bundle of the hourly temperature data of wall 10 was most closely concentrated.

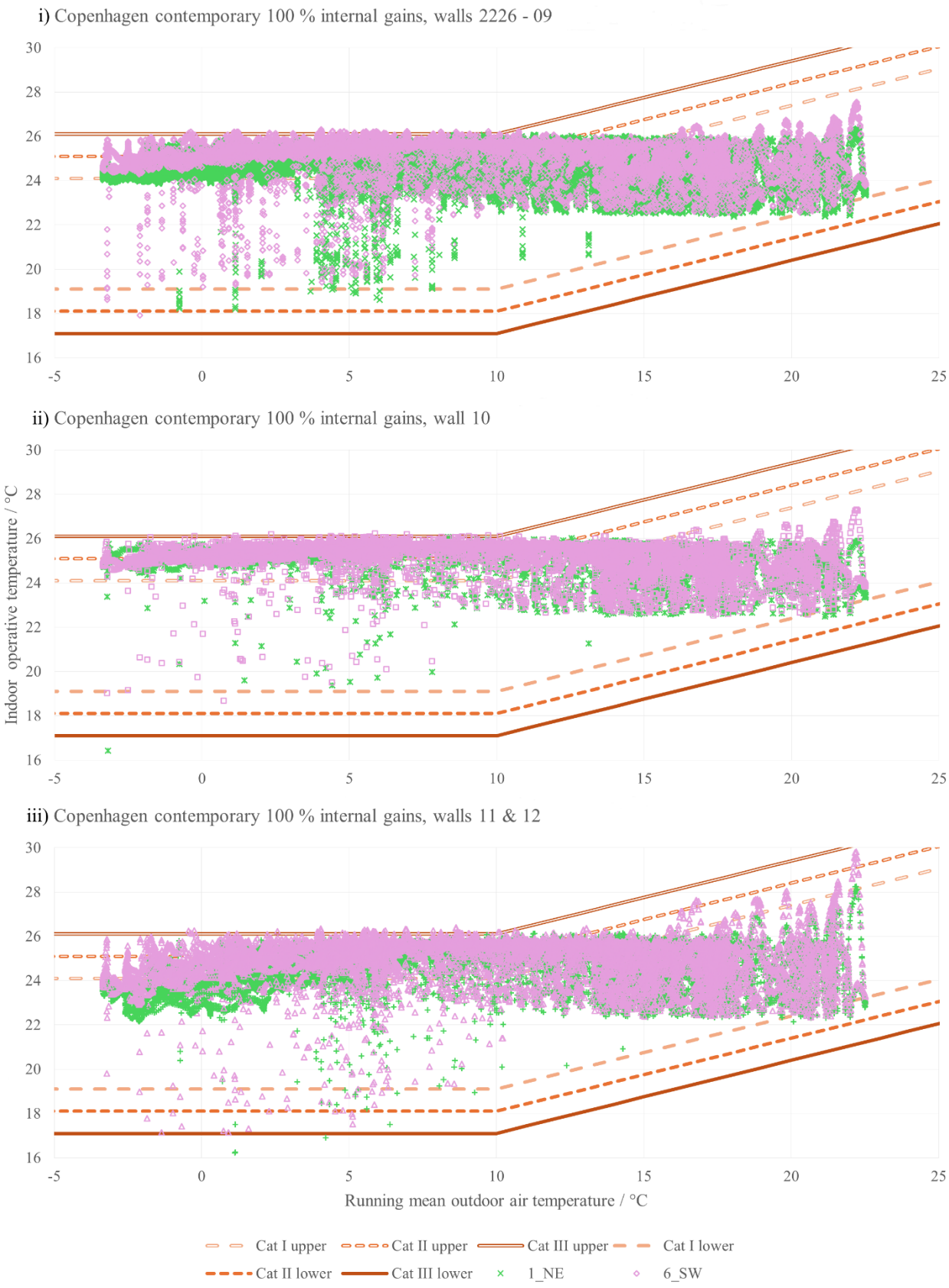

Figure 29. Indoor operative temperature in relation to the outdoor running mean temperature. Hourly zone data for the contemporary climate of Copenhagen and 100 % of internal gains are plotted for different wall assemblies, with marked limits of the thermal comfort categories I – III, according to the EN 16798-1:2019 standard.

In the relatively mild historic and contemporary climates of Copenhagen and Bergen, the indoor operative temperature was rather similar in the south-facing and the north-facing zones. The difference in orientation was more pronounced in the colder and harsher climates, as seen in the example for Karlstad (Figure 30).

Similarly, the difference between 100 % and 200 % of internal gains was not as noticeable in milder climates, while in colder climates, the north-facing zone experienced most of the cold season out of the thermal comfort range (if 100 % of internal gains were simulated). The temperatures dropped to values similar to outdoor conditions, indicating that the windows were frequently open. At 200 % of internal gains, the temperature during winter in the northern zone was much closer to the desired range, as observed in Figure 30.

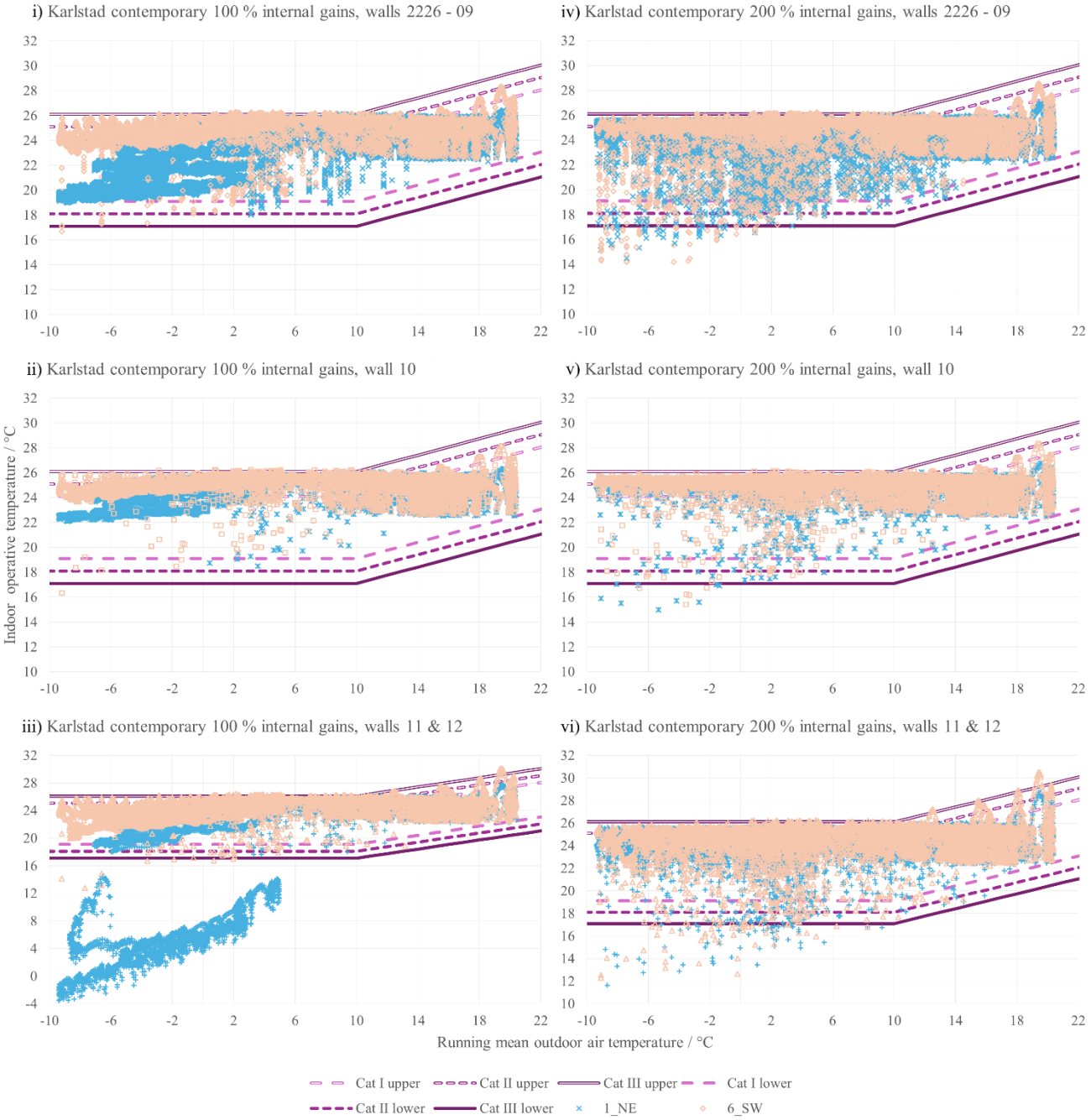

Figure 30. Indoor operative temperature in relation to the outdoor running mean temperature. Hourly zone data for the contemporary climate of Karlstad at 100 % (left) and 200 % (right) of internal gains are plotted for different wall assemblies, with marked limits of the thermal comfort categories I – III, according to the EN 16798-1:2019 standard.

In all future climate scenarios (apart from walls 11 and 12 in the coldest locations of Jyväskylä and Östersund), the wall assemblies managed operative temperature control within the prescribed bounds for more than 97 % of the time, even at 100 % of internal gains. In Jyväskylä and Östersund, a large share of winter time still experienced very cold indoor operative temperatures. In all other locations, the effect of global warming was evident in the better temperature control ability.

However, as depicted in the example from Helsinki in Figure 31, if the future extreme climate was simulated, then, at 100 % of internal gains, temperature control in winter was unobtainable, and at 200 % of internal gains, there was an increased occurrence of overheating.
In many simulated combinations of extreme future climate, the considerable temperature out of control was observed only in low-mass walls 11 and 12.

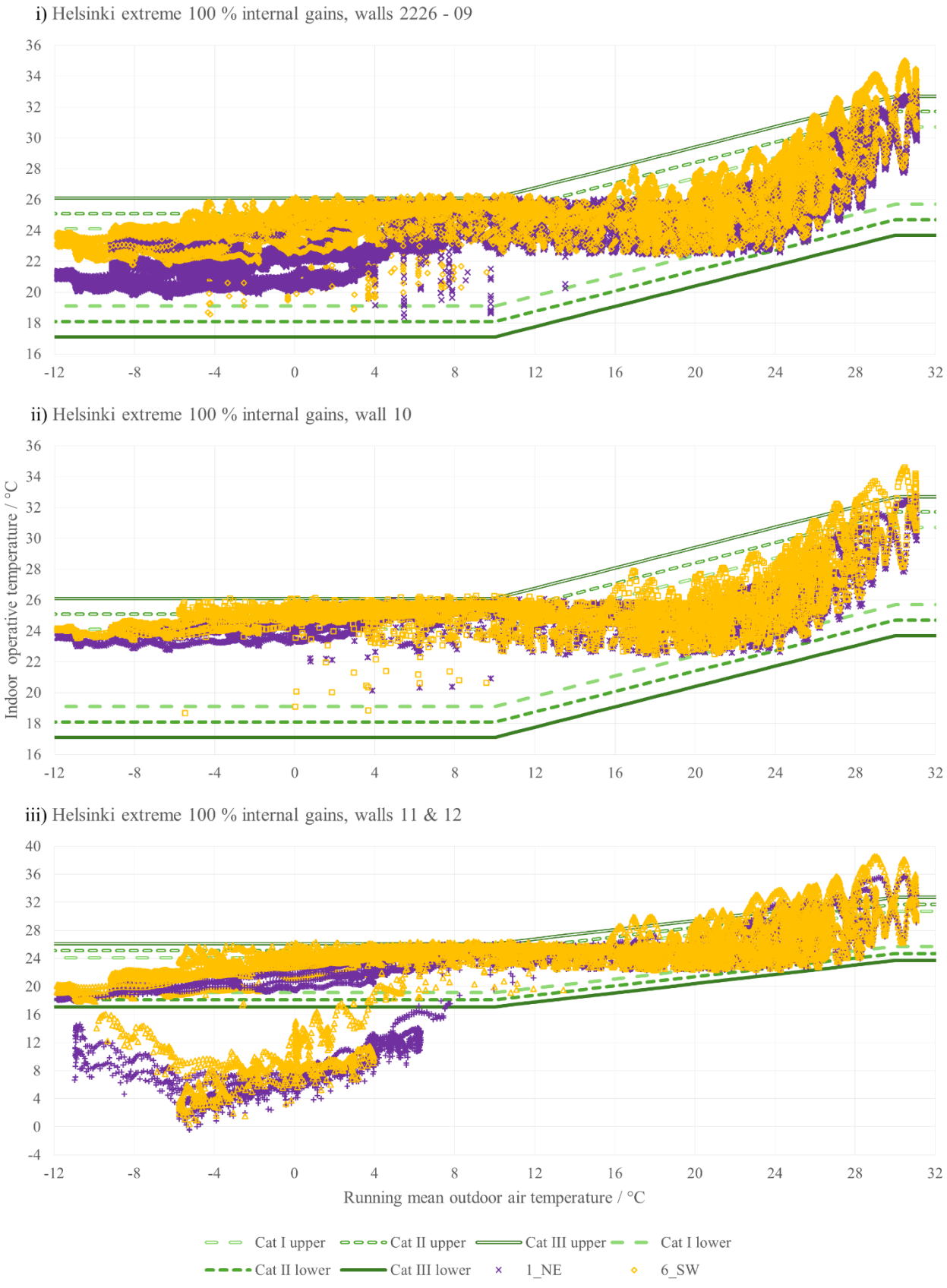

Figure 31. Indoor operative temperature in relation to the outdoor running mean temperature. Hourly zone data for the future extreme climate of Helsinki and 100 % of internal gains are plotted for different wall assemblies, with marked limits of the thermal comfort categories I – III, according to the EN 16798-1:2019 standard.

The exceedance of temperature limits was evaluated for warm months. In cold months, the algorithm kept the temperature within the limits, but at the expense of not opening the windows for weeks or months, as further explained in sections 5.3and 5.4. In summer, the results revealed, as shown in Figure 32, that walls 11 and 12 were the most susceptible to overheating risk.
Over the whole summer, in the extreme future scenario, overheating was on average still a temporary event causing a low discomfort, seen as a weekly occurrence that did not last more than a day. However, in each location, there was a critical period of several consecutive days of overheating.
If the temperature was constantly above the upper limit during this period, it meant that indoor space could not be cooled even during the night. Such prolonged discomfort is a significant threat to occupants‘ health. The highest overheating risk was found in Copenhagen and Helsinki, while the lowest overheating risk was found in Bergen and Östersund. In Copenhagen, shown in Figure 32, the worst cases resulted in several days in a row of high-intensity overheating (up to 6 K higher than the upper comfort limit), while yielding less than several hours in a row of temperatures dropping below the adaptive maximum.

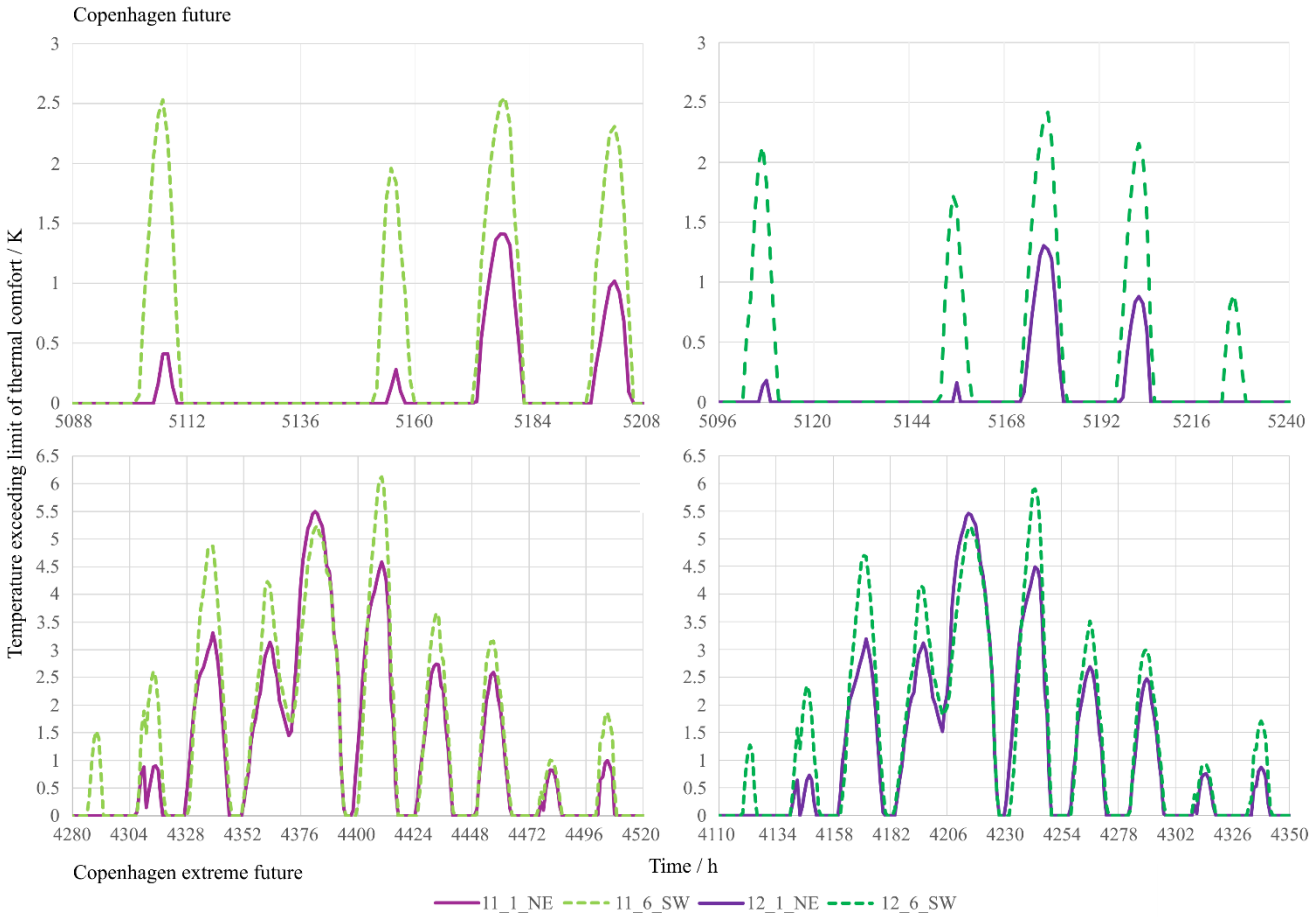

Figure 32. Overheating in walls 11 (left) and 12 (right). Hourly data of indoor temperature exceeding limits of thermal comfort during the hottest part of the year: the future climate of Copenhagen is shown on the top row and the future extreme climate of Copenhagen on the bottom row.

5.3 Relative Humidity

The results for indoor relative humidity reveal a common denominator for all scenarios with 100 % internal gains: free-running buildings were not viable because they contained too much indoor moisture, which would almost certainly cause mold growth and other health risks. Although these results did not take into account the moisture storage/buffer capacity of walls, the distribution of relative humidity towards saturation point (100 % relative humidity) signals that frequent occurrences of exceedingly humid indoor environments would most likely be unavoidable.

As illustrated in the example of Bergen in Figure 33, the boxplots for 100 % of internal gains showed that indoor humidity was significantly high for long periods in the north-facing zones. Similarly, the south-facing zones experienced high humidity periods, as the whiskers of the boxplot reached up to maximum relative humidity. The results also showed that walls 01 – 09 performed almost identically as the 2226 wall. The negligible deviation from these results is seen in walls 10 – 12. When observed over the year, the relative humidity exhibited similar patterns as seen in Figure 19 and Figure 21 (section 4.1), which means that saturation occurred during winter.

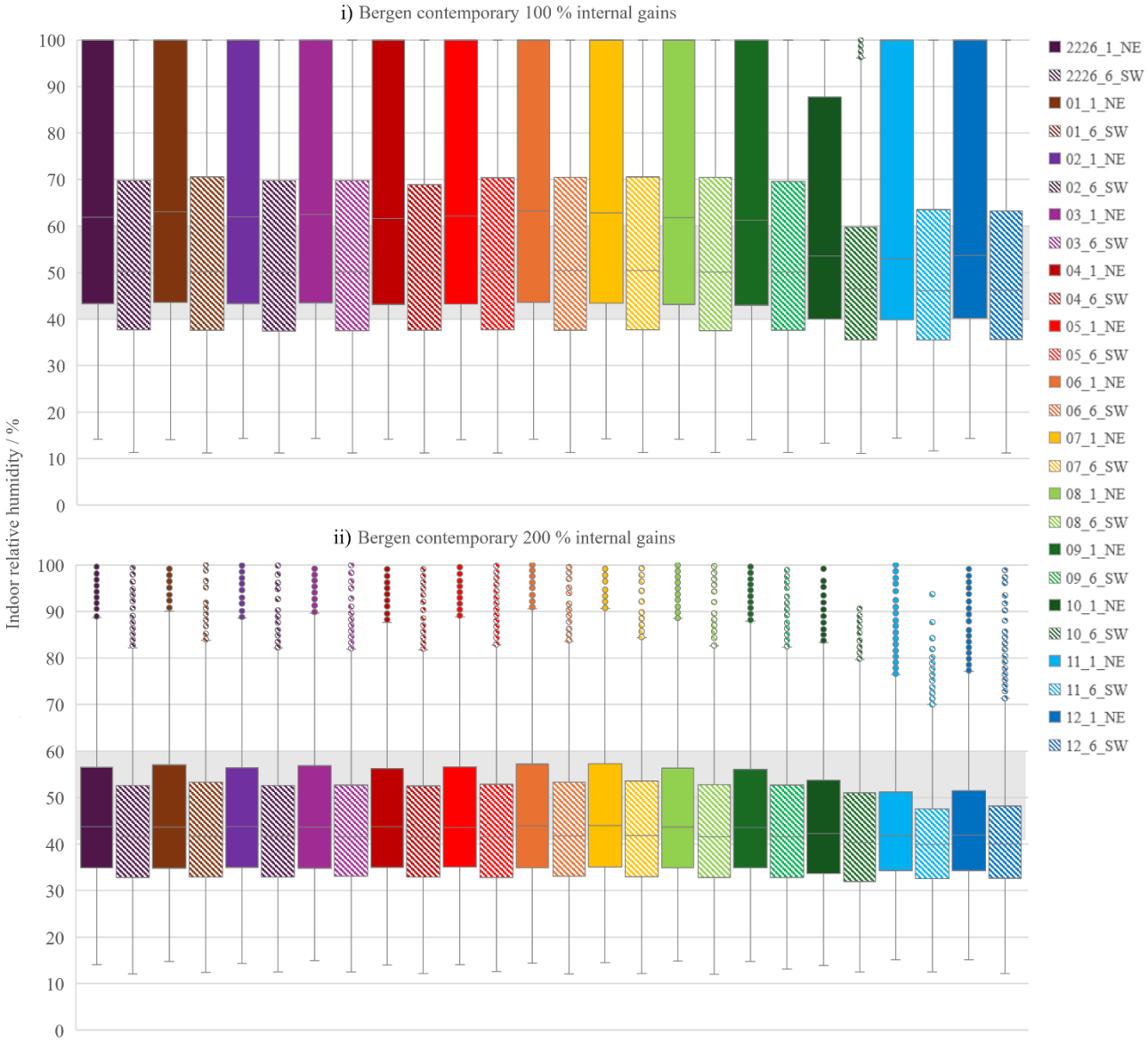

Figure 33. Boxplots of indoor relative humidity for all wall assemblies in the contemporary climate of Bergen, with 100 % of internal gains on top, and 200 % of internal gains on the bottom.

In most future climate scenarios, the results at 200 % of internal gains indicated a favorable indoor climate, as the range of boxplot whiskers was reduced, and the majority of hourly data was in the desired relative humidity range. However, as shown in the example for Jyväskylä in Figure 34, these conditions were diminished in the extreme future climate scenarios, where the whiskers stretched again up to 100 % relative humidity, regardless of the room orientation.

In the framework of the provided simulation setup, only the results for Copenhagen and Bergen showed a potential for enduring the harsher humidity conditions of the extreme future climate, as in those cases, only outlier data reached 100 % relative humidity.

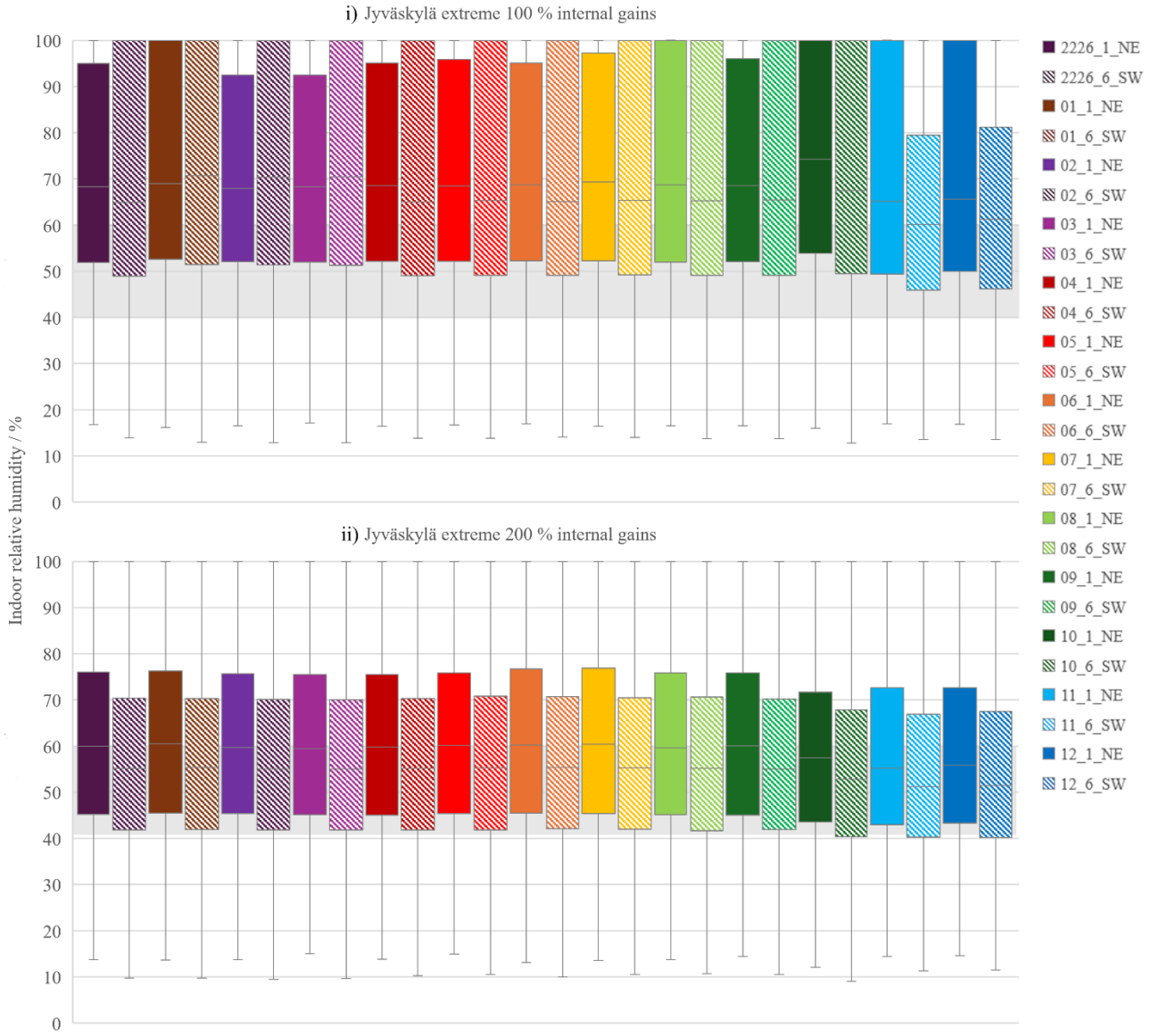

Figure 34. Boxplots of indoor relative humidity for all wall assemblies in the future extreme climate of Jyväskylä, with 100 % of internal gains on top, and 200 % of internal gains on the bottom.

5.4 Carbon Dioxide

The simulations show that the historic and contemporary climates have not allowed sufficiently low CO_2 concentrations. Combinations with 100 % internal gains yielded undesirably high concentrations, which is a result of weeks/months-long avoidance of window opening during winter. Likewise, a significant difference is observed between the south-facing and north-facing zones.

In colder climates of Östersund (Figure 35) and Jyväskylä, indoor CO_2 concentrations were too high even in the future and future extreme warming scenarios. In Helsinki and Karlstad, the results were slightly too high, with median values above 1500 ppm in the best-case scenario.

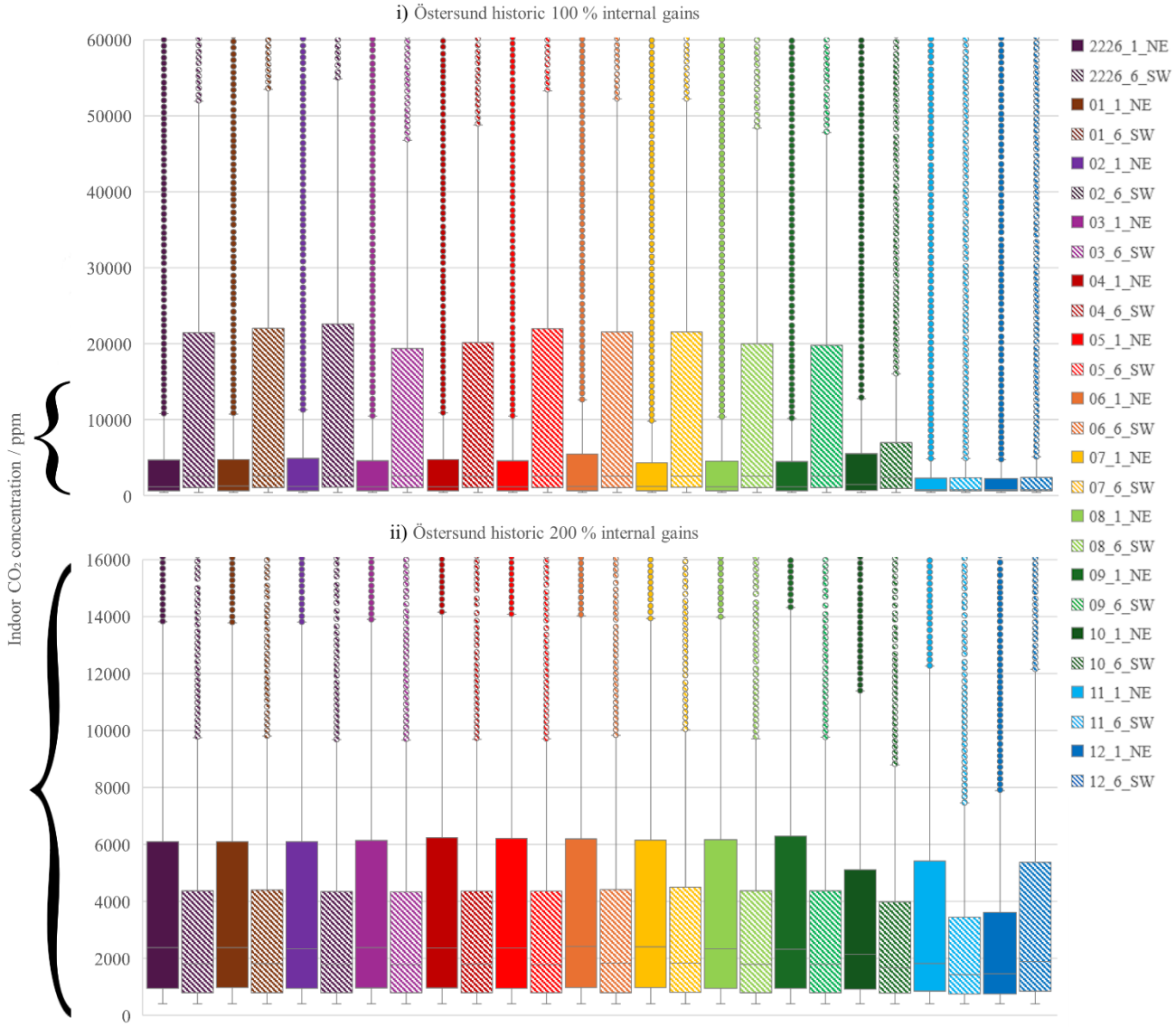

Figure 35. Boxplots of indoor carbon dioxide concentrations for all wall assemblies in the historic climate of Östersund, with 100 % of internal gains on top, and 200 % of internal gains on the bottom. The brackets on the left illustrate the scale of the graphs.

The results for Bergen (Figure 36) and Copenhagen showed promising results, as in all four climate scenarios, the indoor CO_2 concentrations were below 2000 ppm at least 75 % of the time for south-facing walls 11 and 12, while the median concentration value was around 1000 ppm. The south-facing wall 10 came close to these boundaries in the contemporary climate. Especially low CO_2 levels were obtained for all 13 south-facing wall assemblies in the future climate, where for at least 75 % of the time, the concentrations were below 1700 ppm, with the best-case being below 1400 ppm in the same timespan (walls 11 and 12). When observing the patterns over the whole year, it is noticeable that the CO_2 concentrations were not homogeneous. Instead,

relatively frequent spikes of higher concentration are witnessed, with spikes in winter being higher than those in summer.

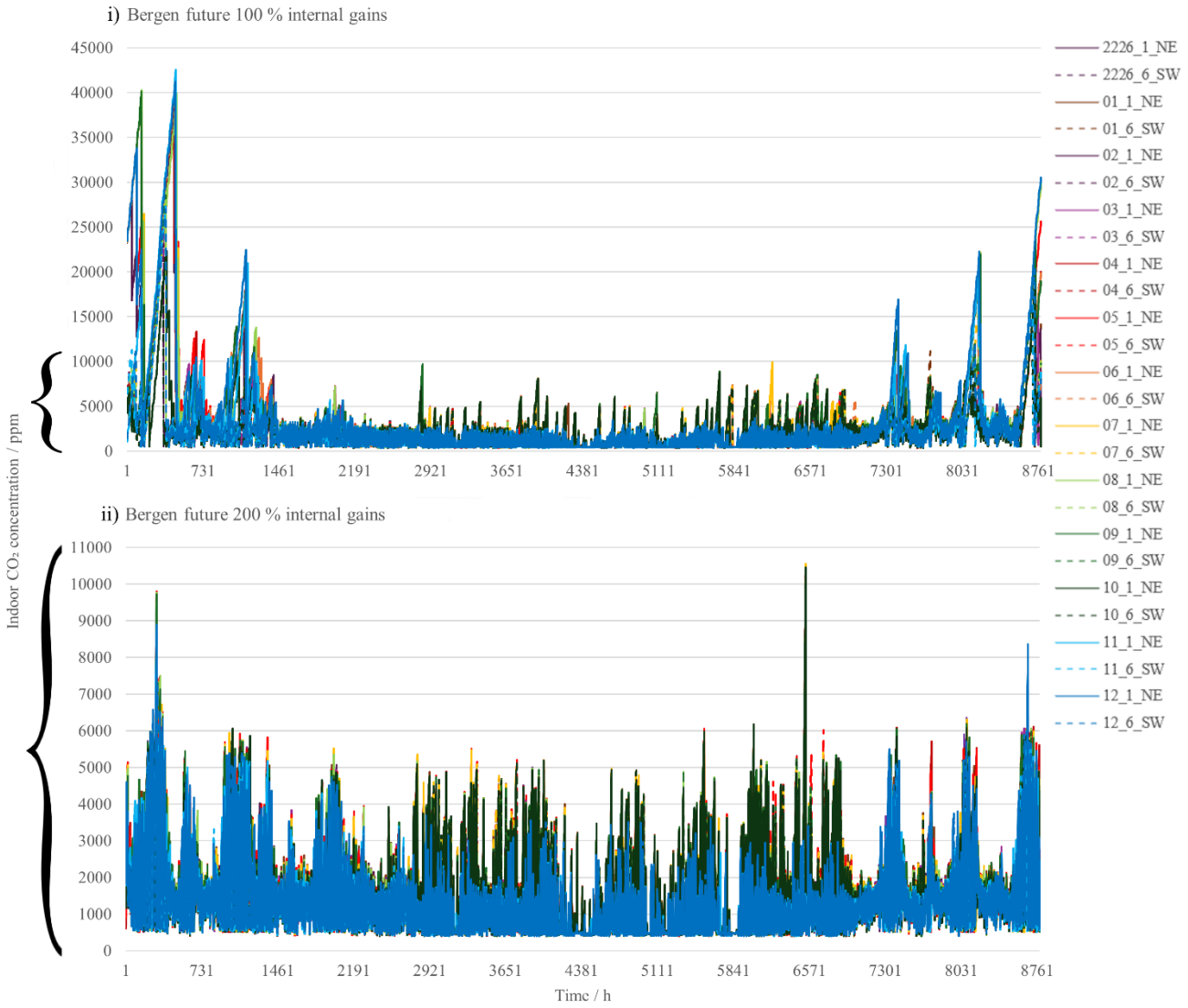

Figure 36. Indoor carbon dioxide concentrations over time for all wall assemblies in the future climate of Bergen, with 100 % of internal gains on top, and 200 % of internal gains on the bottom. The brackets on the left illustrate the scale of the graphs.

5.5 Discussion

Here, the simulation results are discussed with wider implications on free-running building performance.

5.5.1 Temperature and Thermal Inertia

All buildings are subject to dynamic heat and mass transport processes (Hall & Allinson, 2010). We can think of free-running buildings as those where indoor mechanical heating and cooling input was taken out of the heat equation. Therefore, in free-running buildings, the passive internal heat gains, solar gains, and heat dissipation/modulation strategies need to be balanced for successful building operation.
This explains why all north-facing zones, lacking solar gains, performed worse than the south-facing ones. In milder climates, however, the difference between room orientations was diminished, as solar gains there were relatively less significant. Similarly, with sufficiently high internal heat gains, north-facing rooms achieved desired temperatures even in lower outdoor temperatures.

The results emphasized that the simulated options were highly sensitive to the cold waves and heat waves, despite their high thermal insulation and thermal inertia. In particular, the majority of simulated combinations

with the lower rate of internal heat gains had difficulty in obtaining the target temperature range in cold winter, as discussed previously in section 4.4. The observed drop in indoor temperature during low outdoor temperatures, as seen for example in Figure 31, was a result of the inner workings of the natural ventilation algorithm, which evaluated different incoming signals for opening/closing rules from different sensors, with the opening signals manifestly outweighing the closing signals.

Among the walls, it was observed that all high-mass walls behaved almost identically as the original 2226 wall, while the differences were seen in wall 10 (lower *U*-value), and low-mass walls (11 and 12). This came as a surprise, as it was hypothesized that modifications in exterior wall layers would lead to different impacts of thermal inertia, which seemed here to be negligible.

Since low-mass walls had the same *U*-value as other walls (apart from wall 10), this indicated that thermal inertia and thermal insulation both had an impact on indoor thermal comfort.
If the internal areal heat capacity of low-mass exterior walls were equal to or greater than most of the studied high-mass walls, the difference in performance most likely stemmed from the significantly lower areal heat capacities of other interior surfaces, such as the floor, ceiling, and interior wall, which were 50 % – 75 % lower than the assemblies of the 2226 building. In other words, the heat modulation correlated with the exposed surface area of the high-mass materials.
When considering an individual zone, the combined surface area of these building components was greater than that of the external wall, signaling that their impact was more important than the thermal inertia of the external wall, confirming the studies by Feist (2000) and Long & Ye (2016). This can be of direct benefit to designers trying to limit the risk of overheating.

Between low-mass walls, wall 11 usually showed overheating a few decimals of a degree higher than wall 12, which can be considered negligible, and it is explained by the lower internal areal heat capacity of wall 11. Even though hemp-lime brick showed greater thermal mass than the strawbale, the strawbale wall performed better because it was covered by a thick layer of high-mass plaster.

In addition to overheating reduction, the major advantage of thermal inertia is its ability to modulate the impact of sudden weather changes over a day or a week (Karlsson et al., 2013), making outdoor temperature fluctuations less pronounced indoors. The potential for a greater or longer heat wave or cold wave (low-probability, high-risk events) should also not be crossed out.
These scenarios are not covered in the studied weather files, since they cover the assumed long-term climate average, and their temperature values were increased numerically, but not temporally (no heat wave for a longer time than the usual peak in summer). In the future climate with more extreme and severe weather (Patel & Kuttippurath, 2023), thermal inertia could and should be exploited to reduce or eliminate short-term heating and cooling demands.

Moreover, if only the usual future climate files had been investigated, these observations would not have been possible. As seen already in section 4.2 and Appendix B, the generated extreme climate for all weather stations brought cold waves similar to temperatures from historic or contemporary climates while creating heat waves significantly higher than the peaks of the „regular“ future climate.
The extreme future weather files were crucial in understanding the real risks of future weather, as they depicted atypical, but probable cold winters and hot summers.
It needs to be pointed out that these results were obtained without any shading devices, following the wall self-shading principle of the 2226 building. It is not clear how much the overheating risk would be alleviated in case a shading device were employed.

5.5.2 Relative Humidity and Carbon Dioxide

The results for the indoor relative humidity were the consequence of the natural ventilation algorithm that prevented the opening of windows for long periods of cold months. The synthetic occupant was not allowed to bring in the fresh air, so the human-generated humidity kept accumulating until reaching saturation point. Conversely, in instances where the algorithm decided to open the windows, thereby considerably decreasing indoor temperature, the excess humidity of humans was removed, but moisture damage would remain, as all interior surfaces condensed moisture from the air, thereby keeping the indoor environment too humid.
The difference in relative humidity between the north-facing and the south-facing zones was emphasized,

which supported the earlier observation that solar gains had a greater influence on thermal comfort and indoor climate when internal gains were low.

Paradoxically, in many simulated cases, low-mass walls 11 and 12 exhibited greater overlap with the ideal relative humidity range (between 40 % and 60 %). This was caused directly by their poorer temperature control ability, which means that the window-opening signal was more frequently triggered, thereby introducing fresh air more frequently. This is just a reflection of the functionality of the modeled natural ventilation system, and it does not mean that low-mass walls necessarily offer better indoor humidity conditions.

However, since the simulated low-mass materials were bio-based (hempcrete and strawbale insulation), truly accurate results were not obtained because the moisture buffer capacity had not been assessed by the simulation software (for additional context, refer to sections 2.2.2, 2.4.2, and 4.4). The evaporation and condensation cycles of water inside pores of bio-based materials lead to the uptake and release of latent heat, respectively, thereby reducing indoor temperature and humidity variation (Rahim et al., 2017).
Additionally, while maintaining a more stable indoor climate, the hygroscopic nature of bio-based materials might conflict with the thermal conductivity, as higher moisture uptake reduces the insulating properties of the building enclosure, causing uncertainties in building performance. Nonetheless, as shown by Evrard (2008), the thermal inertia of hempcrete (thermal diffusivity α) is unaffected by the increase in relative humidity. Total energy use that takes into account the latent heat cycle of hygroscopic materials and the dynamic behavior of thermal insulation properties needs to be investigated in greater detail.

The results for carbon dioxide support similar observations as stated for relative humidity, as both were connected to the window-opening mechanism. Throughout the year, the CO_2 concentrations experienced periodic spikes, with the highest concentrations observed in winter, in north-facing zones, and with lower internal heat gains.
The low-mass walls provided the lowest annual average CO_2 levels. In all locations, future climate scenarios reduced CO_2 concentrations, but the effect was diminished when the future extreme climate was simulated. At higher rates of internal heat gains, the windows were opened more frequently, allowing more fresh air. Satisfactory results were not attained in any of the simulated combinations with the lower internal heat gains. However, one can notice that most of the high CO_2 concentrations occurred between September and March in all studied locations, signaling that the natural ventilation concept worked successfully only in transitional and warm months when the outdoor temperature was approximately between 10 °C and 30 °C.

Similarly, slightly higher CO_2 levels (spikes) were simulated a few times in summer, coinciding with the strongest heat waves. This means that windows were intentionally not opened during the heat wave to prevent the excessively warm outdoor air from entering the rooms.
In cases where the duration and the intensity of the spike were reasonably short, one could expect the occupant to tolerate such occurrences, as reported in the study of the 2226 building by Junghans & Widerin (2017). Moreover, since the results could have been improved to an extent if the window-opening algorithm had been more fine-tuned, the viability of intermediate locations, such as Karlstad, could not be written off yet with absolute certainty.

5.5.3 Occupant Behavior

It was evident from the simulation results that the internal heat gains were largely insufficient. The standard residential rates of occupancy and the occupants' indoor energy use do not allow for the thermal autonomy of buildings in the Nordic countries. The proposed higher occupancy rate achieved much better results in temperature and indoor climate control. Such housing density might be too high for contemporary Nordic apartment design, but the increase in occupancy is a move towards a more austere/sustainable lifestyle, depending on the perspective. Devising new lifestyle solutions, based on greater living densities, may be an important challenge for planners, architects, and policymakers.

However, if the same building had different occupants (for example, office workers), with higher occupancy per surface area, and higher density of appliances and lighting, the outcome would have been more optimistic. This importance of internal heat gains leads to interesting implications. For example, could the occupants leave their house for an extended period? In the 2226 building in Lustenau, when the occupants are collectively absent during the winter holidays, their absence has to be compensated by continuously switched-

on lighting and other appliances. Otherwise, the indoor temperature drops below 21 °C. How long could the free-running building survive without the occupants before moisture damage is induced? Conversely, the occupants may be incentivized to change their daily habits in summer to generate as low indoor heat as possible. One could also ask how free-running buildings would respond in case of another global pandemic and lockdowns.

The performance of the building often boils down to the expectations and necessities of its users. In times of energy crisis, people are encouraged to wear long-sleeved instead of short-sleeved shirts or to adjust the thermostat setpoints. To what extent are residents willing to tolerate discomfort? For example, people with a higher sense of environmental responsibility/consciousness tend to be more tolerant towards a wider indoor temperature range (Yang et al., 2014).
Necessities will sooner or later provide the answer to such questions.

In the end, just like there are unknown unknowns in the field of climate science, there are also unknown unknowns in potential human responses. The variety of vernacular architecture reminds us that people are capable of devising excellent engineering solutions, as they have been doing throughout the millennia. Looking just at recent local changes in residential buildings in Sweden, it is evident that humans adapt to new challenges quite well (Kärrholm, 2020). This leaves hope that the challenges discussed in this study will also be surmounted.

6 Conclusion

The concluding chapter synthesizes the findings, with a reflection on the study's aim and objectives, evaluating the significance of the research, while highlighting areas for further investigation.

6.1 Aim and Objectives

Coming back to the overall aim and study objectives of this thesis, total work can be evaluated. The overall aim was to assess the viability of free-running residential buildings – relying exclusively on passive design strategies – to ensure future climate resilience in the Nordic region. The focus was on creating future-proof homes that can maintain a specified level of comfort without any use of active heating, cooling, or mechanical ventilation systems.

To meet the overall aim of the study, the objectives of the thesis were to:

1. *Identify possible passive design strategies applicable to the Nordic context, and understand the underlying mechanisms behind their performance.*

Based on the literature review, a variety of passive design measures were investigated. They comprised thermal insulation for heat retention/exclusion in winter/summer, respectively; thermal inertia for heat modulation; and natural ventilation for heat dissipation, as well as for the regulation of indoor air quality. The case study, "2226" building, served as an excellent starting point in understanding the practical aspects of free-running buildings. Additionally, bio-based materials (hemp and straw) were studied because of their low environmental footprint and promising physical properties. Consequently, several new building assembly solutions were proposed, and their performance was simulated.

2. *Specify the performance requirements for thermal comfort and indoor climate quality.*

An adaptive thermal comfort model based on the EN 16798-1:2019 standard was used in determining the thermal comfort of simulated results. The intensity and duration of summer overheating were addressed as well. For indoor environmental quality, the target ranges for desired relative humidity and carbon dioxide concentration have been determined, although the results of relative humidity were recognized to not be as accurate, due to the missing coupled hygrothermal simulations.

3. *Investigate the current and projected Nordic climate conditions to understand risks and vulnerabilities that could be alleviated with the identified passive measures.*

Four climate scenarios were generated using the tool Meteonorm for six Nordic locations to explore the impact of weather files on the practical viability of free-running buildings. They comprised the historic and contemporary climate data, and two future climates for the year 2100 under the IPCC RCP 8.5 scenario – the regular and the extreme (above average summer/below average winter) future weather files. In all locations, the future climate is expected to become significantly warmer, posing risks of overheating. In most cases, relative humidity will decrease in summer and increase in winter, increasing the importance of moisture-safe design.

4. *Evaluate the performance of proposed solutions by comparing the selected passive design strategies.*

The building performance was evaluated through dynamic simulations using the software IDA ICE. The case study building was modeled and modified parametrically to assess thermal comfort and indoor environmental quality. The parameters included various layers of the building enclosure and different rates of internal heat gains, simulated in every climate scenario and every location, amounting to 624 unique simulation configurations.
Thermal inertia and natural ventilation were useful passive conditioning mechanisms, although with partial applicability. The important conclusion for thermal inertia was that internal walls, floors, and ceilings had a far greater impact on heat modulation (expressed as internal areal heat capacity) than external walls.
The simulated relative humidity results indicated a critical limitation of the free-running building design in Nordic countries, revealing that while the concept could manage either temperature or relative humidity/CO_2

concentration, it could not balance all three criteria due to insufficient residential occupancy rates and internal heat gains to compensate for the lack of solar gains throughout the year.

5. *Provide insights into the influence of climate projections on future building performance.*

Since future predictions carry a high degree of uncertainty, no definite measure or recommendation can be described for a specific location. Depending on the exact direction of climate change, the Nordic region could experience extremely varying degrees of warming, and in some scenarios, even sharp cooling.
Although the building materials boasted high thermal inertia and low thermal transmittance, it was found that extreme future outdoor conditions significantly affected indoor conditions, and the thermal properties of the building enclosure had a limited potential to mitigate this effect.
This highlights the importance of assessing the risks of the worst-case scenarios. If it was too cold or too hot, passive building measures on their own simply did not fulfill their necessary functions. This means that the proposed buildings could be considered thermally resilient, but only in certain climate scenarios were they fully thermally autonomous.

By addressing these objectives, insight into free-running buildings was provided for the Nordic region, hopefully contributing to the further development of resilient, future-proof homes.

To conclude, the viability of free-running buildings in the Nordic context may not be answered with a simple "yes" or "no". As already shown by de Wilde & Tian (2012), the performance of the building in a specific climate will always depend on almost all inputs: the location, the user, the schedule, the internal gains, the building design, or thermal comfort preferences. However, every building designer is advised to try and maximize the potential of passive design solutions.

6.2 Significance

This was the first study that tried to quantify the year-round performance of free-running buildings in the Nordic region. The focus was on the potential application of the concept in residential buildings, propelled by the case study building, "2226" in Austria.

The study revealed the critical roles of thermal inertia, thermal transmittance, and natural ventilation, as well as their practical limits. The underwhelming results of the simulations do not mean that the research on passive design strategies is unnecessary. On the contrary, such building measures can lead to energy savings, reduced exposure to external risks, and increased thermal comfort, even if sometimes the occupants have to resort to active space conditioning.

The importance of the thesis is revealed in the decreased dependency on HVAC systems, paving the way for a more resilient building design. In addition, the insights on specific future climate conditions, and the performance of various building materials in combination with control systems provide useful knowledge to the broader field of climate adaptation.

6.3 Future Work

In future studies, different passive strategies could be explored. Many building parameters were left out of this research, which could help improve building performance. It is still an open question on the potential difference between the building geometry that was just copied and pasted in every location, and the one that would be tailor-made and optimized for the specific local climate requirements.

Future investigations should focus on resilient, low-tech design. There is a great variety of materials that may improve on the presented design, while potentially bringing higher environmental and economic benefits. The prospective research could explore the potential of bio-based materials to the fullest. Furthermore, building performance should be linked with the surrounding microclimate (for example, green roofs and green facades), extending the research of climate resilience to outdoor and urban design. Some studies have already paved the way in that direction. For example, "simple" low-energy buildings in Germany, with massive monolithic blocks of timber, clay brick, and concrete, were evaluated by Technische Universität München (2023). Prefabricated solid timber solutions, comprising purely timber joints (without metal connections,

construction adhesives, and typical insulating materials), are seeing commercial applications across several European countries (Holzius, 2024), (Thoma, 2024), (HRW, 2024).

A key understanding of free-running building performance was seen in moisture safety. This could be performed in hygrothermal simulation software, or by testing building assemblies in actual outdoor conditions. This comes with new obstacles. For example, the coupled heat-air-moisture transfer simulations still suffer from high computing requirements (Zu et al., 2020). In IDA ICE, it was not possible to fully assess the dynamic behavior of temperature and humidity transfer in bio-based materials. TRNSYS, for example, enables hygrothermal simulation with a simplified humidity model that does not consider moisture diffusion in hygroscopic materials (Medjelekh et al., 2016). In other software, however, it may not be possible to design advanced control mechanisms such as the automated window-opening algorithm.

The potential research is also seen in more accurate modeling of both sensor-based controls and advanced occupant models. Relatively recently, stochastic occupant models have been developed, allowing for individual differences and preferences, various interactions with the building, different personal activities, as well as the dynamic nature of occupant behavior (Jia et al., 2021). The advanced agent-based models are not yet widely implemented because of their inaccessibility, questionable transferability, and high computing requirements (Gunay et al., 2016). Nevertheless, it is hypothesized by the author of the thesis that there are substantial modeling improvements possible in the careful setup of setpoints and control mechanisms.

Finally, to comprehensively understand future risks, we need to better understand the links between the ecological overshoot, climate change, and resource decline. In future studies, more focus should be given to the understudied worst-case scenarios, such as crossing the planetary climate thresholds (particularly the AMOC collapse for Europe), derived from the latest evidence in climate science research. Only this approach will enable quantifying genuine risks and favorable adaptation strategies.

References

Abdallah, M., Al-Olofi, A., & Ahmed Youssef, H. (2020). Traditional Yemeni Architecture and Its Impact on Energy Efficiency. *International Journal of Engineering Research and Technology*, *13*. https://doi.org/10.37624/IJERT/13.8.2020.2014-2022

Albert, M. J. (2022). Beyond continuationism: Climate change, economic growth, and the future of world (dis)order. *Cambridge Review of International Affairs*, *35*(6), 868–887. https://doi.org/10.1080/09557571.2020.1825334

Allouhi, A., El Fouih, Y., Kousksou, T., Jamil, A., Zeraouli, Y., & Mourad, Y. (2015). Energy consumption and efficiency in buildings: Current status and future trends. *Journal of Cleaner Production*, *109*, 118–130. https://doi.org/10.1016/j.jclepro.2015.05.139

Andersen, R., Fabi, V., Toftum, J., Corgnati, S. P., & Olesen, B. W. (2013). Window opening behaviour modelled from measurements in Danish dwellings. *Building and Environment*, *69*, 101–113. https://doi.org/10.1016/j.buildenv.2013.07.005

Anderson, K. (2015). Duality in climate science. *Nature Geoscience*, *8*(12), 898–900. https://doi.org/10.1038/ngeo2559

Armstrong McKay, D. I., Staal, A., Abrams, J. F., Winkelmann, R., Sakschewski, B., Loriani, S., Fetzer, I., Cornell, S. E., Rockström, J., & Lenton, T. M. (2022). Exceeding 1.5°C global warming could trigger multiple climate tipping points. *Science*, *377*(6611), eabn7950. https://doi.org/10.1126/science.abn7950

Artmann, N., Manz, H., & Heiselberg, P. (2007). Parametric study on the dynamic heat storage capacity of building elements. *28th AIVC Conference*. https://vbn.aau.dk/en/publications/parametric-study-on-the-dynamic-heat-storage-capacity-of-building

Arutyunov, V. S., & Lisichkin, G. V. (2017). Energy resources of the 21st century: Problems and forecasts. Can renewable energy sources replace fossil fuels†. *Russian Chemical Reviews*, *86*(8), 777. https://doi.org/10.1070/RCR4723

Aste, N., Angelotti, A., & Buzzetti, M. (2009). The influence of the external walls thermal inertia on the energy performance of well insulated buildings. *Energy and Buildings*, *41*(11), 1181–1187. https://doi.org/10.1016/j.enbuild.2009.06.005

Bakkour, A., Ouldboukhitine, S.-E., Biwole, P., & Amziane, S. (2024). A review of multi-scale hygrothermal characteristics of plant-based building materials. *Construction and Building Materials*, *412*, 134850. https://doi.org/10.1016/j.conbuildmat.2023.134850

Barclay, M., Holcroft, N., & Shea, A. D. (2014). Methods to determine whole building hygrothermal performance of hemp–lime buildings. *Building and Environment*, *80*, 204–212. https://doi.org/10.1016/j.buildenv.2014.06.003

Bellard, C., Bertelsmeier, C., Leadley, P., Thuiller, W., & Courchamp, F. (2012). Impacts of climate change on the future of biodiversity. *Ecology Letters*, *15*(4), 365–377. https://doi.org/10.1111/j.1461-0248.2011.01736.x

Bellomo, K., Meccia, V. L., D'Agostino, R., Fabiano, F., Larson, S. M., Von Hardenberg, J., & Corti, S. (2023). Impacts of a weakened AMOC on precipitation over the Euro-Atlantic region in the EC-Earth3 climate model. *Climate Dynamics*, *61*(7–8), 3397–3416. https://doi.org/10.1007/s00382-023-06754-2

Benfratello, S., Capitano, C., Peri, G., Rizzo, G., Scaccianoce, G., & Sorrentino, G. (2013). Thermal and structural properties of a hemp–lime biocomposite. *Construction and Building Materials*, *48*, 745–754. https://doi.org/10.1016/j.conbuildmat.2013.07.096

Bergman, T. L., & Levine, A. S. (2019). *Fundamentals of heat and mass transfer* (Eighth edition Wiley loose-leaf print edition). John Wiley & Sons, Inc.

Berkely Earth. (2024). *Temperature Country List*. Berkeley Earth. https://berkeleyearth.org/temperature-country-list/

Borger, C., Beirle, S., & Wagner, T. (2022). Analysis of global trends of total column water vapour from multiple years of OMI observations. *Atmospheric Chemistry and Physics*, *22*(16), 10603–10621. https://doi.org/10.5194/acp-22-10603-2022

Borrelle, S. B., Ringma, J., Law, K. L., Monnahan, C. C., Lebreton, L., McGivern, A., Murphy, E., Jambeck, J., Leonard, G. H., Hilleary, M. A., Eriksen, M., Possingham, H. P., De Frond, H., Gerber, L. R., Polidoro, B., Tahir, A., Bernard, M., Mallos, N., Barnes, M., & Rochman, C. M. (2020). Predicted growth in plastic waste exceeds efforts to mitigate plastic pollution. *Science*, *369*(6510), 1515–1518. https://doi.org/10.1126/science.aba3656

Bournas, I. (2021). *Daylight compliance of multi-dwelling apartment blocks: Design considerations, evaluation criteria and occupant responses* [Doctoral Thesis (compilation)]. Department of Architecture and Built Environment, Lund University.

Brännlund, A., Amcoff, J., Österman, M., Peterson, L., & Brännlund, H. (2024). Jolts at the ballot box: Electricity prices and voting in Swedish manufacturing communities. *Energy Research & Social Science*, *110*, 103419. https://doi.org/10.1016/j.erss.2024.103419

Brauer, H. B., Hasselqvist, H., Håkansson, M., Willermark, S., & Hiller, C. (2024). Re-configuring practices in times of energy crisis – A case study of Swedish households. *Energy Research & Social Science*, *114*, 103578. https://doi.org/10.1016/j.erss.2024.103578

Bravo Dias, J., Soares, P. M. M., & Carrilho Da Graça, G. (2020). The shape of days to come: Effects of climate change on low energy buildings. *Building and Environment*, *181*, 107125. https://doi.org/10.1016/j.buildenv.2020.107125

Bugenings, L. A., & Kamari, A. (2022). Bioclimatic Architecture Strategies in Denmark: A Review of Current and Future Directions. *Buildings*, *12*(2), 224. https://doi.org/10.3390/buildings12020224

Bulińska, A., Popiołek, Z., & Buliński, Z. (2014). Experimentally validated CFD analysis on sampling region determination of average indoor carbon dioxide concentration in occupied space. *Building and Environment*, *72*, 319–331. https://doi.org/10.1016/j.buildenv.2013.11.001

Cao, X., Dai, X., & Liu, J. (2016). Building energy-consumption status worldwide and the state-of-the-art technologies for zero-energy buildings during the past decade. *Energy and Buildings*, *128*, 198–213. https://doi.org/10.1016/j.enbuild.2016.06.089

Cardinale, N., Rospi, G., & Stefanizzi, P. (2013). Energy and microclimatic performance of Mediterranean vernacular buildings: The Sassi district of Matera and the Trulli district of Alberobello. *Building and Environment*, *59*, 590–598. https://doi.org/10.1016/j.buildenv.2012.10.006

Cascione, V., Maskell, D., Shea, A., & Walker, P. (2021). The moisture buffering performance of plasters when exposed to simultaneous sinusoidal temperature and RH variations. *Journal of Building Engineering*, *34*, 101890. https://doi.org/10.1016/j.jobe.2020.101890

Ceballos, G., Ehrlich, P. R., Barnosky, A. D., García, A., Pringle, R. M., & Palmer, T. M. (2015). Accelerated modern human–induced species losses: Entering the sixth mass extinction. *Science Advances*, *1*(5), e1400253. https://doi.org/10.1126/sciadv.1400253

Chen, R., Samuelson, H., Zou, Y., Zheng, X., & Cao, Y. (2024). Improving building resilience in the face of future climate uncertainty: A comprehensive framework for enhancing building life cycle performance. *Energy and Buildings*, *302*, 113761. https://doi.org/10.1016/j.enbuild.2023.113761

Ciancio, V., Falasca, S., Golasi, I., De Wilde, P., Coppi, M., De Santoli, L., & Salata, F. (2019). Resilience of a Building to Future Climate Conditions in Three European Cities. *Energies*, *12*(23), 4506. https://doi.org/10.3390/en12234506

Climate Reanalyzer. (2024). https://climatereanalyzer.org/clim/sst_daily/

Cony Renaud Salis, L., Abadie, M., Wargocki, P., & Rode, C. (2017). Towards the definition of indicators for assessment of indoor air quality and energy performance in low-energy residential buildings. *Energy and Buildings*, *152*, 492–502. https://doi.org/10.1016/j.enbuild.2017.07.054

Country Overshoot Days. (2024). *Earth Overshoot Day*. https://overshoot.footprintnetwork.org/newsroom/country-overshoot-days/

de Dear, R. J., & Brager, G. S. (2002). Thermal comfort in naturally ventilated buildings: Revisions to ASHRAE Standard 55. *Energy and Buildings*, *34*(6). https://doi.org/10.1016/S0378-7788(02)00005-1

de Wilde, P., & Coley, D. (2012). The implications of a changing climate for buildings. *Building and Environment*, *55*, 1–7. https://doi.org/10.1016/j.buildenv.2012.03.014

de Wilde, P., & Tian, W. (2012). Management of thermal performance risks in buildings subject to climate change. *Building and Environment*, *55*, 167–177. https://doi.org/10.1016/j.buildenv.2012.01.018

Egenolf, V., Distelkamp, M., Morland, C., Beck-O'Brien, M., & Bringezu, S. (2022). The timber footprint of German bioeconomy scenarios compared to the planetary boundaries for sustainable roundwood supply. *Sustainable Production and Consumption*, *33*, 686–699. https://doi.org/10.1016/j.spc.2022.07.029

Ejstrup, H., Kjær Frederiksen, L., Hildebrand, L., Stylsvig Madsen, U., Munch-Petersen, P., & Sköld, S. (2019). *Cirkulært Byggeri: Materiale Arkitektur Tektonik*. The Royal Danish Academy of Fine Arts, Schools of Architecture, Design and Conservation.

Energy consumption in households. (2023). https://ec.europa.eu/eurostat/statistics-explained/index.php?title=Energy_consumption_in_households

Eurostat. (2022a). *Average household size* [Dataset]. https://doi.org/10.2908/ILC_LVPH01

Eurostat. (2022b). *Average size of dwelling* [Dataset]. https://doi.org/10.2908/ILC_HCMH02

Eurostat. (2022c). *Under-occupied dwellings* [Dataset]. https://doi.org/10.2908/ILC_LVHO50A

Evrard, A. (2008). *Transient hygrothermal behaviour of lime-hemp materials*. https://www.researchgate.net/profile/Arnaud-Evrard-2/publication/283568943_Transient_hygrothermal_behavior_of_Lime-Hemp_Materials/links/563f849608ae34e98c4e714c/Transient-hygrothermal-behavior-of-Lime-Hemp-Materials.pdf

Fanger, P. O. (1973). Assessment of man's thermal comfort in practice. *Occupational and Environmental Medicine*, *30*(4), 313–324. https://doi.org/10.1136/oem.30.4.313

Fannon, D., Laboy, M., & Wiederspahn, P. (2021). *The Architecture of Persistence: Designing for Future Use*. Routledge. https://doi.org/10.4324/9781003042013

Farahani, A. V., Jokisalo, J., Korhonen, N., Jylhä, K., & Kosonen, R. (2024). Hot Summers in Nordic Apartments: Exploring the Correlation between Outdoor Weather Conditions and Indoor Temperature. *Buildings*, *14*(4), Article 4. https://doi.org/10.3390/buildings14041053

Feist, W. (2000). *Ist Wärmespeichern wichtiger als Wärmedämmen?* Passivhaus Institut. https://shop.passivehouse.com/de/products/ist-warmespeichern-wichtiger-als-warmedammen-90/

Fischer, E. M., & Knutti, R. (2015). Anthropogenic contribution to global occurrence of heavy-precipitation and high-temperature extremes. *Nature Climate Change*, *5*(6), 560–564. https://doi.org/10.1038/nclimate2617

Foldbjerg, P., Asmussen, T., & Holzer, P. (2014). Ventilative Cooling of Residential Buildings—Strategies, Measurement Results and Lessons Learned from Three Active Houses in Austria, Germany and Denmark. *International Journal of Ventilation*, *13*(2), 179–192. https://doi.org/10.1080/14733315.2014.11684047

Gaupp, F., Hall, J., Hochrainer-Stigler, S., & Dadson, S. (2020). Changing risks of simultaneous global breadbasket failure. *Nature Climate Change*, *10*(1), 54–57. https://doi.org/10.1038/s41558-019-0600-z

Grazieschi, G., Gori, P., Lombardi, L., & Asdrubali, F. (2020). Life cycle energy minimization of autonomous buildings. *Journal of Building Engineering*, *30*, 101229. https://doi.org/10.1016/j.jobe.2020.101229

Guide A: Environmental design (2015) | CIBSE. (2015). https://www.cibse.org/knowledge-research/knowledge-portal/guide-a-environmental-design-2015

Gunay, H. B., O'Brien, W., & Beausoleil-Morrison, I. (2016). Implementation and comparison of existing occupant behaviour models in EnergyPlus. *Journal of Building Performance Simulation*, *9*(6), 567–588. https://doi.org/10.1080/19401493.2015.1102969

Gutai, M., & Kheybari, A. G. (2020). *Energy consumption of water-filled glass (WFG) hybrid building envelope*. https://doi.org/10.1016/j.enbuild.2020.110050']

Hall, M. R., & Allinson, D. (2010). Heat and mass transport processes in building materials. In M. R. Hall (Ed.), *Materials for Energy Efficiency and Thermal Comfort in Buildings* (pp. 3–53). Woodhead Publishing. https://doi.org/10.1533/9781845699277.1.3

Hanjra, M. A., & Qureshi, M. E. (2010). Global water crisis and future food security in an era of climate change. *Food Policy*, *35*(5), 365–377. https://doi.org/10.1016/j.foodpol.2010.05.006

Hansen, J. E. (2007). Scientific reticence and sea level rise. *Environmental Research Letters*, *2*(2), 024002. https://doi.org/10.1088/1748-9326/2/2/024002

Hansen, J. E., Sato, M., Hearty, P., Ruedy, R., Kelley, M., Masson-Delmotte, V., Russell, G., Tselioudis, G., Cao, J., Rignot, E., Velicogna, I., Tormey, B., Donovan, B., Kandiano, E., von Schuckmann, K., Kharecha, P., Legrande, A. N., Bauer, M., & Lo, K.-W. (2016). Ice melt, sea level rise and superstorms: Evidence from paleoclimate data, climate modeling, and modern observations that 2 °C global warming could be dangerous. *Atmospheric Chemistry and Physics*, *16*(6), 3761–3812. https://doi.org/10.5194/acp-16-3761-2016

Hansen, J. E., Sato, M., Simons, L., Nazarenko, L. S., Sangha, I., Kharecha, P., Zachos, J. C., von Schuckmann, K., Loeb, N. G., Osman, M. B., Jin, Q., Tselioudis, G., Jeong, E., Lacis, A., Ruedy, R., Russell, G., Cao, J., & Li, J. (2023). Global warming in the pipeline. *Oxford Open Climate Change*, *3*(1), kgad008. https://doi.org/10.1093/oxfclm/kgad008

Hertwich, E. G., Gibon, T., Bouman, E. A., Arvesen, A., Suh, S., Heath, G. A., Bergesen, J. D., Ramirez, A., Vega, M. I., & Shi, L. (2015). Integrated life-cycle assessment of electricity-supply scenarios confirms global environmental benefit of low-carbon technologies. *Proceedings of the National Academy of Sciences*, *112*(20), 6277–6282. https://doi.org/10.1073/pnas.1312753111

HFA-ÖGH. (2024). *Dataholz—Catalogue of reviewed timber building components—Dataholz.eu*. https://www.dataholz.eu/en/index.htm

Hickel, J., & Kallis, G. (2020). Is Green Growth Possible? *New Political Economy*, *25*(4), 469–486. https://doi.org/10.1080/13563467.2019.1598964

Holzius. (2024). *Das Vollholzhaus von holzius*. Holzius. https://www.holzius.com/de/

Hong, T., Malik, J., Krelling, A., O'Brien, W., Sun, K., Lamberts, R., & Wei, M. (2023). Ten questions concerning thermal resilience of buildings and occupants for climate adaptation. *Building and Environment*, *244*, 110806. https://doi.org/10.1016/j.buildenv.2023.110806

HRW. (2024). *HOME*. H.R.W. Vollholzwandsystem Obb. | Natürlich Bauen - Gesund Wohnen! https://hrw-vollholzwandsystem.de/

Huang, L., Krigsvoll, G., Johansen, F., Liu, Y., & Zhang, X. (2018). Carbon emission of global construction sector. *Renewable and Sustainable Energy Reviews*, *81*, 1906–1916. https://doi.org/10.1016/j.rser.2017.06.001

Hugentobler, W., Widerin, P., Junghans, L., & Bruijn, W. (2016, July 31). *DO HEALTHY BUILDINGS NEED TECHNOLOGY?* https://www.researchgate.net/publication/330011167_DO_HEALTHY_BUILDINGS_NEED_TECHNOLOGY

Huo, X., Yang, L., Li, D. H. W., Zhai, Y., & Lou, S. (2023). A novel index for assessing the climate potential of free-running buildings based on the acceptable upper limits of thermal comfort models across China. *Energy Conversion and Management*, *278*, 116692. https://doi.org/10.1016/j.enconman.2023.116692

IEA EBC Annex 69. (2020). https://iea-ebc.org/Data/publications/EBC_Annex_69_Deliverable_3.pdf

International Energy Agency. (2022). *Europe – Countries & Regions*. IEA. https://www.iea.org/regions/europe

IsoHemp. (2024). *Technical documentation IsoHemp* [Text]. IsoHemp - Sustainable Building and Renovating with Hempcrete Blocks. https://www.isohemp.com/en/technical-documentation

Jia, M., Srinivasan, R., Ries, R., Bharathy, G., & Weyer, N. (2021). Investigating the Impact of Actual and Modeled Occupant Behavior Information Input to Building Performance Simulation. *Buildings*, *11*(1), 32. https://doi.org/10.3390/buildings11010032

Jolly, W. M., Cochrane, M. A., Freeborn, P. H., Holden, Z. A., Brown, T. J., Williamson, G. J., & Bowman, D. M. J. S. (2015). Climate-induced variations in global wildfire danger from 1979 to 2013. *Nature Communications*, *6*(1), 7537. https://doi.org/10.1038/ncomms8537

Junghans, L. (2016). Concept 22/26, a High Performance Office Building Without Active Heating, Cooling and Ventilation Systems. *Proceedings of the ISES Solar World Congress 2015*, 1–10. https://doi.org/10.18086/swc.2015.08.07

Junghans, L., & Widerin, P. (2017). Thermal comfort and indoor air quality of the "Concept 22/26", a new high performance building standard. *Energy and Buildings*, *149*, 114–122. https://doi.org/10.1016/j.enbuild.2017.05.020

Kanters, J., Kulsomboon, M., & Bruijn, P. S. (2023). The potential of agricultural residual waste as building material in South Sweden. *Journal of Physics: Conference Series*, *2600*(16), 162005. https://doi.org/10.1088/1742-6596/2600/16/162005

Karlsson, J., Wadsö, L., & Öberg, M. (2013). A conceptual model that simulates the influence of thermal inertia in building structures. *Energy and Buildings*, *60*, 146–151. https://doi.org/10.1016/j.enbuild.2013.01.017

Kärrholm, M. (2020). The Life and Death of Residential Room Types: A Study of Swedish Building Plans, 1750–2010. *Architectural Histories*, *8*(1), Article 1. https://doi.org/10.5334/ah.343

Kemp, L., Xu, C., Depledge, J., Ebi, K. L., Gibbins, G., Kohler, T. A., Rockström, J., Scheffer, M., Schellnhuber, H. J., Steffen, W., & Lenton, T. M. (2022). Climate Endgame: Exploring catastrophic climate change scenarios. *Proceedings of the National Academy of Sciences*, *119*(34), e2108146119. https://doi.org/10.1073/pnas.2108146119

Khovalyg, D., Chatterjee, A., Sellers, A. J., & van Marken Lichtenbelt, W. (2023). Behavioral adaptations to cold environments: A comparative study of active nomadic and modern sedentary lifestyles. *Building and Environment, 243*, 110664. https://doi.org/10.1016/j.buildenv.2023.110664

Kjellström, E., Hansen, F., & Belušić, D. (2022). *Contributions from Changing Large-Scale Atmospheric Conditions to Changes in Scandinavian Temperature and Precipitation Between Two Climate Normals* (1). *74*(1), Article 1. https://doi.org/10.16993/tellusa.49

Klein, C. (2016). Ein Haus im Rheintal \ A House in the Rhine Valley. In D. Eberle & F. Aicher (Eds.), *Be baumschlager eberle 22 26—Die Temperatur der Architektur / The Temperature of Architecture* (pp. 2–15). De Gruyter. https://doi.org/10.1515/9783035603873-001

Korjenic, A., Petránek, V., Zach, J., & Hroudová, J. (2011). Development and performance evaluation of natural thermal-insulation materials composed of renewable resources. *Energy and Buildings*, *43*(9), 2518–2523. https://doi.org/10.1016/j.enbuild.2011.06.012

Kotireddy, R., Hoes, P.-J., & Hensen, J. L. M. (2018). A methodology for performance robustness assessment of low-energy buildings using scenario analysis. *Applied Energy*, *212*, 428–442. https://doi.org/10.1016/j.apenergy.2017.12.066

Kreiger, B. K., & Srubar, W. V. (2019). Moisture buffering in buildings: A review of experimental and numerical methods. *Energy and Buildings*, *202*, 109394. https://doi.org/10.1016/j.enbuild.2019.109394

Latif, E., Lawrence, M., Shea, A., & Walker, P. (2015). Moisture buffer potential of experimental wall assemblies incorporating formulated hemp-lime. *Building and Environment, 93*, 199–209. https://doi.org/10.1016/j.buildenv.2015.07.011

Leo Samuel, D. G., Dharmasastha, K., Shiva Nagendra, S. M., & Maiya, M. P. (2017). Thermal comfort in traditional buildings composed of local and modern construction materials. *International Journal of Sustainable Built Environment*, *6*(2), 463–475. https://doi.org/10.1016/j.ijsbe.2017.08.001

Li, J., Foden, G. W., Chow, S. K. W., & To, L. S. (2024). Integrating sustainable and energy-resilient strategies into emergency shelter design. *Renewable and Sustainable Energy Reviews*, *191*, 113968. https://doi.org/10.1016/j.rser.2023.113968

Ljubas, M. (2024, June 19). *Future-ready Nordic homes: Responding to the Changing Climate with Free-running Buildings; Digital Repository of Obtained Results*. Zenodo. https://doi.org/10.5281/zenodo.12172627

Loeb, N. G., Johnson, G. C., Thorsen, T. J., Lyman, J. M., Rose, F. G., & Kato, S. (2021). Satellite and Ocean Data Reveal Marked Increase in Earth's Heating Rate. *Geophysical Research Letters*, *48*(13), e2021GL093047. https://doi.org/10.1029/2021GL093047

Logan, T. M., Aven, T., Guikema, S. D., & Flage, R. (2022). Risk science offers an integrated approach to resilience. *Nature Sustainability*, *5*(9), 741–748. https://doi.org/10.1038/s41893-022-00893-w

Long, L., & Ye, H. (2016). The roles of thermal insulation and heat storage in the energy performance of the wall materials: A simulation study. *Scientific Reports*, *6*(1), 24181. https://doi.org/10.1038/srep24181

Lönngren, J., & van Poeck, K. (2020). Wicked problems: A mapping review of the literature. *International Journal of Sustainable Development & World Ecology*, *21*(6). https://doi.org/10.1080/13504509.2020.1859415

MacAskill, K., & Guthrie, P. (2014). Multiple Interpretations of Resilience in Disaster Risk Management. *Procedia Economics and Finance*, *18*, 667–674. https://doi.org/10.1016/S2212-5671(14)00989-7

Maierhofer, D., Röck, M., Ruschi Mendes Saade, M., Hoxha, E., & Passer, A. (2022). Critical life cycle assessment of the innovative passive nZEB building concept 'be 2226' in view of net-zero carbon targets. *Building and Environment*, *223*, 109476. https://doi.org/10.1016/j.buildenv.2022.109476

Malik, J., Hong, T., Wei, M., & Rotmann, S. (2024). Prioritize energy sufficiency to decarbonize our buildings. *Nature Human Behaviour*, *8*(3), 406–410. https://doi.org/10.1038/s41562-023-01752-0

Mao, D., Yang, S., Ma, L., Ma, W., Yu, Z., Xi, F., & Yu, J. (2024). Overview of life cycle assessment of recycling end-of-life photovoltaic panels: A case study of crystalline silicon photovoltaic panels. *Journal of Cleaner Production*, *434*, 140320. https://doi.org/10.1016/j.jclepro.2023.140320

Marsh, R., Larsen, V. G., & Kragh, M. (2010). Housing and energy in Denmark: Past, present, and future challenges. *Building Research & Information*, *38*(1), 92–106. https://doi.org/10.1080/09613210903226608

MASEA. (2024). *MASEA Datenbank*. https://www.masea-ensan.com/

McGregor, F., Heath, A., Shea, A., & Lawrence, M. (2014). The moisture buffering capacity of unfired clay masonry. *Building and Environment*, *82*, 599–607. https://doi.org/10.1016/j.buildenv.2014.09.027

Medjelekh, D., Ulmet, L., Abdou, S., & Dubois, F. (2016). A field study of thermal and hygric inertia and its effects on indoor thermal comfort: Characterization of travertine stone envelope. *Building and Environment*, *106*, 57–77. https://doi.org/10.1016/j.buildenv.2016.06.010

Medved, S. (2022). *Building Physics: Heat, Ventilation, Moisture, Light, Sound, Fire, and Urban Microclimate*. Springer International Publishing. https://doi.org/10.1007/978-3-030-74390-1

Meteotest. (2023). *Meteonorm 8.2 Manual*. Meteonorm (En). https://meteonorm.com/en/meteonorm-documents

Michaux, S. (2021). *Assessment of the Extra Capacity Required of Alternative Energy Electrical Power Systems to Completely Replace Fossil Fuels*. https://doi.org/10.13140/RG.2.2.34895.00160

Minke, G., & Krick, B. (2020). *Straw Bale Construction Manual | Design and Technology of a Sustainable Architecture*. Birkhäuser. https://birkhauser.com/books/9783035618754

Moazami, A., Nik, V. M., Carlucci, S., & Geving, S. (2019). Impacts of future weather data typology on building energy performance – Investigating long-term patterns of climate change and extreme weather conditions. *Applied Energy*, *238*, 696–720. https://doi.org/10.1016/j.apenergy.2019.01.085

Morgan Pattison, P., Hansen, M., & Tsao, J. Y. (2018). LED lighting efficacy: Status and directions. *Comptes Rendus Physique*, *19*(3), 134–145. https://doi.org/10.1016/j.crhy.2017.10.013

Moriarty, P., & Honnery, D. (2016). Can renewable energy power the future? *Energy Policy*, *93*, 3–7. https://doi.org/10.1016/j.enpol.2016.02.051

Mustak, Sk. (2022). Climate Change and Disaster-Induced Displacement in the Global South: A Review. In A. R. Siddiqui & A. Sahay (Eds.), *Climate Change, Disaster and Adaptations: Contextualising Human Responses to Ecological Change* (pp. 107–120). Springer International Publishing. https://doi.org/10.1007/978-3-030-91010-5_9

Naumann, G., Schropp, E., & Gaderer, M. (2022). Life Cycle Assessment of an Air-Source Heat Pump and a Condensing Gas Boiler Using an Attributional and a Consequential Approach. *Procedia CIRP*, *105*, 351–356. https://doi.org/10.1016/j.procir.2022.02.058

Nicol, F., & Humphreys, M. (2010). Derivation of the adaptive equations for thermal comfort in free-running buildings in European standard EN15251. *Building and Environment*, *45*(1), 11–17. https://doi.org/10.1016/j.buildenv.2008.12.013

Nicol, J. F., & Humphreys, M. A. (1973). Thermal comfort as part of a self-regulating system. *Building Research and Practice*, *1*(3), 174–179. https://doi.org/10.1080/09613217308550237

Nicol, J. F., & Humphreys, M. A. (2002). Adaptive thermal comfort and sustainable thermal standards for buildings. *Energy and Buildings*, *34*(6), 563–572. https://doi.org/10.1016/S0378-7788(02)00006-3

Nik, V. M. (2016). Making energy simulation easier for future climate – Synthesizing typical and extreme weather data sets out of regional climate models (RCMs). *Applied Energy*, *177*, 204–226. https://doi.org/10.1016/j.apenergy.2016.05.107

Nik, V. M., Mundt-Petersen, S. O., Kalagasidis, A. S., & De Wilde, P. (2015). Future moisture loads for building facades in Sweden: Climate change and wind-driven rain. *Building and Environment*, *93*, 362–375. https://doi.org/10.1016/j.buildenv.2015.07.012

Norén, A., Akander, J., Isfält, E., & Söderström, O. (1999). The effect of thermal inertia on energy requirement in a Swedish building—Results obtained with three calculation models. *International Journal of Low Energy and Sustainable Buildings*, *1*, 1–16.

Norwegian Centre for Climate Service. (2017). *Klima i Norge 2100—Norsk klimaservicesenter*. https://klimaservicesenter.no/kss/rapporter/kin2100

Oropeza-Perez, I., & Østergaard, P. A. (2014). Potential of natural ventilation in temperate countries – A case study of Denmark. *Applied Energy*, *114*, 520–530. https://doi.org/10.1016/j.apenergy.2013.10.008

Osanyintola, O. F., & Simonson, C. J. (2006). Moisture buffering capacity of hygroscopic building materials: Experimental facilities and energy impact. *Energy and Buildings*, *38*(10), 1270–1282. https://doi.org/10.1016/j.enbuild.2006.03.026

Our World in Data. (2018). *CO_2 emissions per capita vs. GDP per capita*. Our World in Data. https://ourworldindata.org/grapher/co2-emissions-vs-gdp

Our World in Data. (2022). *Energy use per person*. Our World in Data. https://ourworldindata.org/grapher/per-capita-energy-use

Palme, M., Inostroza, L., Villacreses, G., Lobato-Cordero, A., & Carrasco, C. (2017). From urban climate to energy consumption. Enhancing building performance simulation by including the urban heat island effect. *Energy and Buildings*, *145*, 107–120. https://doi.org/10.1016/j.enbuild.2017.03.069

Palumbo, M., Lacasta, A. M., Holcroft, N., Shea, A., & Walker, P. (2016). Determination of hygrothermal parameters of experimental and commercial bio-based insulation materials. *Construction and Building Materials*, *124*, 269–275. https://doi.org/10.1016/j.conbuildmat.2016.07.106

Patel, V. K., & Kuttippurath, J. (2023). Increase in Tropospheric Water Vapor Amplifies Global Warming and Climate Change. *Ocean-Land-Atmosphere Research*, *2*, 0015. https://doi.org/10.34133/olar.0015

Pelzeter, A. (2017). *Lebenszyklus-Management von Immobilien – Ressourcen- und Umweltschonung in Gebäudekonzeption und –betrieb*.

Pérez-Lombard, L., Ortiz, J., & Pout, C. (2008). A review on buildings energy consumption information. *Energy and Buildings*, *40*(3), 394–398. https://doi.org/10.1016/j.enbuild.2007.03.007

Persily, A. (2022). Development and application of an indoor carbon dioxide metric. *Indoor Air*, *32*(7), e13059. https://doi.org/10.1111/ina.13059

Peuhkuri, R., Lone, H., Time, B., Gustavsen, A., Ojanen, T., Ahonen, J., Svennberg, K., Harderup, L.-E., & Arfvidsson, J. (2006). *Moisture Buffering of Building Materials*. Technical University of Denmark DTU. https://www.byg.dtu.dk/forskning/publikationer/byg_rapporter

Porotherm 38 H.i Plan. (2023). Austria. https://www.wienerberger.at/produkte/wand/produktkatalog/porotherm-38-h_i-plan.html

Porotherm 38 Plan. (2023). Austria. https://www.wienerberger.at/produkte/wand/produktkatalog/porotherm-38-plan.html

Porras-Salazar, J. A., Flor, J.-F., & Obando Robles, M. (2023). Thermal Performance Assessment of Vernacular Earth Buildings in Tropical Climates: A Case Study in Costa Rica. In L. Marín-Restrepo, A. Pérez-Fargallo, M. B. Piderit-Moreno, M. Trebilcock-Kelly, & P. Wegertseder-Martínez (Eds.), *Removing Barriers to Environmental Comfort in the Global South* (pp. 17–32). Springer International Publishing. https://doi.org/10.1007/978-3-031-24208-3_2

Rahim, M., Douzane, O., Tran Le, A. D., Promis, G., Laidoudi, B., Crigny, A., Dupre, B., & Langlet, T. (2015). Characterization of flax lime and hemp lime concretes: Hygric properties and moisture buffer capacity. *Energy and Buildings*, *88*, 91–99. https://doi.org/10.1016/j.enbuild.2014.11.043

Rahim, M., Douzane, O., Tran Le, A. D., Promis, G., & Langlet, T. (2017). Experimental investigation of hygrothermal behavior of two bio-based building envelopes. *Energy and Buildings*, *139*, 608–615. https://doi.org/10.1016/j.enbuild.2017.01.058

Rashedi, A., & Khanam, T. (2020). Life cycle assessment of most widely adopted solar photovoltaic energy technologies by mid-point and end-point indicators of ReCiPe method. *Environmental Science and Pollution Research*, *27*(23), 29075–29090. https://doi.org/10.1007/s11356-020-09194-1

Richards, C. E., Gauch, H. L., & Allwood, J. M. (2023). International risk of food insecurity and mass mortality in a runaway global warming scenario. *Futures*, *150*, 103173. https://doi.org/10.1016/j.futures.2023.103173

Richardson, K., Steffen, W., Lucht, W., Bendtsen, J., Cornell, S. E., Donges, J. F., Drüke, M., Fetzer, I., Bala, G., von Bloh, W., Feulner, G., Fiedler, S., Gerten, D., Gleeson, T., Hofmann, M., Huiskamp, W., Kummu, M., Mohan, C., Nogués-Bravo, D., … Rockström, J. (2023). Earth beyond six of nine planetary boundaries. *Science Advances*, *9*(37), eadh2458. https://doi.org/10.1126/sciadv.adh2458

Robert, A., & Kummert, M. (2012). Designing net-zero energy buildings for the future climate, not for the past. *Building and Environment*, *55*, 150–158. https://doi.org/10.1016/j.buildenv.2011.12.014

Röck, M., Saade, M. R. M., Balouktsi, M., Rasmussen, F. N., Birgisdottir, H., Frischknecht, R., Habert, G., Lützkendorf, T., & Passer, A. (2020). Embodied GHG emissions of buildings – The hidden challenge for effective climate change mitigation. *Applied Energy*, *258*, 114107. https://doi.org/10.1016/j.apenergy.2019.114107

Rockström, J., Norström, A. V., Matthews, N., Biggs, R., Folke, C., Harikishun, A., Huq, S., Krishnan, N., Warszawski, L., & Nel, D. (2023). Shaping a resilient future in response to COVID-19. *Nature Sustainability*, *6*(8), 897–907. https://doi.org/10.1038/s41893-023-01105-9

Rockström, J., Steffen, W., Noone, K., Persson, Å., Chapin, F. S. I., Lambin, E., Lenton, T., Scheffer, M., Folke, C., Schellnhuber, H. J., Nykvist, B., de Wit, C., Hughes, T., van der Leeuw, S., Rodhe, H., Sörlin, S., Snyder, P., Costanza, R., Svedin, U., … Foley, J. (2009). Planetary Boundaries: Exploring the Safe Operating Space for Humanity. *Ecology and Society*, *14*(2). https://doi.org/10.5751/ES-03180-140232

Rodrigues, L., Sougkakis, V., & Gillott, M. (2016). Investigating the potential of adding thermal mass to mitigate overheating in a super-insulated low-energy timber house. *International Journal of Low-Carbon Technologies*, *11*(3), 305–316. https://doi.org/10.1093/ijlct/ctv003

Rohde, R. (2024, January 12). *Global Temperature Report for 2023*. Berkeley Earth. https://berkeleyearth.org/global-temperature-report-for-2023/

Roostaie, S., Nawari, N., & Kibert, C. J. (2019). Sustainability and resilience: A review of definitions, relationships, and their integration into a combined building assessment framework. *Building and Environment*, *154*, 132–144. https://doi.org/10.1016/j.buildenv.2019.02.042

Rosenow, J., Gibb, D., Nowak, T., & Lowes, R. (2022). Heating up the global heat pump market. *Nature Energy*, *7*(10), 901–904. https://doi.org/10.1038/s41560-022-01104-8

Rüdisser, D. (2018). *A brief guide and free tool for the calculation of the thermal mass of building components (according to ISO 13786)*. https://doi.org/10.13140/RG.2.2.18312.72967/1

Salvalai, G., Pfafferott, J., & Sesana, M. M. (2013). Assessing energy and thermal comfort of different low-energy cooling concepts for non-residential buildings. *Energy Conversion and Management*, *76*, 332–341. https://doi.org/10.1016/j.enconman.2013.07.064

Schaffernicht, S. K., Türk, A., Kogler, M., Berger, A., Scharf, B., Clementschitsch, L., Hammer, R., Holzer, P., Formayer, H., König, B., & Haluza, D. (2023). Heat vs. Health: Home Office under a Changing Climate. *Sustainability*, *15*(9), 7333. https://doi.org/10.3390/su15097333

Schandl, H., Fischer-Kowalski, M., West, J., Giljum, S., Dittrich, M., Eisenmenger, N., Geschke, A., Lieber, M., Wieland, H., Schaffartzik, A., Krausmann, F., Gierlinger, S., Hosking, K., Lenzen, M., Tanikawa, H., Miatto, A., & Fishman, T. (2018). Global Material Flows and Resource Productivity: Forty Years of Evidence. *Journal of Industrial Ecology*, *22*(4), 827–838. https://doi.org/10.1111/jiec.12626

Scheffer, M., Carpenter, S., Foley, J. A., Folke, C., & Walker, B. (2001). Catastrophic shifts in ecosystems. *Nature*, *413*(6856), 591–596. https://doi.org/10.1038/35098000

Schneider, T., Kaul, C. M., & Pressel, K. G. (2019). Possible climate transitions from breakup of stratocumulus decks under greenhouse warming. *Nature Geoscience*, *12*(3), 163–167. https://doi.org/10.1038/s41561-019-0310-1

Schumacher, D. L., Singh, J., Hauser, M., Fischer, E. M., Wild, M., & Seneviratne, S. I. (2024). Exacerbated summer European warming not captured by climate models neglecting long-term aerosol changes. *Communications Earth & Environment*, *5*(1), 1–14. https://doi.org/10.1038/s43247-024-01332-8

Schwalm, C. R., Glendon, S., & Duffy, P. B. (2020). RCP8.5 tracks cumulative CO2 emissions. *Proceedings of the National Academy of Sciences*, *117*(33), 19656–19657. https://doi.org/10.1073/pnas.2007117117

SECO, S. für W. (2010). *Schweizerische Befragung in Büros (SBiB-Studie)*. https://www.seco.admin.ch/seco/de/home/Publikationen_Dienstleistungen/Publikationen_und_Formulare/Arbeit/Arbeitsbedingungen/Studien_und_Berichte/schweizerische-befragung-in-bueros--sbib-studie-.html

Shea, A., Lawrence, M., & Walker, P. (2012). Hygrothermal performance of an experimental hemp–lime building. *Construction and Building Materials*, *36*, 270–275. https://doi.org/10.1016/j.conbuildmat.2012.04.123

Sicurella, F., Evola, G., & Wurtz, E. (2012). A statistical approach for the evaluation of thermal and visual comfort in free-running buildings. *Energy and Buildings*, *47*, 402–410. https://doi.org/10.1016/j.enbuild.2011.12.013

Skjærseth, J. B., Hansen, T., Donner-Amnell, J., Hanson, J., Inderberg, T. H. J., Nielsen, H. Ø., Nygaard, B., & Steen, M. (2023). *Wind Power Policies and Diffusion in the Nordic Countries: Comparative Patterns*. Springer Nature Switzerland. https://doi.org/10.1007/978-3-031-34186-1

Sorrell, S. (2009). Jevons' Paradox revisited: The evidence for backfire from improved energy efficiency. *Energy Policy*, *37*(4), 1456–1469. https://doi.org/10.1016/j.enpol.2008.12.003

Statistics Sweden. (2024). *Electricity prices and electricity contracts*. Statistikmyndigheten SCB. https://www.scb.se/en/finding-statistics/statistics-by-subject-area/energy/price-trends-in-the-energy-sector/electricity-prices-and-electricity-contracts/

Steffen, W., Rockström, J., Richardson, K., Lenton, T. M., Folke, C., Liverman, D., Summerhayes, C. P., Barnosky, A. D., Cornell, S. E., Crucifix, M., Donges, J. F., Fetzer, I., Lade, S. J., Scheffer, M., Winkelmann,

R., & Schellnhuber, H. J. (2018). Trajectories of the Earth System in the Anthropocene. *Proceedings of the National Academy of Sciences*, *115*(33), 8252–8259. https://doi.org/10.1073/pnas.1810141115

Stern, D. I., & Kander, A. (2012). The Role of Energy in the Industrial Revolution and Modern Economic Growth. *The Energy Journal*, *33*(3), 125–152. https://doi.org/10.5547/01956574.33.3.5

Strandberg-de Bruijn, P., Donarelli, A., & Balksten, K. (2019). Full-scale Studies of Improving Energy Performance by Renovating Historic Swedish Timber Buildings with Hemp-lime. *Applied Sciences*, *9*(12), Article 12. https://doi.org/10.3390/app9122484

Sun, K., & Hong, T. (2017). A framework for quantifying the impact of occupant behavior on energy savings of energy conservation measures. *Energy and Buildings*, *146*, 383–396. https://doi.org/10.1016/j.enbuild.2017.04.065

Sun, Y., Gu, L., Wu, C. F. J., & Augenbroe, G. (2014). Exploring HVAC system sizing under uncertainty. *Energy and Buildings*, *81*, 243–252. https://doi.org/10.1016/j.enbuild.2014.06.026

Sundell, J., Levin, H., Nazaroff, W. W., Cain, W. S., Fisk, W. J., Grimsrud, D. T., Gyntelberg, F., Li, Y., Persily, A. K., Pickering, A. C., Samet, J. M., Spengler, J. D., Taylor, S. T., & Weschler, C. J. (2011). Ventilation rates and health: Multidisciplinary review of the scientific literature. *Indoor Air*, *21*(3), 191–204. https://doi.org/10.1111/j.1600-0668.2010.00703.x

Swedish Meteorological and Hydrological Institute. (2020). *Advanced Climate Change Scenario Service | SMHI*. https://www.smhi.se/en/climate/future-climate/advanced-climate-change-scenario-service/met/sverige/medeltemperatur/rcp85/2071-2100/year/anom

Tawalbeh, M., Al-Othman, A., Kafiah, F., Abdelsalam, E., Almomani, F., & Alkasrawi, M. (2021). Environmental impacts of solar photovoltaic systems: A critical review of recent progress and future outlook. *Science of The Total Environment*, *759*, 143528. https://doi.org/10.1016/j.scitotenv.2020.143528

Taylor, R. A., & Miner, M. (2014). A metric for characterizing the effectiveness of thermal mass in building materials. *Applied Energy*, *128*, 156–163. https://doi.org/10.1016/j.apenergy.2014.04.061

Technische Universität München. (2023). *Einfach bauen*. https://www.einfach-bauen.net/

TEK 17. (2017). Direktoratet for byggkvalitet. https://www.dibk.no/regelverk/byggteknisk-forskrift-tek17/13/ii/13-4

The Danish portal for Climate Change Adaptation. (2023). *Denmark's future climate*. https://en.klimatilpasning.dk/knowledge/climate/denmarksfutureclimate/

The Energy Institute. (2023). *Statistical Review of World Energy*. Statistical Review of World Energy. https://www.energyinst.org/statistical-review/home

Thoma. (2024). *Gesund und nachhaltig wohnen im Thoma Holzhaus*. https://www.thoma.at/

Thomas, C. D., Cameron, A., Green, R. E., Bakkenes, M., Beaumont, L. J., Collingham, Y. C., Erasmus, B. F. N., de Siqueira, M. F., Grainger, A., Hannah, L., Hughes, L., Huntley, B., van Jaarsveld, A. S., Midgley, G. F., Miles, L., Ortega-Huerta, M. A., Townsend Peterson, A., Phillips, O. L., & Williams, S. E. (2004). Extinction risk from climate change. *Nature*, *427*(6970), 145–148. https://doi.org/10.1038/nature02121

Trainer, T. (2021). Degrowth: How Much is Needed? *Biophysical Economics and Sustainability*, *6*(2), 5. https://doi.org/10.1007/s41247-021-00087-6

UNEP. (2021). *A Practical Guide to Climate-resilient Buildings and Communities*. United Nations Environment Programme (UNEP).

UNFCCC. (2017). *Finland National Communication 7*. UNFCCC. https://unfccc.int/documents/198252

Vadeboncoeur, M. A., Hamburg, S. P., Yanai, R. D., & Blum, J. D. (2014). Rates of sustainable forest harvest depend on rotation length and weathering of soil minerals. *Forest Ecology and Management*, *318*, 194–205. https://doi.org/10.1016/j.foreco.2014.01.012

Vadén, T., Lähde, V., Majava, A., Järvensivu, P., Toivanen, T., Hakala, E., & Eronen, J. T. (2020). Decoupling for ecological sustainability: A categorisation and review of research literature. *Environmental Science & Policy*, *112*, 236–244. https://doi.org/10.1016/j.envsci.2020.06.016

Van Vuuren, D. P., Edmonds, J., Kainuma, M., Riahi, K., Thomson, A., Hibbard, K., Hurtt, G. C., Kram, T., Krey, V., Lamarque, J.-F., Masui, T., Meinshausen, M., Nakicenovic, N., Smith, S. J., & Rose, S. K. (2011). The representative concentration pathways: An overview. *Climatic Change*, *109*(1–2), 5–31. https://doi.org/10.1007/s10584-011-0148-z

van Westen, R. M., Kliphuis, M., & Dijkstra, H. A. (2024). Physics-based early warning signal shows that AMOC is on tipping course. *Science Advances*, *10*(6), eadk1189. https://doi.org/10.1126/sciadv.adk1189

Verbeke, S., & Audenaert, A. (2018). Thermal inertia in buildings: A review of impacts across climate and building use. *Renewable and Sustainable Energy Reviews*, *82*, 2300–2318. https://doi.org/10.1016/j.rser.2017.08.083

Villacis-Ormaza, M. (2024). The Progression and Shift from Sustainable to Regenerative Architecture Design Concept. In T. Kang (Ed.), *Proceedings of 5th International Conference on Civil Engineering and Architecture* (Vol. 369, pp. 291–302). Springer Nature Singapore. https://doi.org/10.1007/978-981-99-4049-3_24

Vogel, J., & Hickel, J. (2023). Is green growth happening? An empirical analysis of achieved versus Paris-compliant CO2–GDP decoupling in high-income countries. *The Lancet Planetary Health*, *7*(9), e759–e769. https://doi.org/10.1016/S2542-5196(23)00174-2

Vohra, K., Vodonos, A., Schwartz, J., Marais, E. A., Sulprizio, M. P., & Mickley, L. J. (2021). Global mortality from outdoor fine particle pollution generated by fossil fuel combustion: Results from GEOS-Chem. *Environmental Research*, *195*, 110754. https://doi.org/10.1016/j.envres.2021.110754

von Schuckmann, K., Minière, A., Gues, F., Cuesta-Valero, F. J., Kirchengast, G., Adusumilli, S., Straneo, F., Ablain, M., Allan, R. P., Barker, P. M., Beltrami, H., Blazquez, A., Boyer, T., Cheng, L., Church, J., Desbruyeres, D., Dolman, H., Domingues, C. M., García-García, A., … Zemp, M. (2023). Heat stored in the Earth system 1960–2020: Where does the energy go? *Earth System Science Data*, *15*(4), 1675–1709. https://doi.org/10.5194/essd-15-1675-2023

Wang, L.-S., Ma, P., Hu, E., Giza-Sisson, D., Mueller, G., & Guo, N. (2014). A study of building envelope and thermal mass requirements for achieving thermal autonomy in an office building. *Energy and Buildings*, *78*, 79–88. https://doi.org/10.1016/j.enbuild.2014.04.015

Wang, P., Yang, Y., Xue, D., Ren, L., Tang, J., Leung, L. R., & Liao, H. (2023). Aerosols overtake greenhouse gases causing a warmer climate and more weather extremes toward carbon neutrality. *Nature Communications*, *14*(1), 7257. https://doi.org/10.1038/s41467-023-42891-2

Wienerberger. (2023). *Wienerberger Press Release*. Corporate Website. https://www.wienerberger.com/en/media/press-releases/2023/20231127-2226-ein-Gebaudekonzept-mit-Zukunft-Technology-made-in-Austria.html

Witkowski, C. R., von der Heydt, A. S., Valdes, P. J., van der Meer, M. T. J., Schouten, S., & Sinninghe Damsté, J. S. (2024). Continuous sterane and phytane δ13C record reveals a substantial pCO2 decline since the mid-Miocene. *Nature Communications*, *15*(1), 5192. https://doi.org/10.1038/s41467-024-47676-9

Wolkoff, P. (2018a). Indoor air humidity, air quality, and health – An overview. *International Journal of Hygiene and Environmental Health*, *221*(3), 376–390. https://doi.org/10.1016/j.ijheh.2018.01.015

Wolkoff, P. (2018b). The mystery of dry indoor air – An overview. *Environment International*, *121*, 1058–1065. https://doi.org/10.1016/j.envint.2018.10.053

World Health Organization (Ed.). (2010). *Who guidelines for indoor air quality: Selected pollutants*. WHO.

Xu, C., Kohler, T. A., Lenton, T. M., Svenning, J.-C., & Scheffer, M. (2020). Future of the human climate niche. *Proceedings of the National Academy of Sciences*, *117*(21), 11350–11355. https://doi.org/10.1073/pnas.1910114117

Xu, L., Feng, K., Lin, N., Perera, A. T. D., Poor, H. V., Xie, L., Ji, C., Sun, X. A., Guo, Q., & O'Malley, M. (2024). Resilience of renewable power systems under climate risks. *Nature Reviews Electrical Engineering*, *1*(1), 53–66. https://doi.org/10.1038/s44287-023-00003-8

Yang, L., & Li, Y. (2008). Cooling load reduction by using thermal mass and night ventilation. *Energy and Buildings*, *40*(11), 2052–2058. https://doi.org/10.1016/j.enbuild.2008.05.014

Yang, L., Yan, H., & Lam, J. C. (2014). Thermal comfort and building energy consumption implications – A review. *Applied Energy*, *115*, 164–173. https://doi.org/10.1016/j.apenergy.2013.10.062

Zhang, M., Qin, M., Rode, C., & Chen, Z. (2017). Moisture buffering phenomenon and its impact on building energy consumption. *Applied Thermal Engineering*, *124*, 337–345. https://doi.org/10.1016/j.applthermaleng.2017.05.173

Zhao, J., Uhde, E., Salthammer, T., Antretter, F., Shaw, D., Carslaw, N., & Schieweck, A. (2024). Long-term prediction of the effects of climate change on indoor climate and air quality. *Environmental Research*, *243*, 117804. https://doi.org/10.1016/j.envres.2023.117804

Zhu, L., Hurt, R., Correia, D., & Boehm, R. (2009). Detailed energy saving performance analyses on thermal mass walls demonstrated in a zero energy house. *Energy and Buildings*, *41*(3), 303–310. https://doi.org/10.1016/j.enbuild.2008.10.003

Zou, Y., Lou, S., Xia, D., Lun, I. Y. F., & Yin, J. (2021). Multi-objective building design optimization considering the effects of long-term climate change. *Journal of Building Engineering*, *44*, 102904. https://doi.org/10.1016/j.jobe.2021.102904

Zu, K., Qin, M., Rode, C., & Libralato, M. (2020). Development of a moisture buffer value model (MBM) for indoor moisture prediction. *Applied Thermal Engineering*, *171*, 115096. https://doi.org/10.1016/j.applthermaleng.2020.115096

Appendices

Appendix A: Generative Artificial Intelligence (GAI) Use

1) I used a GAI tool in my report.	**YES**/NO	Only as a language editor.
2) I used a GAI tool as a language editor.	**YES**/NO	Tool Grammarly was used to check grammar, spelling, style, and tone.
3) I used GAI to retrieve information.	YES/**NO**	
4) I used GAI to get help in writing code.	YES/**NO**	
5) I used GAI for translations.	YES/**NO**	
6) I used GAI to generate graphs/images.	YES/**NO**	
7) I used GAI to help structure my content.	YES/**NO**	

Appendix B: Generated Weather Files

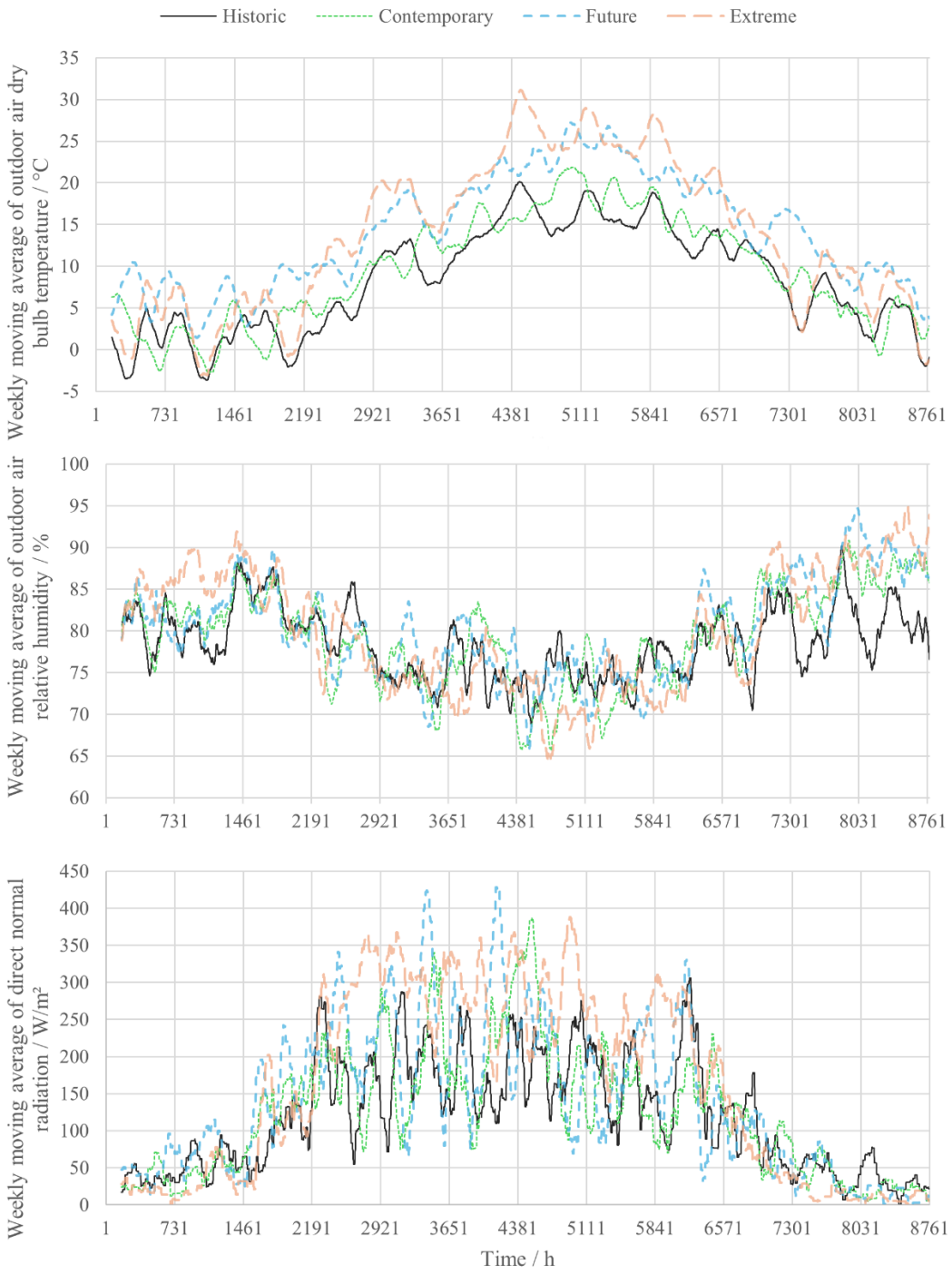

Figure 37. Weekly moving averages of outdoor air dry bulb temperature, outdoor air relative humidity, and direct normal radiation in four climate scenarios of Copenhagen.

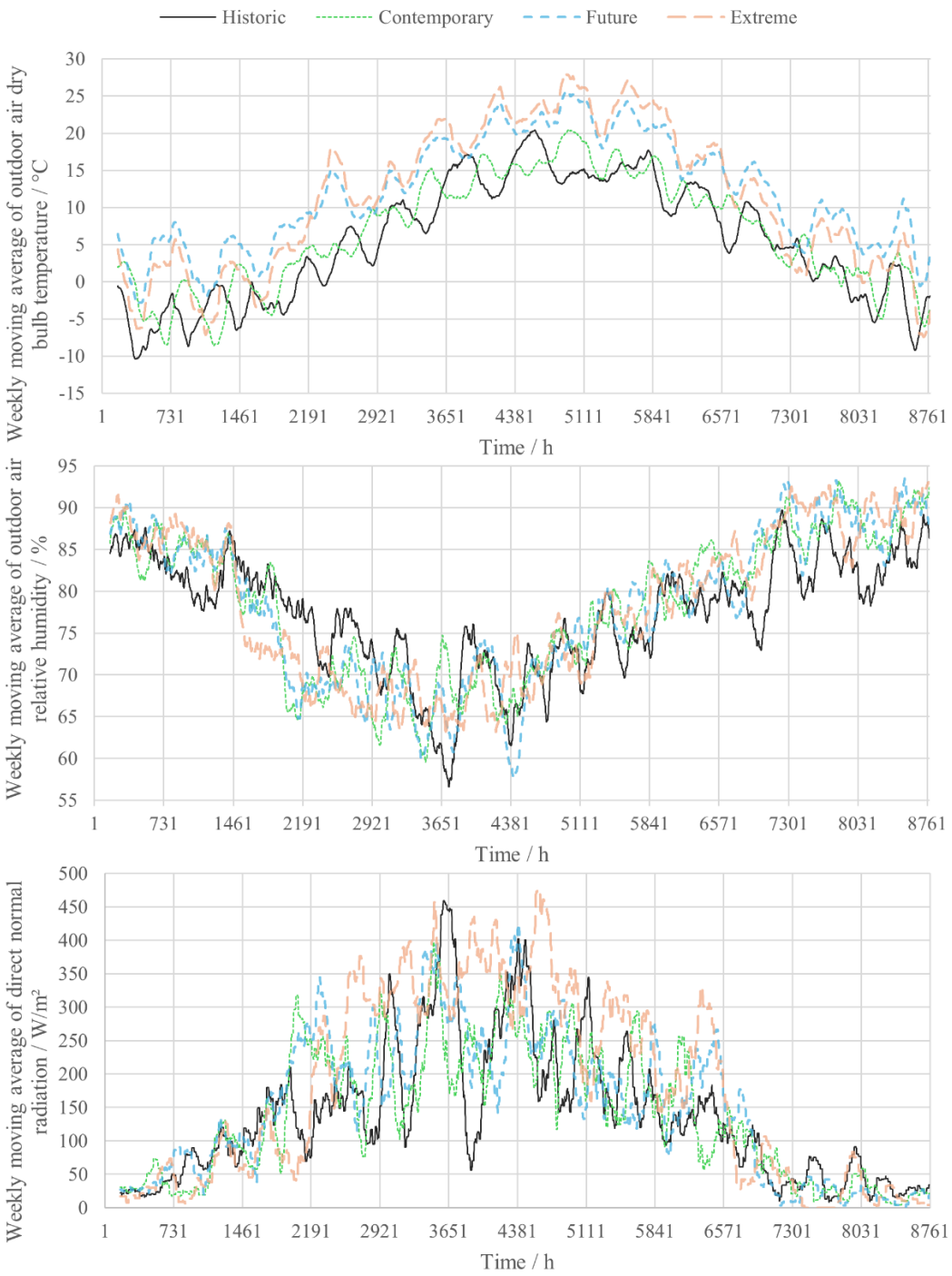

Figure 38. Weekly moving averages of outdoor air dry bulb temperature, outdoor air relative humidity, and direct normal radiation in four climate scenarios of Karlstad.

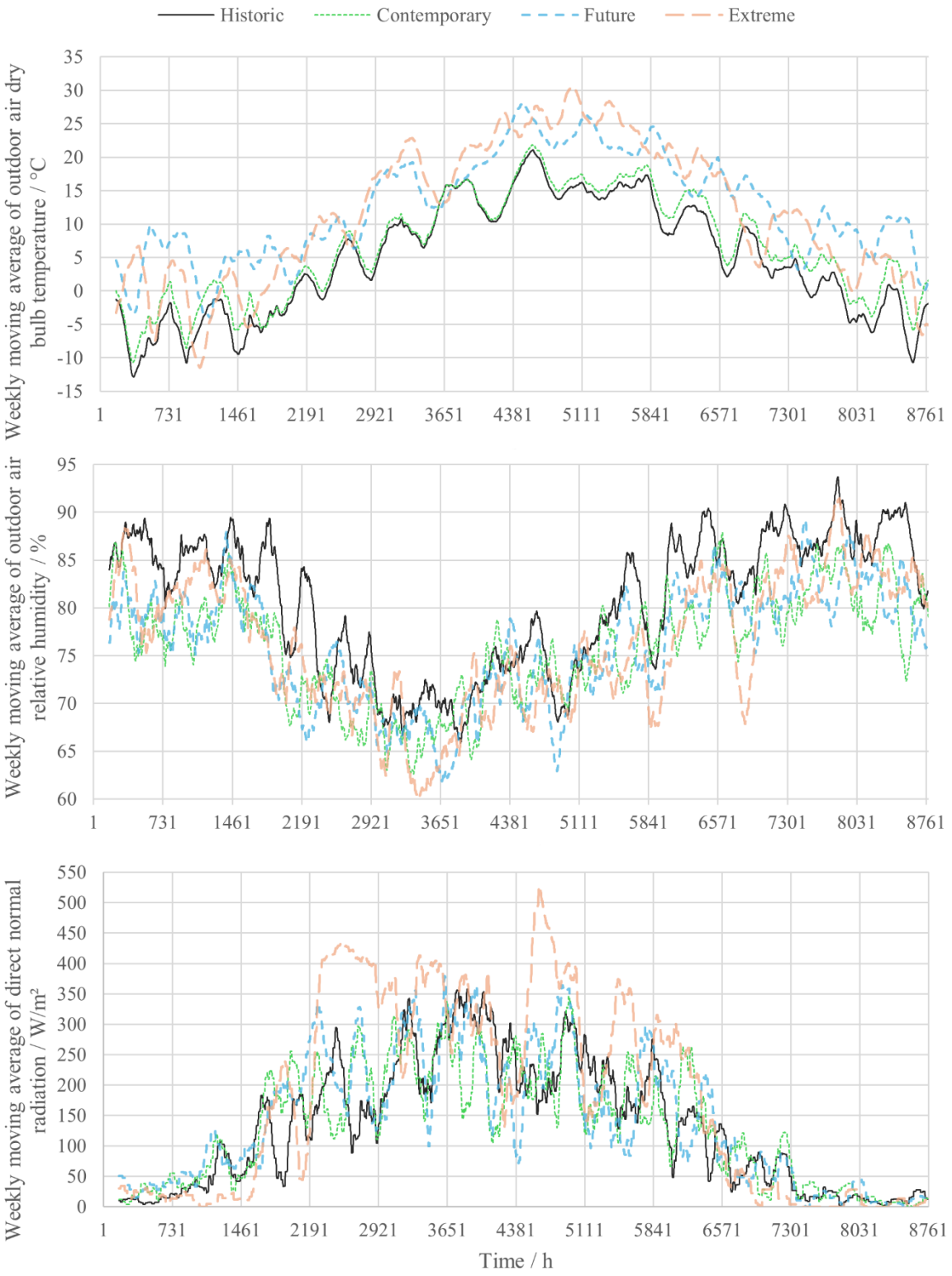

Figure 39. Weekly moving averages of outdoor air dry bulb temperature, outdoor air relative humidity, and direct normal radiation in four climate scenarios of Helsinki.

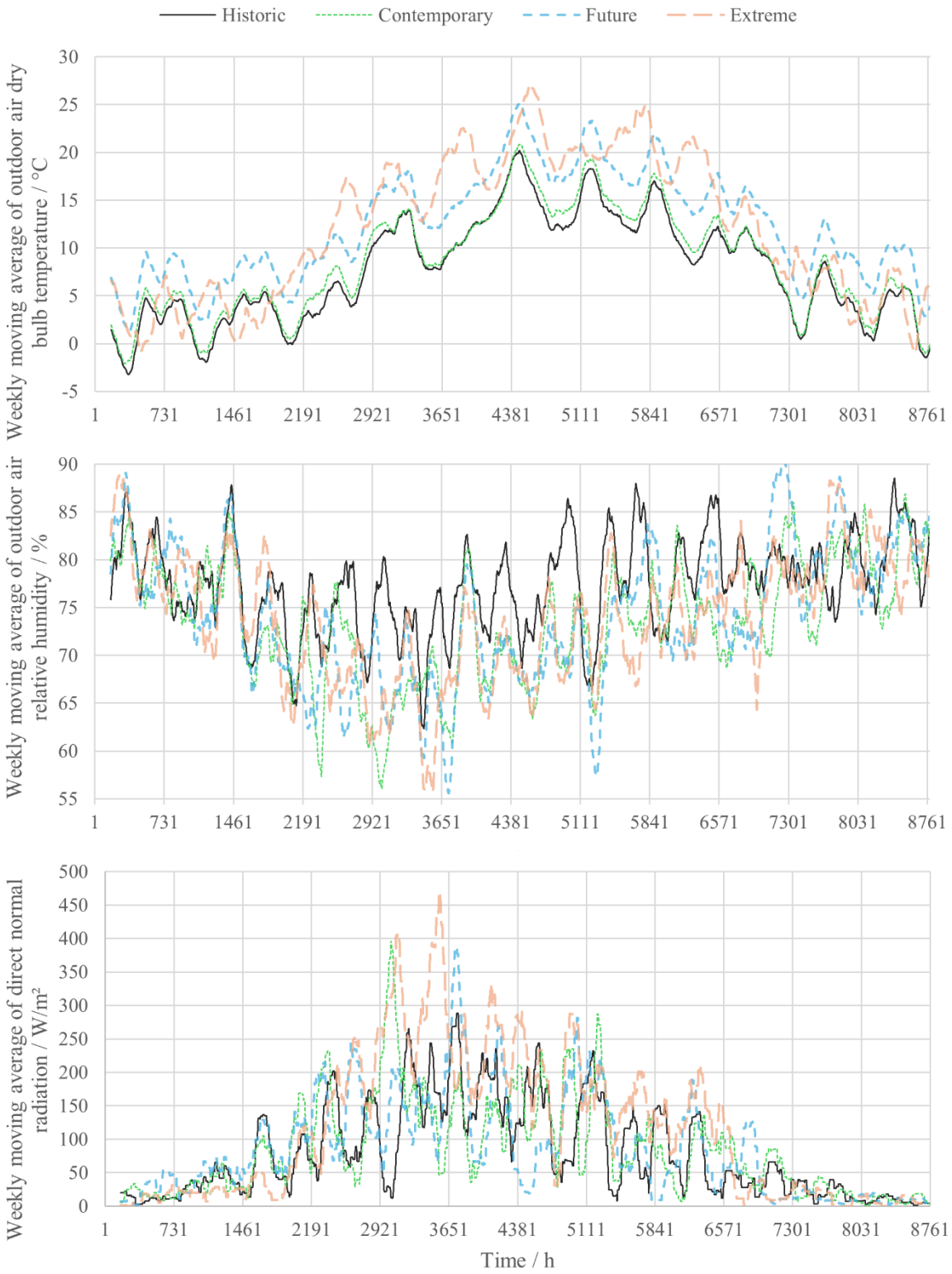

Figure 40. Weekly moving averages of outdoor air dry bulb temperature, outdoor air relative humidity, and direct normal radiation in four climate scenarios of Bergen.

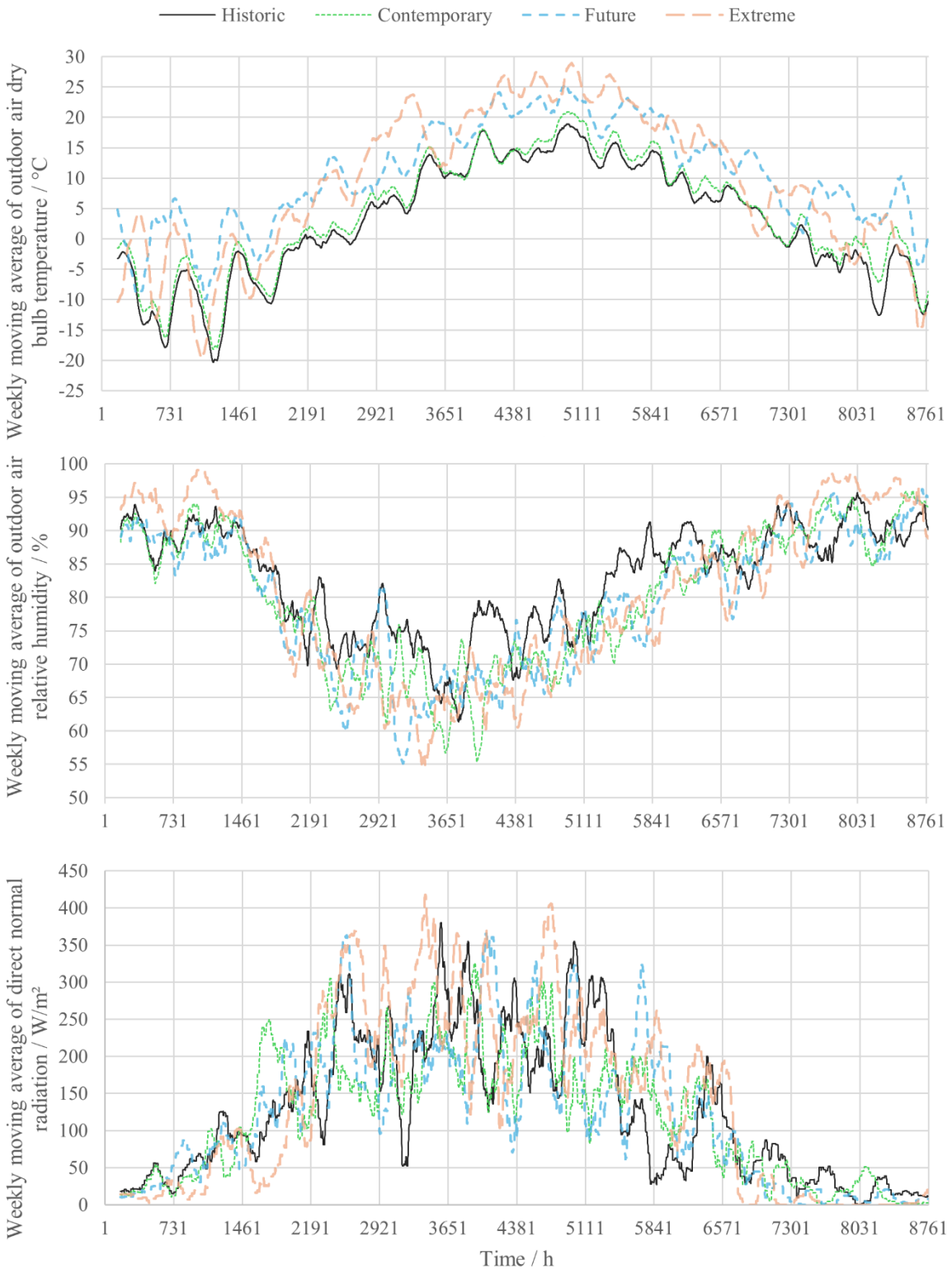

Figure 41. Weekly moving averages of outdoor air dry bulb temperature, outdoor air relative humidity, and direct normal radiation in four climate scenarios of Jyväskylä.

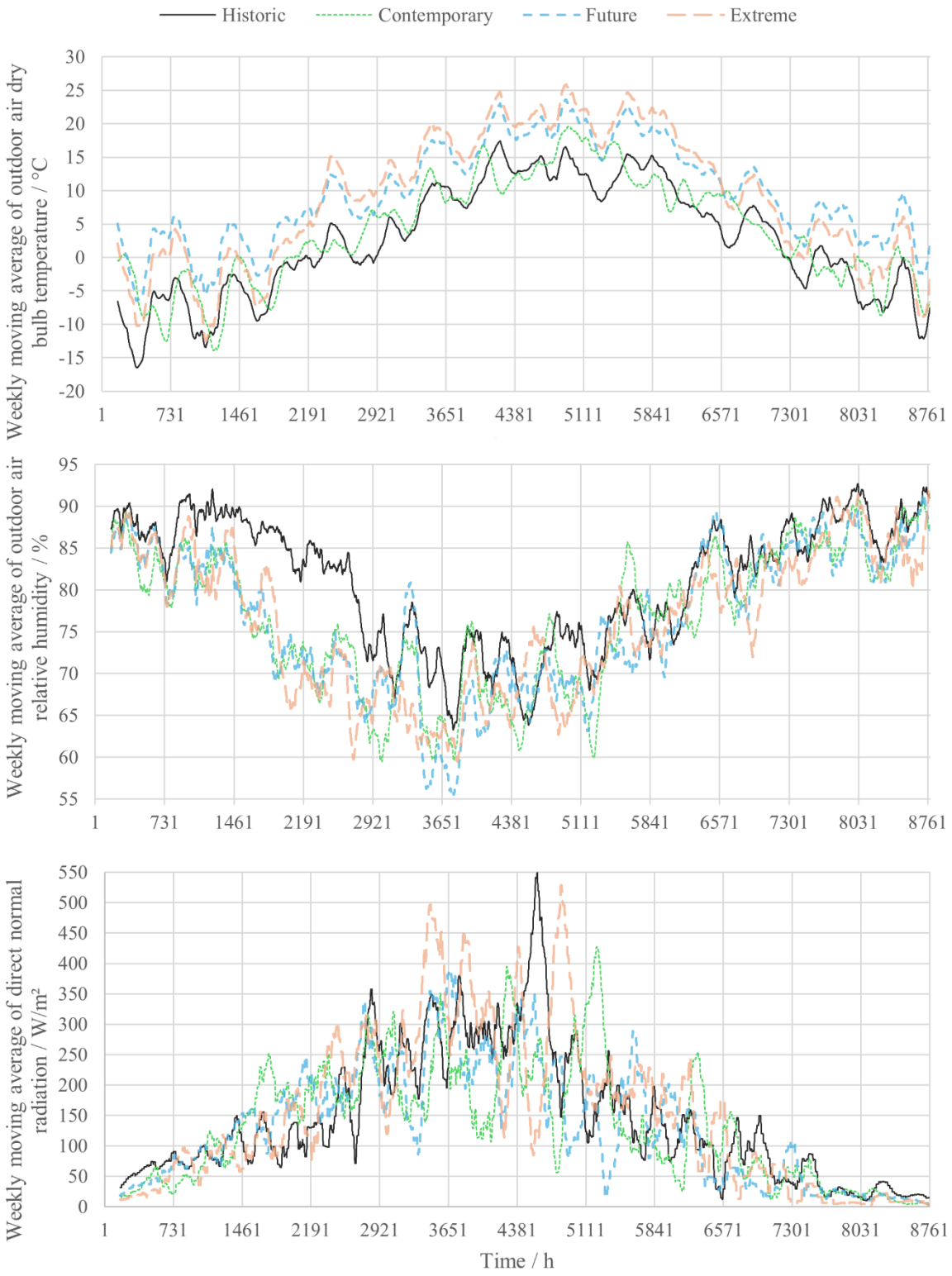

Figure 42. Weekly moving averages of outdoor air dry bulb temperature, outdoor air relative humidity, and direct normal radiation in four climate scenarios of Östersund.

LUND UNIVERSITY

Divisions of Energy and Building Design, Building Physics and Building Services
Department of Building and Environmental Technology